

Non-thermal messengers from the Universe - High energy physics processes in astrophysics

Pasquale D. Serpico

LAPTh, CNRS and Univ. of Savoie Mont Blanc, 9 chemin de Bellevue - BP 110, 74941 Annecy-Le-Vieux, France

It was the wonders of the night sky, observed by Indians, Sumerians or Egyptians, that started science several thousand years ago. It was the question why the wanderers - the planets - moved as they did that triggered off the scientific avalanche several hundred years ago. [...] if the night sky on which we observe them is at a high latitude, outside this lecture hall - perhaps over a small island in the archipelago of Stockholm - we may also see in the sky an aurora, which is a cosmic plasma, reminding us of the time when our world was born out of plasma. Because in the beginning was the plasma. (H. Alfvén Nobel lecture, 11/12/1970)

The main goal of the present lectures is to outline the main mechanisms and processes through which *high-energy* (or non-thermal) particles evolve in space and momentum in typical galactic and extragalactic environments. This realm is much more rich and hard to describe than the *thermal* one you are most familiar with, where the collisional interactions are frequent enough that the distribution in momentum/energy attains the *universal* Maxwell-Boltzmann function (or Fermi-Dirac/Bose-Einstein when quantum effects are relevant). Clearly we are dealing with systems which are *not* at thermodynamical equilibrium. The important concept of collisionless diffusion of charged particles will be tackled, followed by a description of particle interactions and loss mechanisms in the Galactic and extragalactic medium. These interactions are an important ingredient entering the propagation equation and contribute shaping the spectrum of high-energy charged particles, whose population observed at the Earth (top of the atmosphere) is known as "Cosmic Rays" (CR). The neutral byproducts of the charged energetic particle interactions (gamma rays and neutrinos) point back to their production point, and are themselves signals one can look for and study.

A gentle introduction to the topic is [1]. For the CR propagation part, classical texts like [2] remain useful. Specialised literature, such as [3–5], or reviews like [6, 7] can and should be addressed for more advanced concepts, but hopefully will not be required to make you grasp the fundamentals of this wide topic, which is my goal here. An original recent book, that fills the widening gap in modern physicists' training in advanced *classical physics* notions, is [8]: I would like to recommend notably Part II and Part VI on statistical physics and plasma physics, respectively. It may be the single best reference to go also to consolidate auxiliary concepts I must introduce very quickly and that may be unfamiliar to you.

These lecture notes also include other references (including reviews and articles), but have not undergone a deep proof-reading, nor can be considered complete. Their essential goal is to make you focus on following the arguments (rather than frantically taking notes) and ease the task especially of those following remotely. Exercises are typically not very advanced since you do not have much time, so are meant to help you consolidating the notions and guide you through some literature. Some more advanced projects are also suggested, notably for after the school. Obviously, the only way to learn is *by doing*, so I invite you to repeat all derivations presented below. Do not hesitate to signal me typos and mistakes, if you find any.

Contents

I Introductory notions

I. Prolegomena	3
A. On Units	3
B. The Galactic and extragalactic environments	4
1. Magnetic fields	5
2. Photon fields	5
II. Some dates and facts about cosmic rays	6
A. Cosmic ray spectra, fluxes, and observational techniques	8
1. Units	8
2. Direct techniques	9
3. Indirect techniques	9
B. Chemical composition	11

II Cosmic ray propagation

III. Elementary considerations	12
A. Motion in a constant field	12
B. Heuristic derivation of the diffusive propagation	13
IV. CR propagation in phase space	16
A. Diffusion in the phase space description	17
B. Alternative approach: Quasi-linear theory (QLT)	17
C. Solving the diffusion problem	19
D. Basics of Galactic propagation	20
III Cosmic ray acceleration	
V. Towards a theory of cosmic ray acceleration	21
A. Moving scattering centers	21
B. The CR transport equation: moving scattering centers	22
VI. How to accelerate CRs?	24
1. (First order) Fermi acceleration theory.	25
2. Generalities of stochastic acceleration and (Second order) Fermi mechanism.	27
3. Some notions on supernova remnants.	28
4. Confinement condition	29
IV Collisions	
A. Pair production and the “gamma-ray horizon”	31
VII. Synchrotron radiation	31
1. Beaming effect from relativistic motion	33
2. Characteristic frequency of emission	34
VIII. Inverse Compton	35
A. Thomson cross-section	35
1. Energy loss rate	35
B. The Klein-Nishina regime	36
1. Compton kinematics	37
C. Notions on SSC	37
IX. Leptonic interactions with matter	38
A. Ionization and Coulomb interactions	38
B. Bremsstrahlung	39
X. Hadronic interactions	40
A. Generalities and spallation	40
B. Adiabatic energy losses	41
C. Bethe-Heitler process	42
D. Nuclear photodisintegration	42
E. Inelastic pp collisions	43
F. $p\gamma$ collisions	43
XI. The diffusion-loss equation: Including collisional effects	44
A. Catastrophic losses	44
B. Continuous energy losses	44
C. The “complete” diffusion-loss equation and some benchmark solutions	44
1. E-loss dominated propagation	45
2. Catastrophic loss for diagnostics: Secondaries over primaries	45
3. Principles underlying dark matter searches via CRs	45
D. On some limitations of the theory presented	46

V Multimessenger astrophysics

XII. Spectra of pion decay byproducts	47
A. Gamma spectra emitted in neutral pion decays	47
B. Neutrino spectra emitted in charged pion decays	48
XIII. Diffuse extragalactic fluxes	49
A. Recap: Collisional random motions	51
B. From Liouville equation to BBGKY hierarchy	52
a. Liouville Equation	52
b. BBGKY hierarchy	53
References	54

Part I

Introductory notions

I. PROLEGOMENA

A. On Units

As in particle physics, astroparticle physics practitioners tend to use *natural units* for microscopic scales (where $c = k_B = \hbar = 1$), so that e.g. energy, mass, momenta, temperature, inverse length and inverse time have the same unit. Astrophysical units are instead common for astrophysical distances, in particular. Typically, energy is measured in eV (and multiples) for microscopic applications or ergs for macroscopic/astrophysics scales; distances are given in parsecs (and multiples), cross sections in barns (and multiples), etc. On the other hand, differently from some convention frequent among quantum gravity *aficionados*, in astroparticle we retain $G_N \equiv M_P^{-2} = (1.22 \times 10^{19} \text{ GeV})^{-2}$. Finally, in agreement with most astrophysical literature, the Gaussian electromagnetic convention is used (with the 4π 's in Maxwell equations, not in Coulomb or Biot-Savart laws). The charge of the positron is $e \simeq \sqrt{\alpha} \simeq \sqrt{1/137} \simeq 0.085$. The magnetic field energy density is for instance $B^2/(8\pi)$, etc. Some rough conversions are

- $1 \text{ s} = 3 \times 10^{10} \text{ cm} = 1.5 \times 10^{15} \text{ eV}^{-1}$
- $1 \text{ J} = 10^7 \text{ erg} = 6.25 \times 10^{18} \text{ eV}$
- $1 \text{ pc} = 3.1 \times 10^{16} \text{ m}$
- $1 \text{ barn} = 10^{-24} \text{ cm}^2$
- $1 \text{ G} = 10^{-4} \text{ T} \simeq 0.069 \text{ eV}^2$

If you are unfamiliar with natural units, practice a bit!

Exercises

- Compute your typical body temperature (assuming you are still alive) and your mass in eV.
- Check the working frequency of your mobile phone. Rephrase it into eV.
- Compute your height and age in eV^{-1} .
- Compute your density (estimated with $\mathcal{O}(10\%)$ error!) in eV^4 .

B. The Galactic and extragalactic environments

These environments are *extremely rarified*, if compared with terrestrial conditions. Typical benchmark densities of matter:

- $\lesssim 1 \text{ cm}^{-3}$ in the Galaxy, apart in regions close to the center and in dense molecular clouds.
- $\lesssim 10^{-6} \text{ cm}^{-3}$ on average, in a cosmological setting.

Sizes and distances are also *much bigger* than terrestrial scales. Typical benchmark distances are ($1 \text{ pc} \simeq 3.26 \text{ lyr} \simeq 3.086 \times 10^{16} \text{ m}$):

- Several kpc, for Galactic objects (Earth-Gal. Center is $\simeq 8 \text{ kpc}$).
- hundreds of Mpc, or Gpc, for cosmologically distant objects (at low redshift, the relation $d \simeq 40(z/0.01) \text{ Mpc}$ holds).

System can also evolve over *very long timescales*. Typical benchmark timescales are:

- $\sim 230 \text{ Myr}$ for a solar orbit in the Milky Way.
- $\sim 14 \text{ Gyr}$, age of the Universe.

Besides via the “general-purpose” equatorial coordinate system ¹, Galactic and extragalactic astronomers locate objects in angular space via Galactic coordinates, illustrated in Fig. 1. Another (less standardised!) frame used is the Galactocentric one, here intended as the cylindrical coordinates centered on the Galactic Center, where r denotes the distance in the plane, θ is the angle as illustrated in Fig. 2, and z is the height above the plane. More precise and operational definitions, as well as algorithms for conversions, can be found at <https://docs.astropy.org/en/stable/coordinates/index.html#module-astropy.coordinates>.

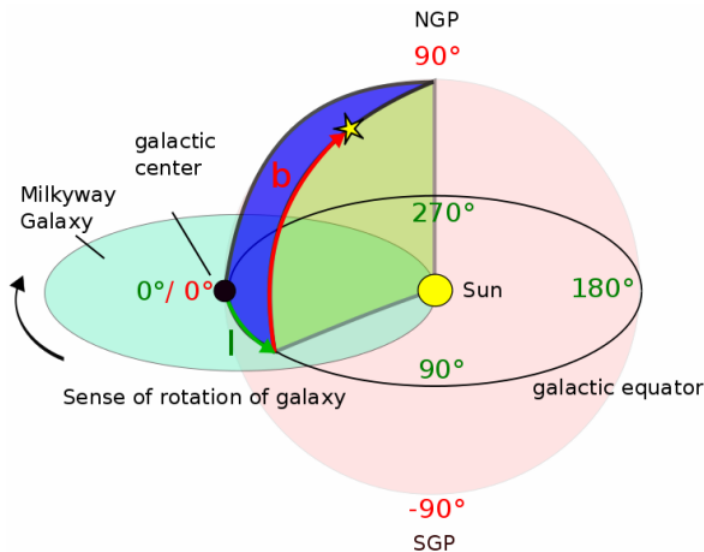


FIG. 1: Illustration of Galactic coordinates; NGP: North Galactic Pole; SGP: South Galactic Pole; l : galactic longitude; b : galactic latitude; from https://auger.org/education/Auger_Education/galacticcoordinates.html.

¹ The eq. coord. system is a *celestial* ‘projection’ of the terrestrial coordinate systems, with the role of latitude played by *declination* and the longitude by *Right Ascension*; instead of El Hierro or Greenwich, the prime meridian (zero R.A.) is taken as the vernal equinox point of the intersection of the equatorial plane with the *ecliptic* (=plane of Earth revolution orbit in the sky, or solar motion plane in geocentric frame).

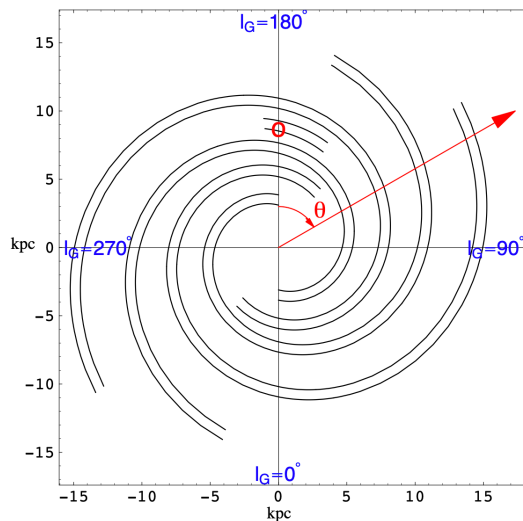


FIG. 2: Galactocentric (cylindrical) coordinates, r is the distance from the Galactic center in the plane, z the distance above the plane, θ the angle shown measured starting at zero along the GC-Sun direction. The indicative (in the sense that these are defined wrt to a frame centered on the Sun, see Fig. 1!) galactic longitudes are shown by comparison. From [9].

1. Magnetic fields

The interstellar medium (ISM) of our Galaxy, as well as external ones, is magnetized. This is most clearly revealed by radio observations (Faraday rotation, synchrotron radiation) but also via polarized light emission (due to dust grains) or, in some cases, via Zeeman splitting. A magnetic field coherent (at least) up to scales comparable to several kpc-long Galactic structures, such as spiral arms, has been detected. Radio observations of external Galaxies as well as our own, notably via synchrotron emission (see below), indicate several kpc thick magnetized halos embedding the stellar disks, as *alfajores* embed their *dulce de leche*. The ISM magnetic field extends to small scales down to at least the typical pc-scale distance between neighbouring stars, where the field orientation is believed to fluctuate following the turbulence of the ISM. Typical inferred intensities of Galactic fields (typically via radio synchrotron emission, its polarization and its Faraday rotation) are in the 1-10 μ G range, where 1 G is the order of magnitude of the Earth magnetic field. There are also indications that the extragalactic medium is magnetized, with magnetic fields exceeding 10^{-19} G at least [10], and not exceeding ~ 2 nG in the truly extragalactic medium [11]. Fields reaching μ G in proximity of Galaxy clusters have been inferred. For a relatively recent review and ample references on Galactic and cosmic magnetism, including microphysics and simulations, see for instance [12]. Another review worth looking at is [13].

2. Photon fields

The most important extragalactic backgrounds are (see Fig. 3, left):

- The CMB (blackbody of cosmological origin and temperature of about 2.7 K), pervading the whole universe (Galaxy and extragalactic sky alike). While today its energy density is only ~ 0.3 eV/cm³, it scales with redshift as $(1+z)^4$ (number density of photons as $(1+z)^3$).
- The extragalactic background light (EBL), pervading the whole universe, due to primary stellar emission and secondary radiation from reprocessing, with a benchmark number density of roughly a photon /cm³; a recent determination of its spectral energy density can be found in [15]. Other backgrounds also exist (e.g. radio) but are less important for what follows.

For the Galactic environment, besides the CMB, UV, optical, and IR backgrounds are important (comparable or larger than the CMB, in energy density) and non-homogeneously distributed (peaking towards inner Galaxy), see Fig. 3, right.

Sometimes, a different classification is made in terms of “starlight” (SL) or primary emission and “dust” or reprocessed emission, with SL loosely covering the UV and optical range, while the dust, responsible for absorbing SL and re-emitting it at longer wavelengths, mostly contributes in the IR. Note however that this “matching” is not absolute in physical units, as considering emission of the same object at higher redshift makes obviously clear.

It turns out that energy densities of magnetic fields, radiation and cosmic rays are roughly comparable (equal within less than one order of magnitude) in our Galaxy, amounting to about $\lesssim 1$ eV/cm³ each.

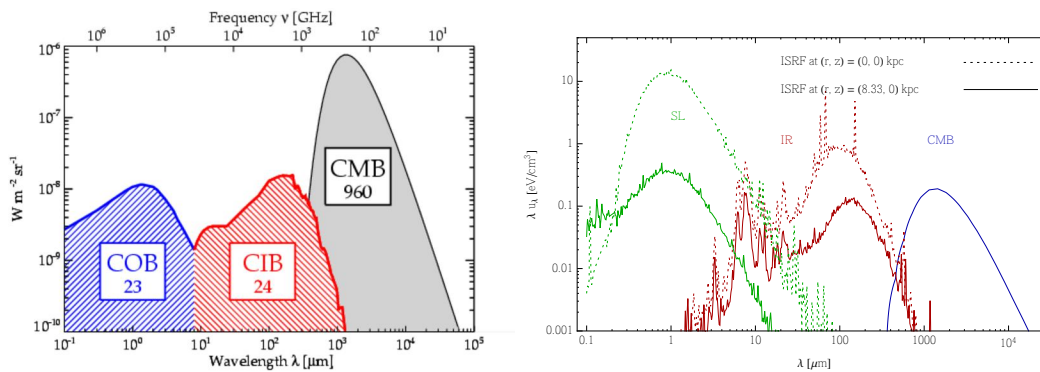


FIG. 3: Left: Typical energy budgets of extragalactic photon backgrounds, in the optical, infrared and microwave band, from https://www.ias.u-psud.fr/irgalaxies/SpitzerPR2006/Dole_v7.html. Numbers in the boxes provide the relative brightness. Right: Typical photon densities in the Galactic regions, from [14].

II. SOME DATES AND FACTS ABOUT COSMIC RAYS

- 1785: Coulomb observes that insulated electroscopes discharge over time.
- 1879: Crookes finds that the discharge rate scales with pressure of gas.
- 1896: Becquerel discovers spontaneous radioactivity (Radioactive materials known to cause discharge of electroscopes)
- 1911: Pacini measured the ionisation level in the deep sea of the Genova gulf, finding that there was 20% less radiation 3 metres below the water compared to on the surface, concluding that the ionizing radiation must come from the atmosphere rather than the "terrestrial radioactivity".
- 1912: Victor Hess performed a series of balloon flights measuring the discharge rate at increasing altitude, discovering that it increases with altitude: Evidence of ionising extraterrestrial radiation that penetrates the atmosphere, no correlation with day/night, i.e. Sun: "Galactic" origin?
- 1926: Millikan confirms findings and, favouring photon interpretation over charged particles one (Compton's view, instead), named them "cosmic rays".
- 1932: Anderson discovers the positron in magnetized cloud chambers; positron is produced by cosmic ray interactions in the atmosphere.
- 1933: *Latitude effect*, first observed by Clay in 1929: The cosmic ray intensity grows with the geomagnetic latitude. Bothe and Kolhoerster correctly interpreted this effect as evidence that (the primary) cosmic rays are charged, see compilation by Compton [16].
- 1934: *East-West effect*: low-energy CR preferentially arrive from the West than the East, suggesting an excess of positively charged particles (For a review of these earlier phenomena, see [17]).
- 1936: Nobel Prize in Physics for Hess & Anderson.
- 1936: Anderson & Neddermeyer discover the muon.
- 1938: Auger (and, independently, Rossi) discovers extended air showers (via coincident measurements in ground arrays) from CR interactions in atmosphere.
- 1947: Powell & Occhialini discover the pion in photographic emulsions.
- 1947: First strange hadron (Kaon) discovered in CR by G. Rochester and C. Butler.
- 1949: First "theory" of cosmic ray origin, by Fermi.
- 1953: Cosmic Ray Conference at Bagnères de Bigorre, marking the divorce entre particle and CRs, see [18].
- 1970: Nobel Prize in Physics to Alfvén for his work on magnetohydrodynamics.

- 1998: the Super-Kamiokande experiment discovers atmospheric neutrino oscillations.
- 2012: the IceCube experiment discovers a diffuse astrophysical neutrino flux at PeV energies.

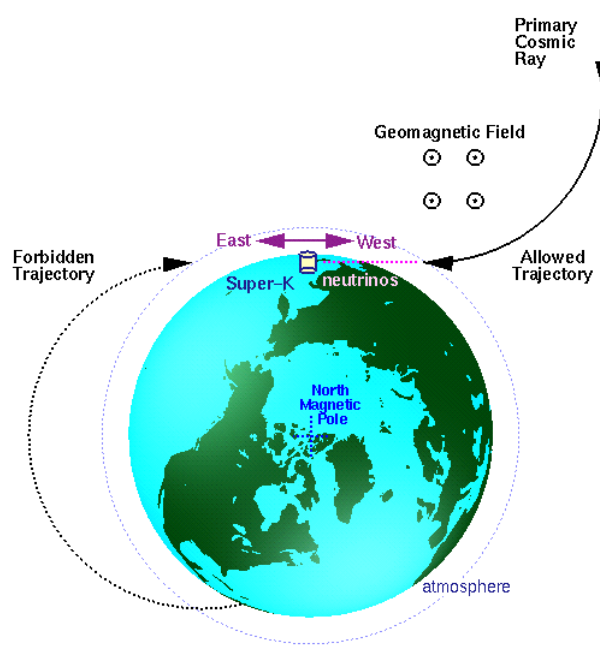


FIG. 4: Illustration of the East-West effect at the Super-Kamiokande location, from <http://hep.bu.edu/~superk/ew-effect.html>

Exercise: Argue that cosmic rays impinging on the Earth along the magnetic field (fraction of a G) direction travel unimpeded, while CR arriving along the magnetic equator suffer a deflection. Compute the radius of curvature and determine the momentum/charge (known as rigidity, measured in GV) below which this radius is smaller than the Earth radius. Discuss how this depends on the latitude. A charged CR nature clearly predicts that an isotropic flux far away from Earth would be observed in a “magnetic-latitude” modulated way. The critical rigidity is known as *rigidity (or magnetic) cutoff*. For estimates, you can use the following dipole model of the Earth:

$$B_r = -2B_0 \left(\frac{R_E}{r} \right)^3 \cos \theta \quad (1)$$

$$B_\theta = -B_0 \left(\frac{R_E}{r} \right)^3 \sin \theta \quad (2)$$

$$|B| = B_0 \left(\frac{R_E}{r} \right)^3 \sqrt{1 + 3 \cos^2 \theta} \quad (3)$$

where $B_0 = 3.12 \times 10^{-5} \text{ T} = 0.321 \text{ G}$, R_E is the mean radius of the Earth (approximately 6370 km), r is the radial distance from the center of the Earth, and θ is the geomagnetic co-latitude measured from the north magnetic pole (if λ is the magnetic latitude, $\theta = \pi/2 - \lambda$). For more professional modeling and links with geographical coordinate systems, you can have a look at <https://www.ngdc.noaa.gov/IAGA/vmod/igrf.html>. Be aware that the magnetic dipole is tilted (by something like 11° , but depends on time!) with respect to the rotation axis of the Earth. For rough calculations you can confound the two, otherwise please use dedicated software like at http://www.geomag.bgs.ac.uk/data_service/models_compass/coord_calc.html for conversions.

Advanced reading suggestions: The motion of a charged particle in a magnetic dipole-field is today called the Størmer problem (e.g. <https://dynamical-systems.org/stoermer/info.html>) in honor of Størmer’s pioneering studies [19]. Stoermer problem. Since a long time, physicists and mathematicians have been interested in how a charged particle moves in the magnetic field of the Earth, in the context of the northern lights and cosmic radiation. After decades of searching for an additional integral besides the energy and the angular momentum, it has been realized that the problem is not integrable. In an early example of qualitative study of diff. equations, Størmer showed the existence of an inner forbidden region that a

particle arriving from a large distance away cannot access. Have a look at a modern take on the problem in [20]. Numerical calculations of magnetic cutoffs remain nonetheless of importance today for many reasons (from computing dose rates of astronauts to atmospheric neutrino fluxes).

A. Cosmic ray spectra, fluxes, and observational techniques

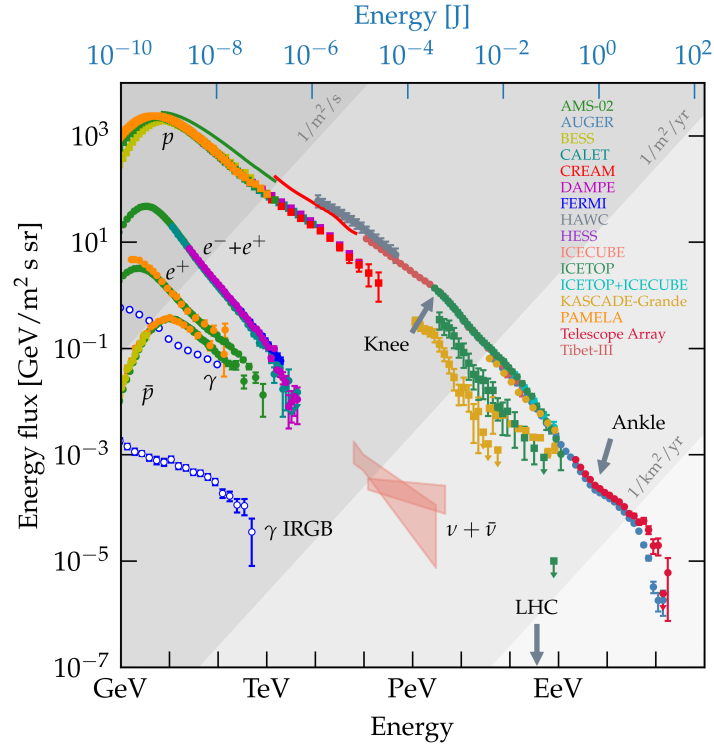


FIG. 5: Synoptic view of CR fluxes (in a broad sense, i.e. including neutral particle components), compiled by C. Evoli. The total spectrum (all constituents) is shown, as well as some elemental constituents, notably the dominant proton flux, the leading antiparticle components (e^+ and \bar{p}), the overall photon flux, its isotropic flux, and the diffuse neutrino flux.

What we typically care about are CR above the Earth atmosphere, to avoid contaminations by secondaries produced in collisions of CRs with the atmosphere. Instead, this is exactly what was used in the early days to do particle physics with CRs! Apart from effects due to the geomagnetic field, the CRs appear to be rather isotropic in arrival directions (anisotropies typically $\lesssim \mathcal{O}(0.1\%)$ level), with an energy spectrum well-distinct from thermal, closely resembling a decreasing broken power-law (spectral index around 2.7 or so, albeit with a few changes of slopes) above about a few GeV. Their fluxes range from $1 \text{ cm}^{-2}\text{s}^{-1}$ @ 1 GeV to $1 \text{ m}^{-2}\text{day}^{-1}$ @ 100 TeV to $1 \text{ km}^{-2}\text{century}^{-1}$ @ 10^{20} eV, the highest energies at which they have been detected (see Fig. 5 for a synoptic view). This means that a transition from *direct* (i.e. high-atmosphere, space) to *indirect techniques* (from ground) is needed around 100 TeV to cope with the tiny fluxes.

1. Units

- Momentum: \mathbf{p} , with $p \equiv |\mathbf{p}| = m\beta\gamma$ in terms of velocity β and gamma-factor $\gamma = (1 - \beta^2)^{-1/2}$. Measured in GeV in natural units, GeV/c otherwise. Used often in theoretical considerations, when working in phase space.
- (Total) Energy $E = m\gamma = \sqrt{m^2 + p^2} \simeq \sqrt{A^2 m_N^2 + p^2}$, measured in GeV (latter approximate relation for nuclei, in terms of the nucleon mass $m_N \simeq (m_p + m_n)/2 \simeq 0.939$ GeV and mass number A). Useful e.g. if gauging the type of particle processes CR can be involved in.
- Energy per nucleon, $E_N = E/A$, measured in GeV/nuc: Useful especially in the GeV-TeV energy range, when caring about spallation processes, since this variable is roughly preserved in these interactions.

- (Total) Kinetic energy: $T = E - A m_N$, less frequently used, apart from low energies.
- Kinetic energy/nucleon: $T_N = T/A = E_N - m_N$, as above.
- Rigidity: $\mathcal{R} = p/q$, momentum over charge, measured in GV. Useful if focusing on “magnetic” properties of CRs, since CR of the same rigidity are deflected the same way (via Lorentz force).

Exercise: Practice to compute the Jacobians relating such quantities, if you want to convert a flux given in some units into another one, or rely on dedicated software (e.g. the CR DataBase <https://1psc.in2p3.fr/crdb/> does that for you on actual databases, upon request!)

2. Direct techniques

In principle, ordinary particle physics detectors onboard balloons and satellites can be used to measure the relevant information on CRs: direction, charge, momentum, energy, velocity via:

- Spectrometers, magnets & trackers: determine Q and \mathbf{p} of the particles.
- Calorimeters: measure E of particles & allow for particle discrimination.
- Cherenkov detectors: measure the particle v from width of the Cherenkov cone.
- Transition radiation detectors: measure the mass of particles via its Lorentz factor γ .
- Time of flight: measure the time difference and thus the velocity.

Some peculiar difficulties & differences wrt colliders: weight and size matter! Unusual backgrounds (for example number e.m. particles \ll hadrons!), challenges in assuring alignment in space (cannot go out there to measure...), etc. The most advanced detector of this class for CR currently running is AMS-02, onboard the International Space Station, see <https://ams02.space>. For photons, Fermi-LAT is the best example: <https://fermi.gsfc.nasa.gov>

3. Indirect techniques

What can be measured from the ground are (the effects of) secondary particles (notably γ , e^\pm , μ^\pm , some hadron like nucleons and pions) produced when the primary CR interacts in the atmosphere, triggering a multiplicative cascade (known as extensive air shower, EAS), first characterised via coincidence detections over an extended area. Quantities like the fluorescent light in clear moonless nights allow one to infer the longitudinal development of the showers in dedicated telescopes, otherwise a “EAS slice” can be inferred by the timing of the signals, the number of particles, and the types of particles detected (e.g. mostly electrons via scintillators, mostly muons via Cherenkov tanks). This allows one to reconstruct the incident direction of the primary, its energy and to some extent learn about the nature of the primary. Below, we will give a brief sketch to some of the principles. Both the Pierre Auger observatory and the Telescope Array for UHECRs are of this class. Among gamma-ray detectors, Imaging Atmospheric Cherenkov Telescopes like HESS, MAGIC, Veritas (and the forthcoming CTA) as well as non-pointing gamma detectors like HAWC, Tibet-AS $_\gamma$ and LHAASO belong to this class.

Due to the highly indirect inference method, models of hadronic interactions in EAS development are needed. Simple, semi-analytical models are possible for purely QED showers, such as the ones triggered by primary γ , impinging on the atmosphere, generating a pair after crossing a characteristic grammage λ (The grammage is defined as density integrated along trajectory $\int d\ell \rho(\ell)$, and measured in g/cm^2); each lepton in turn generates a γ via bremsstrahlung after crossing about the same λ (*Heitler model*, see Fig. 6). After crossing a grammage $X = n\lambda$, the shower will contain a number of particles of the order of $N(X) = 2^n = 2^{X/\lambda}$, each one with average energy $\langle E \rangle = E_0/2^n$. Under the assumption that there is a (sharp) critical energy E_c below which particles lose energy collisionally (e.g. via ionization) rather than radiating new particles, the shower reaches a maximum number of particles

$$N_{\max} = E_0/E_c @ X_{\max} = \lambda \log_2(E_0/E_c). \quad (4)$$

A more elaborated cascade theory developed around 1940 (see [21]) corroborates at least qualitatively these results. Since $\lambda \approx 35 \text{ g}/\text{cm}^2$ (see PDG, at chapter E -losses in matter) and $E_c \approx 80 \text{ MeV}$ are “atmospheric constants”, once calibrated, the method can provide an estimate e.g. of primary energy via an estimate of X_{\max} or the number of particles at a given depth X . Anyway, nowadays such a pure QED cascade can be simulated in a rather reliable way. Hadronic processes are more challenging, especially at the highest energies. A simple generalisation of Heitler’s model to the hadronic case

can be found in [22]. A first approximation is to assume that pions dominate the particles produced in the hadronic interaction; neutral pions promptly decay into photons (thus triggering secondary e.m. showers), while charged pions initiate new hadronic cascades, until their energy falls below a characteristic energy E_d , below which they rather decay than interact. Eventually, when decaying they generate muons, which are very penetrating and useful for diagnostics. For an isospin-symmetric production, after n steps we expect the energy still in hadronic particles to be $E_{\text{had}} = (2/3)^n E_0$, while $E_{\text{e.m.}} = [1 - (2/3)^n] E_0$. The average energy of charged pions at step n in terms of the multiplicity ν_{\pm} is

$$\langle E_{\pm} \rangle (X) = \frac{E_0}{\left(\frac{3}{2}\nu_{\pm}\right)^n}, \quad (5)$$

while the maximum number of particles is reached when average E drops to E_d :

$$n_{\text{max}}^{\pm} = \frac{\ln(E_0/E_d)}{\ln(3\nu_{\pm}/2)}, \quad (6)$$

which also leads to the prediction for the number of muons

$$N_{\mu} = N_{\pm} = \nu_{\pm}^{n_{\text{max}}^{\pm}} \Rightarrow \ln N_{\mu} = n_{\text{max}}^{\pm} \ln \nu_{\pm} = \beta \ln(E_0/E_d), \quad (7)$$

where

$$\beta = \frac{\ln \nu_{\pm}}{\ln(3\nu_{\pm}/2)} \approx 0.85. \quad (8)$$

Also, under the assumption that a nucleus of mass number A and energy E_0 acts like A independent nucleons of energy $E_N = E_0/A$, one deduces

$$N_{\mu}^A = A \left(\frac{E_0/A}{E_d} \right)^{\alpha} \approx N_{\mu}^p A^{0.15} \quad (9)$$

and

$$X_{\text{max}}^A = X_{\text{max}}^p - \lambda_p \ln A \quad (10)$$

while

$$N_{\text{max}} = A E_N / E_c = E_0 / E_c \quad (11)$$

i.e. the maximum number of particles is independent of the chemical nature of the primary (at fixed energy), but the maximal depth is smaller for heavier nuclei² and the number of muons expected larger.

While this picture is qualitatively ok, more refined predictions are heavily based on simulations and are subject to uncertainties not easy to quantify. In fact, they rely on extrapolations of “shaky” models of non-perturbative QCD, not based on first principles! Over the past decade, the calibration of some observables to LHC results has helped, but note that most LHC results not applicable since focused on the rare, high- p_T results instead of the dominating *forward* physics of interest for CRs (more on that in Part IV on Collisions).

Exercise: Consider an isothermal (exponential) model for the (upper) atmosphere,

$$\rho(h) \simeq \rho_0 \exp(-h/h_0) \quad h_0 \simeq 6.4 \text{ km} \quad \rho_0 h_0 \simeq 1300 \text{ g/cm}^2 \quad (12)$$

$$X(\ell, \theta) = \int_{\ell}^{\infty} d l \rho(h(l, \theta)) \quad (13)$$

$$h(l, \theta) = \sqrt{R_{\oplus}^2 + 2lR_{\oplus} \cos \theta + l^2} \approx l \cos \theta + \frac{l^2}{2R_{\oplus}} \sin^2 \theta. \quad (14)$$

- Estimate what is the height in the above model of atmosphere, Eqs. (12)(13),(14) at which the first interaction of a downgoing energetic photon takes place.
- Based on the Heitler model, how many particles are expected in a 1 TeV (100 GeV) gamma-ray induced shower? In the above model, what is the typical height of this maximum for a downgoing photon?

² One can also prove, as intuitively clear, that once considered as a stochastic variable, also the variance of X_{max}^A is smaller.

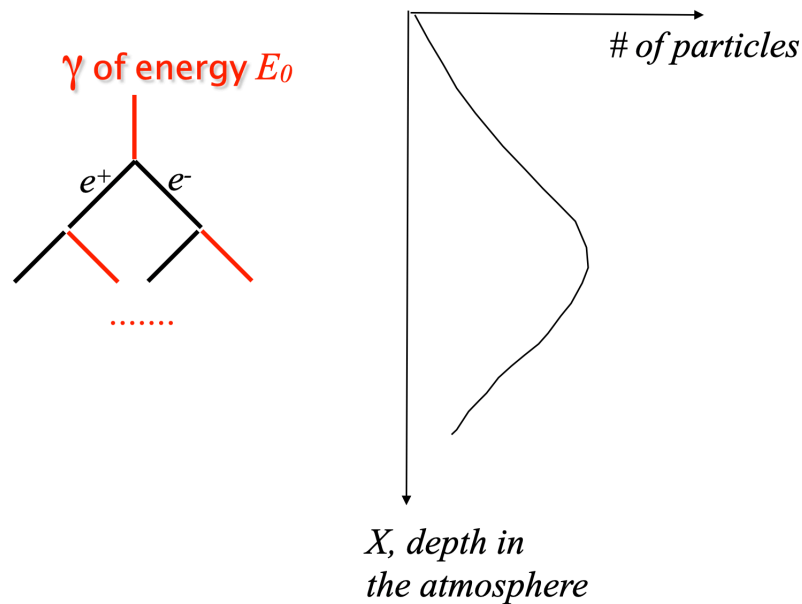


FIG. 6: Sketch to illustrate the Heitler model for a shower development.

B. Chemical composition

In short, the CR composition is overall consistent with solar system abundances, see Fig. 7, apart for Li-Be-B and sub-iron species overabundances (plus deuterium and helium-3, also overabundant; isotopic measurements are however rather difficult, so we will not discuss that in details). Nuclei such as Li-Be-B are *fragile* from the thermonuclear point of view: Due to their small nuclear binding energy, they are easily burned in stellar thermonuclear processes and are only present in traces in conventional astrophysical environments, such as the ISM. Their sizeable presence among CR nuclear fluxes is interpreted as the consequence of spallation of heavier nuclei, such as C or O—which are common in the ISM—onto the ISM gas during their propagation. This is also why such nuclei are also referred to as “secondary” CR species, in the sense that ISM mimics (in a much more rarefied settings!) the kind of processes that take place in the Earth atmosphere. Given the known density of the ISM medium of $\mathcal{O}(1) \text{ cm}^{-3}$, the abundances of these species at the tens of percent of their progenitors require CR residence times in the Galaxy which are orders of magnitude larger than the ballistic crossing time, as outlined in the exercise below. This is the oldest (and still perhaps the most convincing) evidence for some sort of diffusive CR propagation.

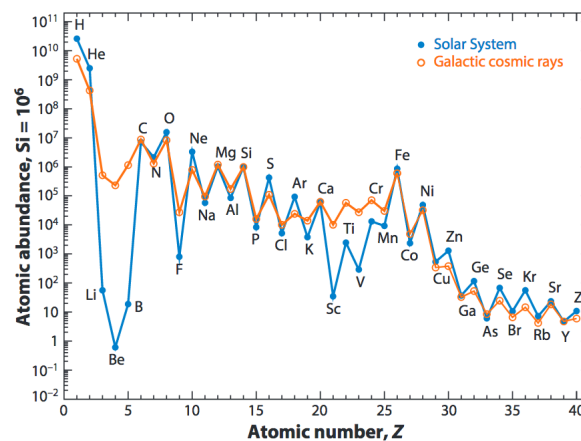


FIG. 7: Relative abundances of CR species, compared to Solar System values, normalized to Si = 10⁶. From [23].

Exercise: Consider two CR species: primaries with number density n_p and secondaries (initially not produced!) with number density n_s . If the two are coupled by the spallation process $p \rightarrow s + \dots$, then

$$\frac{dn_p}{dX} = -\frac{n_p}{\lambda_p} \quad (15)$$

$$\frac{dn_s}{dX} = -\frac{n_s}{\lambda_s} + \frac{p_{p \rightarrow s} n_p}{\lambda_p} \quad (16)$$

where $X \equiv \int d\ell \rho(\ell)$ is the *grammage*, the density integrated along the actual path followed by the particle, measured in g/cm^2 ; $\lambda_i = \rho_{ISM}/(n_{ISM}\sigma_i) = m_{ISM}/\sigma_i$ is the *interaction length* of the species i in the ISM medium, in terms of the effective ISM mass $m_{ISM} \simeq m_p$, and total inelastic cross-section σ_i (appropriately weighted by the medium composition); it is measured in g/cm^2 , as X ; $p_{p \rightarrow s}$ is the probability that, in an inelastic interaction of species p , the species s is produced (the relevant b.r.), and is dimensionless. Note that λ_i are dependent from laboratory measurements and the ISM composition, not really from the CR path. For instance, one has $\sigma_{\text{CNO}} \simeq 6.7 \text{ g}/\text{cm}^2$, $\sigma_{\text{LiBeB}} \simeq 10 \text{ g}/\text{cm}^2$, and $p \simeq 0.35$ between these two groups. From the measured value $n_s/n_p \simeq 0.25$, deduce X , and compare with the predictions for X for straight lines crossing the Milky Way disk with an angle between 30° and 60° , assuming a density of 1 hydrogen atom/ cm^3 and a Galactic half-thickness $h \simeq 100 \text{ pc}$. Based on this, estimate the typical timescales the CRs spent in the gaseous disk.

Part II

Cosmic ray propagation

III. ELEMENTARY CONSIDERATIONS

A. Motion in a constant field

In order to gain an intuitive understanding of the CR movement, let us start with the description of the evolution in a constant (large scale) field of intensity $B_0 \equiv |\mathbf{B}_0|$, neglecting (small scale) field fluctuations. The trajectory of a particle of charge $q = Z|e|$ of mass m moving with velocity \mathbf{v} (associated to Lorentz factor $\gamma(v)$) obeys the EoM

$$\frac{d(m\gamma\mathbf{v})}{dt} = q\mathbf{v} \times \mathbf{B}_0 \Rightarrow m\gamma \frac{d\mathbf{v}}{dt} = q\mathbf{v} \times \mathbf{B}_0, \quad (17)$$

since (**Exercise:** prove it, from $\gamma = (1 - v_j v^j)^{-1/2}$)

$$\frac{d(m\gamma\mathbf{v})}{dt} = m\gamma \frac{d\mathbf{v}}{dt} + m\gamma^3 \mathbf{v} \frac{d(\mathbf{v} \cdot \mathbf{a})}{dt} = m\gamma \frac{d\mathbf{v}}{dt}, \quad (18)$$

the last step following from the fact that in a \mathbf{B}_0 field, the acceleration is always orthogonal to the velocity. This is equivalent to the fact that γ is constant, which we can see also from

$$m\gamma \frac{d(\mathbf{v} \cdot \mathbf{v})}{dt} = 2m\gamma \mathbf{v} \cdot \frac{d\mathbf{v}}{dt} = 2\mathbf{v} \cdot (q\mathbf{v} \times \mathbf{B}_0) = 0. \quad (19)$$

So, both v and $p = m\gamma v$ are constant. The EoM also imply that the velocity component parallel to \mathbf{B}_0 is constant. If we choose the z direction aligned with \mathbf{B}_0 , this means $v_z = \text{const.}$ and $p_z = m\gamma v_z = \text{const.}$ If we denote with μ (the cosine of the angle (dubbed *pitch angle*) formed by the particle momentum \mathbf{p} with the magnetic field direction, this means that $\mu = p_z/p$ is also constant. Hence, the momentum component in the $x - y$ plane, $p_\perp \equiv \sqrt{p_x^2 + p_y^2} = \sqrt{1 - \mu^2} p$ is also constant. In the $x - y$ plane, the particle gyrates with a radius given by equating the acceleration in the $x - y$ plane to the centripetal acceleration

$$\frac{dv_\perp}{dt} = \frac{q}{m\gamma} v_\perp B_0 \quad \text{and} \quad \frac{dv_\perp}{dt} = \frac{v_\perp^2}{r} \Rightarrow r = \frac{m\gamma v_\perp}{q B_0}. \quad (20)$$

With respects to the non-relativistic *Larmor radius* or *gyroradius* r_g , *angular gyrofrequency* or *cyclotron frequency* ω_g , and *gyrofrequency* ν_g defined as

$$r_g \equiv \frac{v_\perp}{\omega_g}, \quad \omega_g \equiv \frac{q B_0}{m}, \quad \nu_g = \frac{\omega_g}{2\pi} \equiv \frac{q B_0}{2\pi m} = 2.8 \text{ Hz } Z \left(\frac{m_e}{m} \right) \left(\frac{B_0}{\mu\text{G}} \right), \quad (21)$$

the relativistic generalizations are thus

$$r_L = \gamma r_g = \sqrt{1 - \mu^2} \frac{\mathcal{R}}{B_0} \simeq 10^{-6} \sqrt{1 - \mu^2} \frac{\mathcal{R}}{\text{GV}} \frac{\mu\text{G}}{B_0} \text{pc}, \quad (22)$$

where we introduced the rigidity \mathcal{R} , or momentum over charge (measured typically in GV), and

$$\Omega = \frac{\omega_g}{\gamma} = \frac{q B_0}{E} \simeq 10^{-2} Z \frac{B_0}{\mu\text{G}} \frac{\text{GeV}}{E} \text{rad/s}. \quad (23)$$

Note that the timescales or equivalently spatial scales of this movement are very small for Galactic astrophysics standards. . .

Exercise

. . . up to which rigidity? Compute the energy at which a proton and a iron nucleus gyroradius exceeds the kpc scale, if $B_0 = 3 \mu\text{G}$. If I told you that the skymap of CRs at $E \simeq 10^{19}$ eV looks roughly isotropic, what would you infer about the source locations?

The gyrating motion means that (with a suitable choice of initial time)

$$v_x = v_\perp \cos(\Omega t), \quad v_y = v_\perp \sin(\Omega t), \quad v_z = v\mu = \text{const}. \quad (24)$$

and equivalently

$$x = x_g + r_L \sin(\Omega t), \quad y = y_g - r_L \cos(\Omega t), \quad z = z_g + v_z t = z_g + v\mu t, \quad (25)$$

with the point $\{x_g, y_g, z(t)\}$, around which the particle rotates, which is called *guiding center*.

B. Heuristic derivation of the diffusive propagation

Let us now add an ensemble of *small-scale, stochastic perturbations* to the B-field, orthogonal to its regular value, i.e. $|\delta\mathbf{B}| \ll |\mathbf{B}_0|$ and $\delta\mathbf{B} \perp \mathbf{B}_0$. For clarity and simplicity, the perturbation has been chosen so that p_z —or better $\mu = p_z/p$ —is affected by the perturbation since the new term yields the leading non-vanishing force, while the $x - y$ trajectory is left unchanged. Also, assume the magnetostatic limit for the field perturbation, which should capture the dominant effect in the ultrarelativistic limit for the CR (under which one also has $E \simeq p$). Under these conditions, for a single plane wave perturbation of wavenumber k and phase ψ , $\delta\mathbf{B} = \{\cos(-kz + \psi), \sin(-kz + \psi), 0\}$ one gets

$$\frac{d\mu}{dt} = \frac{q \sqrt{1 - \mu^2} |\delta\mathbf{B}|}{E} [\cos(\Omega t) \cos(-kz + \psi) - \sin(\Omega t) \sin(-kz + \psi)] = C \cos[w t + \psi], \quad (26)$$

where at the second step we defined the quantities $C \equiv q \sqrt{1 - \mu^2} |\delta\mathbf{B}|/E$ and $w \equiv (\Omega - k v\mu)$. Below, we assume a *random phase approximation* for the perturbations; *ensemble-averaging* over phase ψ :

$$\left\langle \frac{d\mu}{dt} \right\rangle_\psi \propto \int_0^{2\pi} d\psi \cos(A + \psi) = 0. \quad (27)$$

If we compute however the variance after some finite interval of time

$$\Delta\mu^2(t) = C^2 \int_0^t dt' \int_0^t dt'' \cos[wt' + \psi] \cos[wt'' + \psi]. \quad (28)$$

We can express the integrand as a sum of cosine of the sum and the difference of the arguments, i.e. use

$$\cos(A) \cos(B) = \frac{\cos(A - B) + \cos(A + B)}{2}, \quad (29)$$

the piece depending on the sum ensemble-averages to zero; but the one depending on the difference survives. As a consequence, one can prove that *in the limit* $\Delta t \gg \Omega^{-1}$

$$\frac{d\langle \Delta\mu^2 \rangle}{dt} \rightarrow \pi C^2 \delta(w) = \pi (1 - \mu^2) \Omega \frac{|\delta\mathbf{B}|^2}{B_0^2} k_{\text{res}} \delta(k - k_{\text{res}}), \quad k_{\text{res}} \equiv \frac{\Omega}{v\mu}. \quad (30)$$

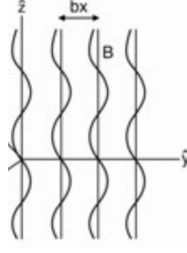


FIG. 8: Example of the perturbed B-field, with static perturbation orthogonal to the background.

(remember that $\pi\delta(w) = \lim_{\epsilon \rightarrow 0} \frac{\sin(w/\epsilon)}{w}$)

We see that on average μ remains constant, but its variance linearly grows with time: This is the typical behaviour of a *diffusive* process, see Eq. (A7). We also deduce that the diffusion process is (quasi)resonant [there are corrections to that at least due to the fact that $1/(\Delta t\Omega)$ is not zero!], with the momentum direction along the regular field only changing if the CR finds a fluctuation whose wavelength matches the gyroradius of the CR in the field, modulo a geometric projection. In Fig. 9 we provide a cartoon interpretation of this effect: a CR “surfs” along field lines whose fluctuations have very long wavelengths, “ignores” fluctuations of the field at too small scales compared with its Larmor radius, but undergoes a significant deflection with respect to its unperturbed trajectory if the perturbation matches r_L . It is straightforward

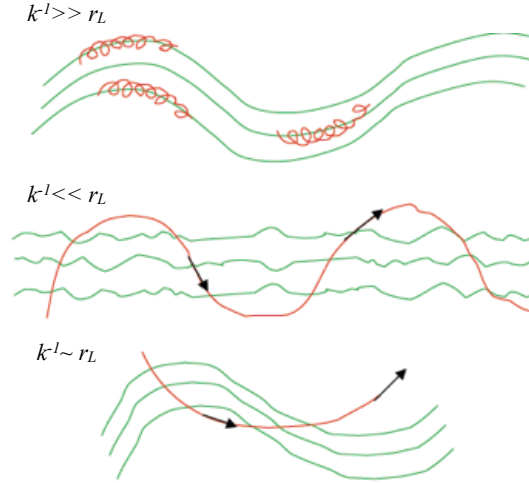


FIG. 9: Sketch of the resonant CR diffusion mechanism. The direction of the CR is significantly affected when the Larmor radius matches the wavelength of the perturbation (bottom panel); otherwise the CR just ‘surfs’ the wave if its Larmor radius is very small (top panel) or “ignores the perturbation”, if its Larmor radius is very large (middle panel).

to generalize the previous derivation to an ensemble of perturbations with different wavelengths. From the analogy with the random-motion (see Appendix A and in particular Eq. (A7) for a reminder), it makes sense to introduce the diffusion coefficient of the cosine of the pitch angle, $D_{\mu\mu}$, according to

$$D_{\mu\mu}(k) = (1 - \mu^2)\nu_{\theta\theta} \simeq (1 - \mu^2)\Omega \frac{1}{B_0^2} \int dx e^{ikx} \delta B^2(x). \quad (31)$$

which essentially means that the typical frequency $\nu_{\theta\theta}$ (or inverse timescale $\tau_{\theta\theta}^{-1}$) over which the pitch angle (as opposed to its cosine) of CRs whose resonant wavenumber is k_{res} changes by order one is given by the intuitive formula

$$\nu_{\theta\theta}(k_{\text{res}}) \sim \Omega \left(\frac{\delta B}{B_0} \right)^2 (k_{\text{res}}). \quad (32)$$

We will not need precise numerical factors, also because this simplified approach cannot account for quantitative subtleties of the CR propagation problem.

For a relatively broad distribution of magnetic field fluctuation power, we can thus expect CRs to lose complete memory of their initial velocity with respect to the regular magnetic field over a few gyroperiods, which is a very short timescale if compared to astrophysical times, see Eq. (23). It can also be readily checked that this timescale is significantly shorter than the collisional timescale for a typical interstellar plasma with order of magnitude number density of $\mathcal{O}(1) \text{ cm}^{-3}$. Despite the simplifications and unavoidable limitations of our treatment above, it correctly captures two features of the CR propagation phenomenon in an astrophysical medium such as the Galactic ISM:

- The CR movement is essentially a diffusive process.
- It is a *collisionless* (rather than a collisional) diffusion. Namely, CR do not scatter on other particles, but on inhomogeneities of the magnetic field.

A few words on the properties of the magnetic field fluctuations, which in general one can write in terms of Fourier transform,

$$\delta B_j(\mathbf{x}, t) = \int_{-\infty}^{\infty} d^3k \delta \tilde{B}_j(\mathbf{k}, t) e^{-i\mathbf{k}\cdot\mathbf{x}}$$

with the real condition for the B -field requiring

$$\delta \tilde{B}_j^*(\mathbf{k}) = \delta \tilde{B}_j(-\mathbf{k})$$

Under the assumption of homogeneity and stationarity, the two point function

$$\xi_{ij} = \langle \delta B_i(\mathbf{x}, t) \delta B_j(\mathbf{x}', t) \rangle$$

only depends on position difference or time differences, i.e. $\xi_{ij} = \xi_{ij}(|\mathbf{x} - \mathbf{x}'|, t - t')$ thus implying

$$\langle \delta \tilde{B}_i(\mathbf{k}, t) \delta \tilde{B}_j^*(\mathbf{k}', t') \rangle = \delta^{(3)}(\mathbf{k} - \mathbf{k}') \tilde{\xi}_{ij}(\mathbf{k}, t - t'),$$

where

$$\tilde{\xi}_{ij}(\mathbf{k}, t - t') = (2\pi)^{-3} \int_{-\infty}^{\infty} d^3r \xi_{ij}(\mathbf{a}, t - t') e^{i\mathbf{k}\cdot\mathbf{a}}.$$

Note that in the magnetostatic approximation, the above quantities are time-independent.

In the rather idealised case of 3D *isotropic* turbulence, the magnetostatic correlation tensor *in absence of helicity* takes the form

$$\tilde{\xi}_{ij}^{\text{iso}}(\mathbf{k}) = g(k) \left(\delta_{ij} - \frac{k_i k_j}{k^2} \right)$$

with $g(k)$ related to the energy density in the fluctuations (and the spectral density $\mathcal{E}(k)$) by the relations

$$\frac{\delta B^2}{8\pi} \equiv \frac{\langle \delta \mathbf{B}(\mathbf{x}) \rangle}{8\pi} = \int dk k^2 g(k) \equiv \int dk \mathcal{E}(k). \quad (33)$$

All indications are for a typical magnetic turbulence which is not isotropic (not surprisingly, since the background magnetic field singles out a preferred direction), so that more complex modeling involves e.g. some slab turbulence (i.e. no turbulence along z , turbulence along $x-y$ only dependent on z). What is more generic is that the spectral density $\mathcal{E}(k)$ has a power-law dependence ($g(k) \propto k^{-q}$, or $\mathcal{E} \propto k^{-\alpha}$, with $\alpha = q - 2$) in the so-called *inertial regime* between some outer scale (low k) characteristic of injection and some lower scale (large k) where dissipative phenomena kick-in. Turbulence (magnetic turbulence even more) is not a closed field of research. It was defined by Feynman as *the most important unsolved problem of classical physics*. We cannot do justice to this topic, but you should be at least aware of some nomenclature and facts: For a turbulence associated to $\mathcal{E} \propto k^{-\alpha}$, we have $\delta B^2 \propto k^{1-\alpha}$ and $D_{\mu\mu} \propto \Omega^{2-\alpha} \propto \mathcal{R}^{\alpha-2}$: The simplest model of turbulence (inspired by hydrodynamical considerations!) due to Kolmogorov is associated to $\alpha = 5/3$ and is thus associated to a rigidity-dependence of the pitch-angle diffusion coefficient $D_{\mu\mu} \propto \mathcal{R}^{-1/3}$. Another model of turbulence, due to Kraichnan, has $\alpha = 3/2$ and thus predicts $D_{\mu\mu} \propto \mathcal{R}^{-1/2}$.

IV. CR PROPAGATION IN PHASE SPACE

The key quantity in terms of which we want to describe CR theoretically is the (single-particle) phase space density, $f = f(t, \mathbf{x}, \mathbf{p})$, defined so that the number dN_α of particles of species α at time t in a given phase-space volume element $d\Pi \equiv d^3\mathbf{x}d^3\mathbf{p}$ is

$$f_\alpha = \frac{dN_\alpha}{d\Pi}. \quad (34)$$

Note that f is a relativistic invariant, since both the number of particles and the phase-space element (but not $d^3\mathbf{x}$ and $d^3\mathbf{p}$ separately!) are relativistic invariants (see e.g. [24]). Which equation does f obey to? It is sometimes said that f obeys the “Liouville equation” (or its relativistic generalisation),

$$\left[\frac{\partial}{\partial t} + \dot{\mathbf{x}} \cdot \nabla_{\mathbf{x}} + \dot{\mathbf{p}} \cdot \nabla_{\mathbf{p}} \right] f = 0, \quad (35)$$

but this is: a) A misnomer, in the sense that it is not the Liouville equation as typically defined in analytical mechanics, although it has a similar structure; b) strictly speaking false, in the sense that Eq. (35) is only true when we can neglect two-body (or more in general 3-body, ... N-body) interactions, such as (possibly short-range) collisions or more in general microscopic processes of the kind you have learned to describe in particle and nuclear physics (e.g. decays, pair-productions, ...).

A form of eq. (35) is used in fact to describe *collisionless* aspects of CR acceleration and transport, but must be supplemented by a non-vanishing right-hand-side (RHS), often denoted as $\mathcal{C}[f_\alpha]$ and dubbed Boltzmann or collisional operator, in order to account for *collisional* aspects important to describe particle generation/absorption, secondary particle production, etc. We will first concentrate on the collisionless transport, before returning to the collisional aspects in Parts IV and V of the lectures. If you are curious on how Eq. (35) follows from first principles, have a look at Appendix B. The species index α will only be made explicit when ambiguity can arise.

Since CRs are empirically close to isotropic (and we will justify why), it makes sense to introduce appropriate angular averages. It is useful to re-write the element of momentum phase space in spherical coordinates

$$d^3\mathbf{p} = p^2 dp d\Omega \quad (36)$$

and define

$$\phi(t, \mathbf{x}, p) \equiv \frac{1}{4\pi} \int d\Omega f(t, \mathbf{x}, \mathbf{p}) \quad (37)$$

and

$$\Phi(t, \mathbf{x}, p) \equiv \frac{1}{4\pi} \int d\Omega \hat{\mathbf{p}} f(t, \mathbf{x}, \mathbf{p}), \quad (38)$$

where $\hat{\mathbf{p}} \equiv \mathbf{p}/p$. If we also decompose the space volume element in the length element parallel to the direction of motion (or any other reference axis) and the surface element orthogonal to it:

$$d^3\mathbf{x} = \beta dt dA_\perp, \quad (39)$$

starting from f , one can define some quantities closer to observational ones:

- *The spectral intensity*

$$F(t, \mathbf{x}, E, \Omega) = \frac{dN}{dt dA_\perp dE d\Omega} = \frac{f d^3\mathbf{x} d^3\mathbf{p}}{dt dA_\perp dE d\Omega} = \beta p^2 \frac{dp}{dE} f = p^2 f \quad (40)$$

where we used $dp/dE = E/p = 1/\beta$ with p^2 and f expressed in terms of the new variables of interest.

- *The spectral density*

$$n(t, \mathbf{x}, E) = \frac{1}{\beta} \int d\Omega F = \frac{4\pi p^2}{\beta} \phi \quad (41)$$

with p^2 and f expressed in terms of the new variables of interest, notably E instead of p .

A. Diffusion in the phase space description

Let us assume CRs of charge q propagating in an externally assigned, static magnetic field \mathbf{B} , however complicated; we also assume vanishing macroscopic electric field. The CRs obey hamiltonian dynamics, and their phase space distribution f obeys Eq. (35), which we specify into (note that we use the relativistic version of the Lorentz force!)

$$\frac{df}{dt} = \frac{\partial f}{\partial t} + \mathbf{v} \cdot \nabla_{\mathbf{x}} f + q \frac{(\mathbf{p} \times \mathbf{B})}{E} \cdot \nabla_{\mathbf{p}} f = 0. \quad (42)$$

The truth is that we have no precise idea of what the field configuration $\mathbf{B}(\mathbf{x})$ is. At best, we have some idea of the ‘‘coarse grained’’ or (ensemble) average field configuration $\langle \mathbf{B} \rangle$, often taken as a constant (along the z direction, implicitly in the following), so that the field can be decomposed into $\mathbf{B} = \langle \mathbf{B} \rangle + \delta \mathbf{B}$, with the $\delta \mathbf{B}$ only known (or simply parameterised) in a statistical sense. If we ensemble-average Eq. (42), we get:

$$\frac{d\langle f \rangle}{dt} = \frac{\partial \langle f \rangle}{\partial t} + \mathbf{v} \cdot \nabla_{\mathbf{x}} \langle f \rangle + q \frac{(\mathbf{p} \times \langle \mathbf{B} \rangle)}{E} \cdot \nabla_{\mathbf{p}} \langle f \rangle = -q \left\langle \frac{(\mathbf{p} \times \delta \mathbf{B})}{E} \cdot \nabla_{\mathbf{p}} \delta f \right\rangle \neq 0, \quad (43)$$

i.e. the ensemble-averaged phase space density is not conserved! This is not particularly surprising, in the sense that the ensemble-average is associated to a loss of information (and ultimately to an entropy increase). Also note that, formally, the RHS of Eq. (43) looks like a collisional operator for $\langle f \rangle$. Indeed, the simplest description of this term relies on assuming [25, 26]

$$-q \left\langle \frac{(\mathbf{p} \times \delta \mathbf{B})}{E} \cdot \nabla_{\mathbf{p}} \delta f \right\rangle \simeq -\nu_{\theta\theta} (\langle f \rangle - \phi), \quad (44)$$

which is a form of the *BGK Ansatz* [27], amounting to say that the fluctuations in the field are responsible for isotropisation of $\langle f \rangle$ (i.e. it tends to ϕ) with a characteristic frequency $\nu_{\theta\theta}$. In general, we expect that $\langle f \rangle$ is dominated but not fully described by its isotropic part; a better approximation consists in adding a dipolar term, i.e. to write $\langle f \rangle \simeq \langle \phi \rangle + 3\hat{\mathbf{p}} \cdot \langle \Phi \rangle$, with ensemble averages defined analogously to Eqs (37, 38). It is also useful to define the current $\mathbf{j} = \beta \langle \Phi \rangle$. Keeping in mind that $\mathbf{v} = \beta \hat{\mathbf{p}}$, the transport equation with the approximation of Eq. (44) reduces then to

$$\partial_t \langle \phi \rangle + \beta \nabla_{\mathbf{x}} \cdot \langle \Phi \rangle = 0, \iff \partial_t \langle \phi \rangle + \nabla_{\mathbf{x}} \cdot \mathbf{j} = 0 \quad (45)$$

$$\partial_t \langle \Phi \rangle + \frac{\beta}{3} \nabla_{\mathbf{x}} \langle \phi \rangle + \mathbf{\Omega} \times \langle \Phi \rangle \simeq -\nu_{\theta\theta} \langle \Phi \rangle \iff \partial_t \mathbf{j} + \frac{\beta^2}{3} \nabla_{\mathbf{x}} \langle \phi \rangle + \mathbf{\Omega} \times \mathbf{j} \simeq -\nu_{\theta\theta} \mathbf{j}. \quad (46)$$

where we introduced $\mathbf{\Omega} \equiv q \langle \mathbf{B} \rangle / E$. As long as the relaxation time $\nu_{\theta\theta}^{-1}$ is much shorter than the astrophysical flux evolution time, in the second equation we can neglect $\partial_t \mathbf{j}$ with respect to the other terms, and the equation reduces to $j_i \simeq -K_{ij} \partial_j \phi$ (*Fick's law*), yielding a diffusion equation for $\langle \phi \rangle$

$$\frac{\partial \langle \phi \rangle}{\partial t} = \frac{\partial}{\partial x_i} \left(K_{ij} \frac{\partial \langle \phi \rangle}{\partial x_j} \right), \quad (47)$$

where the *spatial* diffusion tensor is

$$K_{ij} = \frac{\beta^2}{3\nu_{\theta\theta}} \frac{\nu_{\theta\theta}^2 \delta_{ij} + \nu_{\theta\theta} \Omega_k \epsilon_{ijk} + \Omega_i \Omega_j}{\nu_{\theta\theta}^2 + \Omega^2}, \quad (48)$$

with eigenvalues $\beta^2/3\nu_{\theta\theta}$ and $\beta^2/3(\nu_{\theta\theta} \pm i\Omega)$ corresponding to diffusion parallel and perpendicular to the magnetic field, respectively. Note that *the spatial diffusion coefficient is inversely proportional to the pitch angle scattering diffusion coefficient*, which is physically reasonable since the easier it is to change momentum direction, the harder it is to propagate away from the original direction in physical space. Also, since in the limit of weak turbulence one has $\nu_{\theta\theta} \ll |\Omega|$, this result confirms that the predominant diffusion is parallel to the background field.

B. Alternative approach: Quasi-linear theory (QLT)

Let us subtract Eq. (43) from Eq. (42). We get

$$\frac{d\delta f}{dt} = \frac{\partial \delta f}{\partial t} + \mathbf{v} \cdot \nabla_{\mathbf{x}} \delta f + (\mathbf{p} \times \mathbf{\Omega}) \cdot \nabla_{\mathbf{p}} \delta f \simeq -q \frac{(\mathbf{p} \times \delta \mathbf{B})}{E} \cdot \nabla_{\mathbf{p}} \langle f \rangle, \quad (49)$$

where we assumed (ok since difference is higher order in perturbation theory!)

$$q \frac{(\mathbf{p} \times \delta \mathbf{B})}{E} \cdot \nabla_{\mathbf{p}} \delta f \simeq q \left\langle \frac{(\mathbf{p} \times \delta \mathbf{B})}{E} \cdot \nabla_{\mathbf{p}} \delta f \right\rangle. \quad (50)$$

Eq. (49), being a first order PDE for δf , can be integrated with the *method of characteristics*, the formal solution being:

$$\delta f = \delta f(t_0, \mathbf{x}, \mathbf{p}) - q \int_{t_0}^t dt' \frac{(\mathbf{p} \times \delta \mathbf{B})}{E} \cdot \nabla_{\mathbf{p}} \langle f \rangle \Big|_{\text{char}(t')}, \quad (51)$$

where the integrand has to be evaluated along characteristic curves of eq. (49), which are the solutions of the EOM with \mathbf{B} replaced by the regular field $\langle \mathbf{B} \rangle$: In practice, along helices along the axis z , in our convention. If we insert Eq. (51) into Eq. (43), we get

$$\frac{d\langle f \rangle}{dt} \simeq \int_{t_0}^t dt' \left\langle q^2 \frac{(\mathbf{p} \times \delta \mathbf{B})}{E} \cdot \nabla_{\mathbf{p}} \left(\frac{(\mathbf{p} \times \delta \mathbf{B})}{E} \cdot \nabla_{\mathbf{p}} \langle f \rangle \right) \right\rangle_{\text{char}(t')}, \quad (52)$$

where we dropped the term $\propto \delta f_0$ (we expect that this averages to zero over the ensemble, assuming the fluctuations are uncorrelated with them). We see that the RHS looks like a diffusion term (pay attention to the two momentum derivatives) and that it depends on a quadratic ensemble average of turbulent magnetic field, integrated along the unperturbed trajectory. It can actually be shown that under some additional hypotheses, namely

- Smallness of perturbations, $|\delta \mathbf{B}| \ll |\langle \mathbf{B} \rangle|$;
- Gyrotropy: $\langle f \rangle$ does not depend on the azimuthal angle around the guiding center, so that $\langle f \rangle = \langle f \rangle(t, \mathbf{x}, p, \mu)$, with μ the cosine of the pitch angle (i.e. $\langle f \rangle$ is intended as gyrophase-averaged, so to speak);
- Adiabaticity: $\langle f \rangle$ only varies on time-scales much larger than the correlation time of the turbulent magnetic field, τ_c , i.e. $\langle f \rangle / \partial_t \langle f \rangle \gg \tau_c$;
- Finite correlation times: the turbulent magnetic field remain correlated over timescales much larger than the Larmor period, i.e. $\tau_c \gg \Omega^{-1}$;
- Homogeneous and stationary turbulence;

then Eq. (52) reduces to the Fokker-Planck form:

$$\frac{\partial \langle f \rangle}{\partial t} + v \mu \frac{\partial \langle f \rangle}{\partial z} = \frac{\partial}{\partial \mu} \left(D_{\mu\mu} \frac{\partial \langle f \rangle}{\partial \mu} \right), \quad (53)$$

describing diffusion in pitch-angle; due to the magnetostatic approximation $D_{\mu p} = D_{p\mu} = D_{pp} = 0$. Loosely speaking, in the simplest situation described we expect $D_{\mu\mu}$ to be given by eq. (31) above, i.e. it is proportional to the dimensionless power-spectrum of magnetic inhomogeneities. In practice, diffusion coefficients (a form of transport coefficients) are computed e.g. numerically in a given turbulence realisation via the Taylor-Green-Kubo relation, like

$$D_{\mu\mu} = \int_0^\infty dt \langle \dot{\mu}(0) \dot{\mu}(t) \rangle. \quad (54)$$

By defining the zeroth and first moment of $\langle f \rangle$ with respect to the pitch angle,

$$f_0(t, z) = \frac{1}{2} \int_{-1}^{+1} d\mu \langle f \rangle, \quad (55)$$

$$f_1(t, z) = \frac{v}{2} \int_{-1}^{+1} d\mu \mu \langle f \rangle, \quad (56)$$

and the quantities

$$K_0 \equiv \frac{v}{4} \int_{-1}^{+1} d\mu \frac{1 - \mu^2}{D_{\mu\mu}} (1 + \mu), \quad K \equiv \frac{v^2}{8} \int_{-1}^{+1} d\mu \frac{(1 - \mu^2)^2}{D_{\mu\mu}}, \quad (57)$$

one can prove that

$$\frac{\partial f_0}{\partial t} \simeq \frac{\partial}{\partial z} \left[K \frac{\partial f_0}{\partial z} \right], \quad (58)$$

confirming that the spatial (actually, parallel) diffusion coefficient $K \propto D_{\mu\mu}^{-1}$, in addition to

$$\frac{f_1}{f_0} \sim -\frac{K}{f_0} \nabla f_0 \sim \mathcal{O} \left(\frac{K}{cH} \right) \ll 1 \quad (59)$$

which is always smaller than 1 as long one the diffusive approximation is fulfilled (see exercise below). This ratio can be used as an estimator of the anisotropy level expected in the CR flux, in terms of the diffusive halo thickness H ; this is why we reinstated c in the last step.

Exercise (more advanced, suggested for when you have time): Try to prove Eq.s (58),(59), via appropriate manipulations of the Fokker-Planck equation. A good reference to help you through is Sec. 4.2 in [7].

Finally, it is worth noting that the QLT approach can be extended to tackle higher-order correlators of phase-space densities, such as $\langle f_A f_B \rangle$. This has been successfully used to gain insight into the anisotropy pattern of CRs, see [28]. Also, it is tacitly assumed that in comparing theoretical ensemble expectations on $\langle f \rangle$ with data (providing us the local value of f) is meaningful, in the sense that the difference between the two is anyway smaller than experimental errors. However, in recent years several works have revised this approach, trying to assess this difference quantitatively, often with monte carlo techniques. This applies to magnetic field realisations, but also to other aspects only known probabilistically at best, such as the distribution of sources, spectra, etc. For some examples, see [29–31].

C. Solving the diffusion problem

Eq. (47), supplemented by a source term Q at the RHS, is the paradigmatic case of a *diffusion equation*. In our case, diffusion is expected to be strongly anisotropic as long as $\delta B \ll B_0$. However this expectation holds over the scales where the large-scale field B_0 does not change. If this happens over scales much smaller than the distance from the sources (say, of $\mathcal{O}(100)$ pc vs. several kpc) the diffusive propagation is often modelled as an *effective isotropic diffusion coefficient*, $K_{ij} \rightarrow K \delta_{ij}$. A good fit to actual data yields is obtained for $K = 0.3(\mathcal{R}/10\text{GV})^{0.5} \text{kpc}^2/\text{Myr}$ [32]. We will not indulge in techniques to solve similar equations, which deserve a course of its own. Let us simply recall here that, if K is homogeneous and stationary, only dependent upon energy,

$$\frac{\partial \phi}{\partial t} - K \nabla^2 \phi = Q(p, t, \mathbf{x}), \quad (60)$$

can be solved with the Green's function technique, i.e. if we know $G_p(t, t', \mathbf{x}, \mathbf{x}')$ such that

$$\frac{\partial G_p}{\partial t} - K(p) \nabla^2 G_p = \delta(\mathbf{x} - \mathbf{x}') \delta(t - t'), \quad (61)$$

and satisfying appropriate boundary conditions, then

$$\phi(p, t, \mathbf{x}) = \int d^3 x' dt' G_p(t, t', \mathbf{x}, \mathbf{x}') Q(p, t', \mathbf{x}'). \quad (62)$$

In the simplest case of *free escape boundary* (i.e. vanishing at infinity), we can take the Fourier transform of Eq. (61) and obtain

$$G_p = \int \frac{d^n \mathbf{k} d\omega}{(2\pi)^4} \frac{\exp[i\mathbf{k} \cdot (\mathbf{x} - \mathbf{x}') - i\omega(t - t')]}{K(p)k^2 - i\omega} = \frac{1}{(4\pi K(t - t'))^{n/2}} \exp \left[-\frac{(\mathbf{x} - \mathbf{x}')^2}{4K(t - t')} \right] \Theta(t - t'), \quad (63)$$

n being the spatial dimensionality, and the latter step follows from taking the residue in the ω integral. Hence, we see that the mean square displacement from the initial position is $\langle r^2 \rangle \equiv \langle \sum_i^n (x_i - x'_i)^2 \rangle = 2nKt$. For actual problems obeying e.g. different geometric boundary conditions, a generalization of the above procedure applies (see e.g. [2]).

Exercise A CR source is at a distance d . For $d \simeq H \simeq 3\text{kpc}$ (a typical Galactic distance), assuming the value of the average Galactic diffusion coefficient is $K = 0.3(\mathcal{R}/10\text{GV})^{0.5} \text{kpc}^2/\text{Myr}$, a) compute the time it takes for the CR of rigidity

10 GV to reach us; compare it with the estimated age of a few famous supernova remnants that you can search on the web: Are you surprised? b) Reverse the previous exercise: For a few SNRs that you found by browsing some catalogue online, take their distance and age, and estimate the minimum energy of CRs that could have reached us. c) The rigidity at which the diffusion approximation breaks down, since the diffusion speed nominally exceeds the speed of light.

Suggestion to go beyond: You can easily convince yourself that the previous diffusion equation leads to superluminal propagation at sufficiently small timescales (compute $d\sqrt{\langle r^2 \rangle}/dt$, you'll find superluminal motion for $t < t_c$: Determine t_c in terms of K). This has to do with the approximation of dropping the term $\partial_t \mathbf{j}$ in Eq.(46): It takes some time for the distribution to relax to its isotropic average, a timescale controlled by $\nu_{\theta\theta}$, as we know. This problem can be amended by replacing

$$\frac{\partial \phi}{\partial t} \rightarrow \frac{\partial \phi}{\partial t} + \frac{1}{\nu_{\theta\theta}} \frac{\partial^2 \phi}{\partial t^2}. \quad (64)$$

The corresponding transport equation is known as *telegrapher's equation*, due to its similarity with the differential equation describing the propagation of electromagnetic waves in electrical transmission lines with losses due to finite resistivity. Some articles on the subject are refs. [33, 34].

D. Basics of Galactic propagation

In general, the spatial and temporal scales associated to the acceleration of CRs are much smaller than the propagation scales from the sources to us. As such, one typically factorises the problem of CRs into: 1. Acceleration. 2. Galactic propagation. 3. Propagation within the Solar system. We shall omit dealing with 3. in these lectures; it suffices to say that not only the Sun has a magnetic field, but this is dynamical, with a magnetized wind propagating outwards from the Sun, and whose pattern is subject to a quasi-periodic cycle of 11 yrs. Under some simplifying assumption, its main effect (within the so-called *Force-field* approximation, introduced by Gleeson & Axford in 1968 [35]) is to slow-down the CRs, corresponding to a momentum shift of the momentum at the Earth, p_{\oplus} , with respect to the momentum outside the Solar System, p , $p_{\oplus} = p - Ze\Phi_{\odot}$. $e\Phi_{\odot} \lesssim 1$ GeV is computable based on the radial velocity of the solar wind, and of the diffusion coefficients within the Solar System. It is often estimated via proxies (search for "neutron monitors"). The flux at the top of the atmosphere (TOA)—now expressed as spectral intensity, $F_{\text{TOA}}(E)$, is suppressed with respect to the interstellar intensity $F_{\text{IS}}(E)$ by

$$F_{\text{TOA}}(E) = \frac{E^2 - m^2}{(E + |Z|e\Phi)^2 - m^2} F_{\text{IS}}(E + |Z|e\Phi), \quad (65)$$

where (Ze) is the charge and m the mass of the CR species.

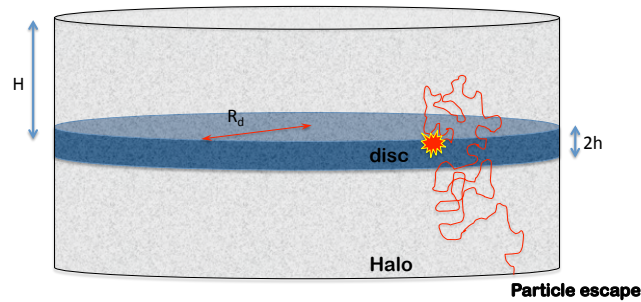


FIG. 10: Propagation setup. The thin disk of sources and interstellar gas of half-thickness h is contained within a cylindrical cosmic ray halo of half-height H and radius R_d (with a hierarchy of scales $R_d > H \gg h$) within which cosmic rays diffuse.

Concerning Galactic CR propagation, it is often considered to be limited to a cylindrical volume of radius R_d and half-height H , where the Galactic thin disk of matter of half-thickness h is contained in, see Fig. 10. Given the rough hierarchy $h : H : R_d \sim 0.1 : 5 : 20$ between the three scales, the gaseous disk of the Galaxy containing the most plausible sources is often considered infinitesimal, and sometimes a further simplification to an effective 1-D models, allowing one to obtain quite transparent analytical solutions. In the 1D case, the Galaxy is considered as a (radially) "infinite" gas thin disk of uniform surface density, sandwiched in a thicker diffusive halo, only the vertical coordinate is relevant. This allows one to

write (omitting $\langle \rangle$ in what follows):

$$\frac{\partial \varphi}{\partial t} - \frac{\partial}{\partial z} \left(K \frac{\partial \varphi}{\partial z} \right) = Q. \quad (66)$$

Exercise: “Leaky box” from slab model

Let us assume that sources are confined to an infinitesimal disk. The steady state transport equation simplifies into

$$-\frac{\partial}{\partial z} \left(K \frac{\partial \phi}{\partial z} \right) = 2 q_0(p) h \delta(z). \quad (67)$$

Find the CR flux $\phi(z, p)$. Compare it with the solution of a “leaky box” type of model, where injection at rate Q happens in a homogeneous and isotropic medium from which cosmic rays take a (momentum dependent) time $\tau_{\text{esc}}(p)$ to escape, leading to the steady state solution $\phi(p) = Q(p) \tau_{\text{esc}}(p)$.

Part III

Cosmic ray acceleration

V. TOWARDS A THEORY OF COSMIC RAY ACCELERATION

A. Moving scattering centers

A major limitation of the previous derivations is that the magnetic field fluctuations are considered static in the Lab (Galactic) frame. You know that a gas supports longitudinal “sound” waves (with frequencies well below the gas collisional frequency) which, in the ideal gas limit, are dissipationless. Continuity eq. (mass conservation) Euler eq. (momentum eq.) and the equation of state (EOS) which write respectively as:

$$\frac{\partial \rho}{\partial t} + \nabla \cdot (\rho \mathbf{v}) = 0, \quad (68)$$

$$\left(\frac{\partial}{\partial t} + \mathbf{v} \cdot \nabla \right) \mathbf{v} = -\frac{\nabla P}{\rho}, \quad (69)$$

$$P = P(\rho, \dots), \quad (70)$$

admit a simple a homogeneous and isotropic solution $\bar{\rho} = \text{const.}$, $\bar{P} = 0$, $\bar{\mathbf{v}} = 0$, for instance. If we perturb it to $\rho(t, \mathbf{x}) = \bar{\rho}(t) + \delta\rho(t, \mathbf{x})$, $P(t, \mathbf{x}) = \delta P$, $\mathbf{v} = \delta\mathbf{v}$, one can derive e.g. in terms of $\delta\rho$ the well-known wave equation

$$\left(\frac{\partial^2}{\partial t^2} - c_s^2 \nabla^2 \right) \delta\rho = 0, \quad (71)$$

where the speed of sound c_s depends on the EOS via $c_s^2 \equiv \delta P / \delta\rho$. Its solution is oscillatory with constant amplitude, i.e. in Fourier space one has

$$\delta\rho(t, \mathbf{x}) = \int \frac{d^3\mathbf{k}}{(2\pi)^{3/2}} \delta\tilde{\rho}_{\mathbf{k}}(t) e^{i\mathbf{k}\cdot\mathbf{x}}, \quad (72)$$

where

$$\delta\tilde{\rho}_{\mathbf{k}} = A_{\mathbf{k}} e^{i\omega_{\mathbf{k}} t} + B_{\mathbf{k}} e^{-i\omega_{\mathbf{k}} t}, \quad (73)$$

with dispersion relation

$$\omega_{\mathbf{k}}^2 = c_s^2 k^2. \quad (74)$$

Similarly, the ISM—as any other magnetized plasma—can support a number of collective excitation modes, with frequencies well below the cyclotron ones. To see this, the simplest way is to write the *ideal* MHD equations (i.e. we use

Maxwell equations in a condition of infinite conductivity and vanishing dissipation)

$$\frac{\partial \rho}{\partial t} + \nabla \cdot (\rho \mathbf{v}) = 0, \quad (75)$$

$$\rho \left(\frac{\partial}{\partial t} + \mathbf{v} \cdot \nabla \right) \mathbf{v} = -\nabla P - \frac{\mathbf{B} \times (\nabla \times \mathbf{B})}{4\pi}, \quad (76)$$

$$P = P(\rho, \dots). \quad (77)$$

$$\frac{\partial \mathbf{B}}{\partial t} = \nabla \times (\mathbf{V} \times \mathbf{B}) \quad (78)$$

(with $\nabla \cdot \mathbf{B} = 0$, of course), obtained adding the electromagnetic force term $\mathbf{j} \times \mathbf{B}$ at the RHS of the Euler equation. If, as before, we search perturbed solutions around the homogeneous case in a cold medium (but this time, not isotropic due to a background field!) $\bar{\rho} = const.$, $\bar{P} = 0$, $\bar{\mathbf{v}} = 0$, $\mathbf{B} = \mathbf{B}_0$, one can reduce oneself to a second-order differential equation for $\delta \mathbf{v}$. By Fourier-transforming it, we obtain a system of equations equivalent to the matrix form $A(\omega, \mathbf{k}) \cdot \delta \mathbf{v}_{\mathbf{k}} = 0$, with A a 3x3 matrix. It admits non-trivial solutions when the determinant of A vanishes, which determines the dispersion relations for the different modes, generalising Eq. (74). The most peculiar of the three types of waves found are the *Alfvén waves*, which are transversal waves (with the ion motion as well as the magnetic field perturbation perpendicular to the velocity) propagating along the magnetic field direction³, and the restoring force is provided purely by magnetic tension, with field lines behaving just like plucked strings. Their characteristics speed is

$$\mathbf{v}_A = \frac{\mathbf{B}_0}{\sqrt{4\pi\rho}}, v_A \simeq 2.2 \frac{\text{km}}{\text{s}} \frac{B_0}{\mu\text{G}} \sqrt{\frac{1 \text{ cm}^{-3}}{\bar{n}}}. \quad (79)$$

In the ideal MHD limit, they are dissipationless. Physically, their long-lived nature is also understandable since—unlike sound waves—they are not associated to a gas compression, which cannot thus radiate, channelling away its energy. The other modes in the above example would be magnetosonic modes, compressional waves subject to both pressure and magnetic tension (fast or slow according if the two forces act together or in opposition), more similar to sound waves. In general, many types of modes can be excited in the medium, whose properties (such as dispersion relation, propagating nature, etc.) depend on the properties of the medium like temperature, composition, etc. The crucial information to retain, however, is that perturbations to the magnetostatic picture we used before are *dynamical*, i.e. they propagate with finite speed in the Lab (Galaxy) frame. This can happen in an incoherent way or also along organised, coherent fronts such as along a shock front. This modifies the transport equation previously derived, and has also some qualitatively new consequences that we will explore in the following.

B. The CR transport equation: moving scattering centers

(This is a sketch; for more, you may want to look at specialised literature, such as [6, 7] and some monographs like [2–4].) Let us consider the case where scattering centers move with some velocity (in general space-dependent) \mathbf{u} . For now, take this velocity as coherent, e.g. of the velocity of a SNR shock front. The goal is, starting from our Vlasov equation (42), to write an equation for the distribution function of the same space and time variable as before (this dependence will thus be omitted in the arguments), but of momentum variable $\bar{\mathbf{p}} = \mathbf{p} - E \mathbf{u}(\mathbf{x})$, i.e. momentum measured in the plasma frame (or scatterers' frame; in the example above, the shock frame). Correspondingly, $\bar{\mathbf{v}} = \mathbf{v} - \mathbf{u}$. Our function of interest, \bar{f} , is

$$\bar{f}(t, \mathbf{x}, \bar{\mathbf{p}}) = f(t, \mathbf{x}, \bar{\mathbf{p}} + E\mathbf{u}). \quad (80)$$

Let us assume for now that $\frac{d\bar{\mathbf{p}}}{dt} \cdot \nabla_{\bar{\mathbf{p}}} = \frac{d\mathbf{p}}{dt} \cdot \nabla_{\mathbf{p}}$, i.e. that the force term is the same as in the original case. This not exact (although it would be so in the limit of constant energy and non-relativistic relative motion, i.e. $|\mathbf{u}| \ll 1$) for a series of reasons, but we will discuss below the main correction to our conclusions that would follow from this term. Given that, Eq. (42) rewrites in terms of \bar{f} as

$$\frac{\partial \bar{f}}{\partial t} + (\bar{\mathbf{v}} + \mathbf{u}) \cdot \nabla_{\mathbf{x}} \bar{f} + (\bar{\mathbf{v}} + \mathbf{u})_i \frac{\partial \bar{f}}{\partial \bar{p}_j} \frac{\partial \bar{p}_j}{\partial x_i} + \frac{d\bar{\mathbf{p}}}{dt} \cdot \nabla_{\bar{\mathbf{p}}} \bar{f} = 0 \quad (81)$$

³ The perturbation considered in previous sections had this property!

from where, considering that $\partial \bar{p}_j / \partial x_i = -E \partial u_j / \partial x_i$, and neglecting terms of order u^2 (so that $\partial f / \partial \bar{p}_j = \partial \bar{f} / \partial \bar{p}_j$)

$$\frac{\partial \bar{f}}{\partial t} + (\bar{\mathbf{v}} + \mathbf{u}) \cdot \nabla_{\mathbf{x}} \bar{f} - \bar{p}_i \frac{\partial u_j}{\partial x_i} \frac{\partial \bar{f}}{\partial \bar{p}_j} + \frac{d\bar{\mathbf{p}}}{dt} \cdot \nabla_{\bar{\mathbf{p}}} \bar{f} = 0. \quad (82)$$

From now on, one can proceed as in the static scattering centers case, writing a monopole plus dipole approximation, and taking an ensemble average,

$$\langle \bar{f} \rangle \simeq \langle \bar{\phi} \rangle + 3 \langle \bar{\Phi} \rangle \cdot \hat{\mathbf{p}}. \quad (83)$$

As a result, one gets a system of two equations by integrating Eq. (82) (with the replacement Eq.(83)) over $\Omega_{\bar{\mathbf{p}}}$ and the product of Eq. (82) (with the replacement Eq.(83)) with \bar{p}_i over $\Omega_{\bar{\mathbf{p}}}$; then, by the same approximation done previously

$$\frac{\partial \langle \bar{\phi} \rangle}{\partial t} - \frac{\partial}{\partial x_i} \left(K_{ij} \frac{\partial \langle \bar{\phi} \rangle}{\partial x_j} \right) + u_i \frac{\partial \langle \bar{\phi} \rangle}{\partial x_i} - \frac{1}{3} \frac{\partial u_i}{\partial x_i} \left(\bar{p} \frac{\partial \langle \bar{\phi} \rangle}{\partial \bar{p}} \right) = 0, \quad (84)$$

where we defined the spatial diffusion coefficient as in Eq. (48). From now on, let us drop the bar over the quantities, to avoid a too cumbersome notation. But don't forget that the functions of interest have their momenta measured with respect to the scattering centers!

This is not the end of the story, however (remember that we have neglected modifications to the force term, in particular!): If the movement of the scattering centers is not coherent (e.g. a distribution of waves with different directions) there is a residual velocity (rather, velocity distribution) of the waves even in the plasma frame. These *moving* magnetic perturbations are then associated to *electric* fields; for an ensemble of "stochastic" waves, we expect a *diffusion* term in momentum space. The more complete equation becomes

$$\boxed{\frac{\partial \langle \phi \rangle}{\partial t} - \frac{\partial}{\partial x_i} \left(K_{ij} \frac{\partial \langle \phi \rangle}{\partial x_j} \right) + u_i \frac{\partial \langle \phi \rangle}{\partial x_i} - \frac{1}{3} \frac{\partial u_i}{\partial x_i} \left(p \frac{\partial \langle \phi \rangle}{\partial p} \right) = \frac{1}{p^2} \frac{\partial}{\partial p} \left(p^2 K_{pp} \frac{\partial \langle \phi \rangle}{\partial p} \right)}, \quad (85)$$

where, schematically, one can show that

$$K_{pp} \simeq \frac{\nu_{\theta\theta} E^2 \langle \delta v^2 \rangle}{3}, \quad (86)$$

with $\langle \delta v^2 \rangle$ being the variance of the velocity distribution of the scattering centers.

Compared to the previously derived Eq. (47), we see three new terms, identified by color-code:

- **convection/advection:** It accounts for spatial transport due to large scale movements like Galactic winds. This term is usually considered mostly perpendicular to the Galactic plane and antisymmetric with respect to it, $u(-z) = -u(z)$. For typical values of $u = \mathcal{O}(10) \text{ km s}^{-1}$ it is relevant at $\mathcal{O}(1) \text{ GeV}$, but its relevance decreases at higher energies.
- **adiabatic energy losses/gains:** Diverging flows lead to adiabatic energy losses, while converging flows to energy gains. While this effect may be important in propagation models with non-uniform galactic winds, it is particularly crucial as a way to *accelerate particles* i.e. in our factorized production-propagation scenario, as a way to produce effectively a source term Q .
- **reacceleration:** If we adopt for the spatial diffusion coefficient its parallel value, we arrive at the estimate $K_{zz} K_{pp} = p^2 \langle \delta v^2 \rangle / 9$ where $\langle \delta v^2 \rangle$ is typically set to the square of the the Alfvén velocity v_A . Acceleration *in the ISM* via this term cannot be the main source of CR acceleration because e.g. of the observed energy dependence of secondary-to-primary ratios (see later). However this term is important in determining the momentum shape of CR fluxes below a few GeV, and this "turbulent" acceleration may also play an important role for acceleration at the sources. A modern treatment of the role of this term in the evolution of the CR distribution (essentially, a diffusive broadening of the energy spectrum) can be found in [36]. An alternative approach to the role of this term is given below, in Sec. VI 2.

In the 1-D case we discussed before, generalising Eq. (66) (but neglecting reacceleration) leads to:

$$\frac{\partial \varphi}{\partial t} - \frac{\partial}{\partial z} \left(K \frac{\partial \varphi}{\partial z} \right) + u \frac{\partial \varphi}{\partial z} - \frac{1}{3} \frac{du}{dz} p \frac{\partial \varphi}{\partial p} = Q. \quad (87)$$

To go beyond: Generalize the solution found to Eq. (66) for the stationary solution in the case $u = \pm \text{const.} \neq 0$ ($+|u|$ above and $-|u|$ below the plane, respectively). You should find a closed-form for the altered z -profile, and a first order differential equation replacing the algebraic Eq. (??) to determine $\phi_0(p)$. Compare the z profiles and the spectra at $z = 0$

for some values of u , keeping the diffusion time and H fixed. If you consider the simplified solution in the limit where $\zeta(p) \equiv uH/K \ll 1$, how does the profile look like? Also, plot the ratio ϕ_0/q (solution in the plane to source term) for a few values of u and the benchmark choice $K = 0.3(\mathcal{R}/10\text{GV})^{0.5}\text{kpc}^2/\text{Myr}$, $H = 4\text{ kpc}$, comparing with the same ratio for the solution found in Eq. (??): In which momentum range do these ratios differ?

Remember that the inhomogeneous first order differential equation:

$$y' + a(x)y = b(x). \quad (88)$$

admits the general solution

$$y(x) = e^{-A(x)} \left(\int_{x_0}^x e^{A(x')} b(x') dx' + y(x_0) \right), \quad (89)$$

where

$$A(x) = \int_{x_0}^x dx' a(x'). \quad (90)$$

VI. HOW TO ACCELERATE CRS?

How to accelerate particles in astrophysics? We need to satisfy several requirements:

- **Energetics:** we must take energy somewhere! For example:
 - Kinetic Energy (translational in SNRs, rotational in pulsars)
 - Gravitational Energy (accretion disks)
 - Magnetic (solar flares)
- **Mechanism for Energy Transfer:** in general, we need to envisage how to transfer energy from macroscopic objects into the (microscopic) acceleration of particles. Ultimately it must be electromagnetic.
- **Confinement:** need to check that the particle stays in the accelerator for the time needed to accelerate it.
- **Lack of (significant) E-losses:** accelerating particles is useless for explaining CRs if they lose Energy too quickly.

While we have several candidates to supply the needed energy, and in astrophysics there is no shortage of objects of large scale, surviving long enough, and with sufficiently rarefied media (first, third and fourth problem), the trickiest problem is the second one, first addressed by Fermi [37]. We start tackling it in the following, which is really introductory. More details can be found for instance in [5].

Almost all ⁴ acceleration mechanisms known are electromagnetic in Nature. Since magnetic field cannot make work on charged particles, one needs electric fields, either coherently on large (astrophysical) scales, or stochastically on small scales. Electric fields are typically not generated by separating charges, since being in a plasma, the unbalance would be quickly compensated/short-circuited. Electric fields are thus due to *moving magnetic fields*.

A coherent generation of electric fields can happen if a front of magnetic disturbances moves coherently in the plasma frame (as in the shock acceleration studied in the following). An alternative is provided by violent transients, like *magnetic reconnection*: Imagine a situation where the pressure of the magnetic field dominates the total pressure; when regions with opposite orientation of magnetic field encounter and merge along a surface (sheet), the decrease of the magnetic pressure due to the dissipation of the magnetic field drives the plasma toward the sheet (dubbed indeed “current sheet”), creating a local electric field $E \sim v_A B$ over the size L of the reconnection region. Of course, this reconnection involves the finite conductivity of the medium, so that perfect MHD conditions are broken. It is a mechanism known to be operational in the sun or in pulsar wind nebulae (PWN).

Another example is the fast rotating magnetic fields in pulsars, acting as a *unipolar rotators* and which are responsible for establishing an electric potential ΔV between the pole and the equator, but also between the surface and infinity. The naive estimate for a pulsar of size R and rotating at angular frequency ω is $\Delta V \sim \omega \Phi_B \simeq \omega B R^2$, although the usable potential turns out to be a factor ωR smaller. This is essentially linked to the fact that there is a region of size $R_L = c/\omega$, known as light cylinder, within which charges are present, co-rotating with the NS (this region is known as pulsar *magnetosphere*,

⁴ In principle, some acceleration is associated to weak or strong processes. Think of the byproducts of a strong or weak decay.

where e.m. forces dominate over gravitational ones in determine the physics), while magnetic lines extending beyond R_L leave to infinity (and particles escape to infinity along these lines). Beyond R_L co-rotation would be impossible, exceeding the speed of light.

The most widely considered acceleration mechanism is however the one associated to shocks. First of all, what is a shock? A shock wave is a propagating disturbance in a medium that moves faster than the local speed of sound in the medium. It is a physical realisation of a mathematical discontinuity, i.e. abrupt changes in macroscopic variables, achieved over microscopic distances. Far from being exotic, shocks arise quite naturally once the non-linear nature of the continuum equations of fluidodynamics or MHD is taken into account. If the disturbance becomes large enough, then nonlinear terms become important: The crest of a wave propagates faster than the leading or trailing edge; The sound speed is greater at the crest, the wave front steepens and a shock may form. Even if the “physics at discontinuities” cannot be understood but in microscopic terms (e.g. finite conductivity determines its actual size), obviously conservation laws continue to hold. Assuming planar geometry, and in the frame of the shock, the conservation of fluxes of mass, momentum energy across the shock write (for stationary conditions ideal fluids)

$$\begin{aligned} [\rho u] &= 0 \\ [\rho u^2 + P_{\text{gas}}] &= 0 \\ \left[\frac{1}{2} \rho u^3 + \frac{\gamma P_{\text{gas}} u}{\gamma - 1} \right] &= 0 \end{aligned} \quad (91)$$

where I am using the rather standard notation $[\mathcal{O}] \iff \mathcal{O}|_2 - \mathcal{O}|_1$ and γ denotes here the adiabatic index, equal to $1+(2/\# \text{dof}) = 5/3$ for a monoatomic gas. This is a special case of the *Rankine-Hugoniot* conditions. The dynamical eqs. in this type of solutions express conservations across the shock, i.e. links between physical quantities at the two sides. For an ideal fluid and using u for upstream (i.e. the unshocked medium) and d for the downstream (post-shock):

$$\frac{\rho_d}{\rho_u} = \frac{v_u}{v_d} = \frac{(\gamma + 1)\mathcal{M}^2}{(\gamma - 1)\mathcal{M}^2 + 2} \rightarrow \frac{(\gamma + 1)}{(\gamma - 1)} \approx 4 \quad (92)$$

where $\mathcal{M} = v_{\text{shock}}/c_s$ is the Mach number. Similarly, the limit conditions for pressure and temperature jump are

$$\begin{aligned} \frac{P_d}{P_u} &\rightarrow \frac{2\gamma\mathcal{M}^2}{(\gamma+1)} \\ \frac{T_d}{T_u} &\rightarrow \frac{2\gamma(\gamma-1)\mathcal{M}^2}{(\gamma+1)^2} \end{aligned}$$

which allow us to conclude that the condition for entropy increase requires $\mathcal{M} > 1$: Shocks can only form in supersonic motion. In shocks, there is a large pressure and T jump; also, the kinetic energy contributes to heating the gas. Shock waves are huge heating machines!

In case e.m. fields are present, similar jump conditions hold in MHD, remembering from elementary courses on electromagnetism that the B-field normal to this surface (i.e. parallel to the normal, hence indicated with B_{\parallel}) and the E-field parallel to the shock surface (again, indicated with E_{\perp} since perpendicular to the normal) and are continuous. In MHD for a planar shock, one gets

$$\begin{aligned} [\rho u_{\perp}] &= 0 \\ \left[P + \rho u_{\perp}^2 + \frac{B_{\parallel}^2 - B_{\perp}^2}{8\pi} \right] &= 0 \\ \left[\rho u_{\perp} u_{\parallel} + \frac{B_{\perp} B_{\parallel}}{4\pi} \right] &= 0 \\ \left[\rho u_{\perp} \left(\frac{1}{2} u^2 + \frac{\gamma P}{(\gamma-1)\rho} \right) + \frac{u_{\perp} B^2 - B_{\perp} (\mathbf{u} \cdot \mathbf{B})}{4\pi} \right] &= 0 \\ [B_{\perp}] &= 0 \\ [B_{\perp} u_{\parallel} - B_{\parallel} u_{\perp}] &= 0 \end{aligned}$$

So that, in particular when $u_{\parallel} = 0$, B_{\parallel} jumps as density since $[B_{\parallel}/\rho]=0$; as a consequence this component of the field gets compressed by $\simeq 4$ in strong shocks.

1. (First order) Fermi acceleration theory.

We want to study what Eq. (87) implies for ϕ in presence of a shock front, at $z = 0$, assuming that CR are sources/injected only at the shock, i.e. a $\delta(z)$ like before. Far from the discontinuity, at steady state, it holds

$$u \frac{\partial \phi}{\partial z} = \frac{\partial}{\partial z} \left(K \frac{\partial \phi}{\partial z} \right) \quad (93)$$

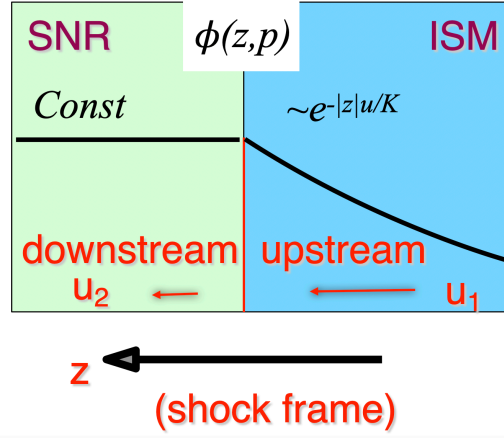


FIG. 11: Scheme to describe the planar shock wave, our SNR proxy.

with the values of u and K different at the two sides of the shock. Let us denote with 1 the upstream, unshocked medium (negative z coordinates), and 2 the downstream (post-shock) positive z coordinates (see sketch in Fig. 11). Upstream we can balance convection and diffusion and, after imposing boundary conditions, one obtains

$$\phi(z, p) = \phi_{-\infty}(p) + [\phi_0(p) - \phi_{-\infty}(p)] \exp\left(-\frac{u_1 |z|}{K_1}\right), \quad z < 0, \quad (94)$$

which gives an exponentially vanishing profile upstream away from the shock. Downstream (post-shock) the only acceptable solution is $\phi = \text{const}$.

$$\phi(z, p) = \phi_0(p), \quad z > 0. \quad (95)$$

If we integrate Eq. (66) across the shock, we find:

$$\left(K \frac{\partial \phi}{\partial z}\right)_2 - \left(K \frac{\partial \phi}{\partial z}\right)_1 + \frac{1}{3}(u_2 - u_1)p \frac{\partial \phi_0}{\partial p} = q_0(p) \implies 0 - u_1 \phi_0 + \frac{1}{3}(u_2 - u_1)p \frac{\partial \phi_0}{\partial p} = q_0(p), \quad (96)$$

from which, setting $r \equiv u_1/u_2$ and assuming a monochromatic injection $q_0 = \kappa u_1 p_i \delta(p - p_i)$ we deduce (see eq.(89))

$$\phi_0(p) = \frac{3\kappa r}{r-1} \left(\frac{p}{p_i}\right)^{-\frac{3r}{r-1}}. \quad (97)$$

Since $r \rightarrow 4$, the spectrum tends to $\phi_0(p) \simeq p^{-4}$, equivalent to p^{-2} in spectral intensity or spectral density. This is known as *Fermi spectrum*. Note that:

- The spectral shape is actually independent of the injected momentum at the shock. A superposition of Fermi spectra will be a Fermi spectrum.
- The result does not really depend on the diffusion coefficient at the shock (great, since we know so little about that!).
- The spectrum of accelerated particle is a power-law extending formally to infinite momenta: without E-losses, in the stationary approach there's no limit!
- The slope depends uniquely on the compression factor, is universal for strong shocks and is notably independent of the diffusion properties.
- The normalization (equivalently, the efficiency of the acceleration, if expressed in terms of the background plasma density) is a free parameter, depending on the details of the injection in the acceleration zone.
- The scattering centers have been assumed to be at rest in the shock frame. That is not necessarily true.
- A planar geometry was assumed, and implicitly that the shock is "parallel", i.e. the field responsible for diffusion is along the shock normal.
- The universal "Fermi spectrum" is obtained for energetic particles at the source (hence should reflect in remote observations as gamma rays), does not necessarily hold for the CRs escaping in the ISM!

2. Generalities of stochastic acceleration and (Second order) Fermi mechanism.

One can also analyse the mechanism previously described from a “microscopic” point of view, i.e. looking at the particles undergoing acceleration. To understand how, let us be more generic, first.

Think of any cyclic process, requiring a time τ per cycle, with escape probability P_{esc} , repeating for a time T leading to an average fractional energy gain ξ per cycle. Then, with probability $(1 - P_{esc})$, a particle with energy E_n will be accelerated to $E_{n+1} = (1 + \xi)E_n$, which implies that a particle with initial energy E_0 will have reached energy $E_n = E_0(1 + \xi)^n$ with probability $(1 - P_{esc})^n$, where the number of cycles $n \simeq T/\tau$. This takes into account that reaching higher energies requires longer times. After a sufficiently long time, the resulting (cumulative) spectrum of non-thermal particles above energy $E = E_0(1 + \xi)^n$ can be obtained as the sum of a geometric series with $x = (1 - P_{esc})$, i.e.

$$\phi(> E) \propto \sum_{m=n}^{\infty} (1 - P_{esc})^m = \frac{(1 - P_{esc})^n}{P_{esc}} = \frac{(1 - P_{esc})^{\frac{\ln(E/E_0)}{\ln(1+\xi)}}}{P_{esc}} = \frac{1}{P_{esc}} \left(\frac{E}{E_0} \right)^{-\alpha} \quad (98)$$

where (remember that $a^{\ln b} = b^{\ln a}$, just take the logs!)

$$\alpha = \frac{\ln(1 - P_{esc})^{-1}}{\ln(1 + \xi)} \simeq \frac{P_{esc}}{\xi}, \quad (99)$$

the last equality holding when escape probability and gain are small. Historically, the first process of this type proposed to

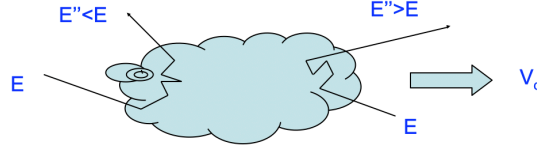


FIG. 12: Scheme to describe the second order Fermi acceleration theory, with the energy at the exit of the cloud E'' sometimes greater and sometimes smaller than the one at the entrance E .

accelerate CR is due to Fermi [37], who made the hypotheses that the CR gain energy in colliding with “magnetised clouds” in the Galaxy, in modern terms disturbances in the magnetic field such as Alfvén waves. Denoting by $\beta = V_c/c \simeq v_A$ the cloud velocity wrt the Lab, the initial particle energy, which is E_i in the Lab/Galaxy frame, i in the cloud frame writes $E'_i = \gamma E_i(1 - \beta\mu)$ where $\mu = \cos(\text{relative angle})$ of incoming particle momentum with respect to the cloud direction.

The particle is only subject to elastic scattering in the cloud, so that its energy E'_f at exiting the cloud is unchanged *in the cloud frame*, $E'_f = E'_i$. Back into the Lab (ISM), its energy E_f at exiting the cloud writes

$$E_f = \gamma E'_f(1 + \beta\tilde{\mu}) = \gamma^2 E_i(1 - \beta\mu)(1 + \beta\tilde{\mu}) \quad (100)$$

(obviously, if β is the cloud velocity wrt the Lab, $-\beta$ is the Lab velocity wrt the cloud).

Both losses and gains are possible in this context, since μ and $\tilde{\mu}$ are random, but the clever observation by Fermi is that they do not compensate, on average! Taking into account that the exiting angle is isotropically distributed (flat distribution of $\tilde{\mu}$ between -1 and 1), one gets

$$\left\langle \frac{E_f - E_i}{E_i} \right\rangle_{\tilde{\mu}} = \gamma^2(1 - \beta\mu) - 1. \quad (101)$$

Since the probability P of entering the cloud depends on the (non-relativistic) relative velocity between cloud and particle, which is given by

$$P(\mu) \propto \frac{v - \beta\mu}{1 - v\beta\mu} = 1 - \beta\mu + \mathcal{O}(\beta^2) \Rightarrow P(\mu) = \frac{(1 - \beta\mu)}{2}, \quad (102)$$

as a result, we get on average a net gain of energy of the particles at the expense of the cloud bulk energy:

$$\xi = \left\langle \frac{\Delta E}{E} \right\rangle_{\mu} = \int_{-1}^1 d\mu \frac{(1 - \beta\mu)}{2} [\gamma^2(1 - \beta\mu) - 1] = \frac{\gamma^2\beta^2}{3} + \gamma^2 - 1 = \frac{4}{3}\beta^2 + \mathcal{O}(\beta^4). \quad (103)$$

The quadratic dependence of the energy gained per cycle from the cloud velocity gives the mechanism its name. Note that for $\beta \simeq v_A \simeq 10^{-5} \div 10^{-4}$, the mechanism is poorly efficient. Also, the value of the predicted power-law index is rather uncertain, depending in particular on how long the particle remains in the cloud, and their mean free path between a cloud encounter and the next, see eq. (99). While historically important, we do not believe that the bulk of CR acceleration in our Galaxy is due to this mechanism, which is thought of more as “post-processing” of already accelerated CRs.

However, the shock acceleration mechanism previously introduced can also be described in similar terms, with Eq. (100) yielding the final energy in terms of $\beta = (u_1 - u_2)/c$. The difference is essentially geometric, since the coherent shock motion only allows for some angles: In particular in order to exit the shock, the particle must go to the right, i.e. restricted to $\tilde{\mu} > 0$, while in order to enter it, the particle must go to the left, i.e. restricted to $\mu < 0$. As a consequence, by projecting an isotropic flux through a plane shock, one infers the probabilities as being

$$P(\mu) = -2\mu\Theta(-\mu)\Theta(1+\mu), \quad P(\tilde{\mu}) = 2\tilde{\mu}\Theta(\tilde{\mu})\Theta(1-\tilde{\mu}), \quad (104)$$

hence the net gain of energy of the particles is first order in the velocity difference across the shock:

$$\xi = \left\langle \frac{\Delta E}{E} \right\rangle = \int_{-1}^0 d\mu(-2\mu) \int_0^1 d\tilde{\mu}2\tilde{\mu} [\gamma^2(1-\beta\mu)(1+\beta\tilde{\mu}) - 1] = \frac{4}{3}\beta + \mathcal{O}(\beta^2) \quad (105)$$

Note that for an isotropic flux of particles, we have $j = \phi c/(4\pi)$. The rate of particles thus entering the shock (in the right direction to get accelerated) is

$$\int d\Omega_{\text{sh}} j = \int_{-1}^0 d\mu \int_0^{2\pi} d\phi(-\mu)j = \pi j = \frac{\phi_{\text{CR}}c}{4} \quad (106)$$

On the other hand, the rate of particles advected away downstream, is given by $\phi_{\text{CR}}u_2$.

The probability that a particle will escape (and not return to the shock) is

$$P_{\text{esc}} = \frac{\phi_{\text{CR}}u_2}{\frac{\phi_{\text{CR}}c}{4}} = 4\frac{u_2}{c} \quad (107)$$

This allows us to compute the cumulative spectral index

$$\alpha \simeq \frac{P_{\text{esc}}}{\xi} = 3\frac{u_2}{u_1 - u_2} = \frac{3}{r-1} \simeq 1 + \frac{4}{\mathcal{M}^2} \quad (108)$$

we recover the universality of the Fermi spectrum consistent with eq. (97), but now starting from a microscopic consideration rather than a distribution function approach.

Exercise Starting from Newton’s law in presence of electromagnetic fields, show that the rigidity of a particle obeys the equation

$$\frac{d\vec{\mathcal{R}} \cdot \vec{\mathcal{R}}}{dt} = 2\vec{\mathcal{R}} \cdot \mathbf{E} \quad (109)$$

i.e. any electromagnetic acceleration process orders particle distribution functions with respect to their rigidity. Use this to justify why, in the relativistic limit ($E_N \gg m_N$), we must expect that electrons are subleading to the hadronic (approximate, protonic) CR component, and estimate by how much, expressing them in terms of ratio of fluxes with respect to kinetic energy, $J(T)$. Consider both species accelerated from a non-relativist bath with typical kinetic energy $T_0 \ll m_e$, for which charge neutrality applies (so that equal numbers of particles are accelerated above T_0 for both species). For momentum power-spectra of index s , you should find

$$\frac{J_e(T)}{J_p(T)} \rightarrow \left(\frac{m_e}{m_p} \right)^{(s-1)/2} \quad (110)$$

in the relativistic limit.

3. Some notions on supernova remnants.

In the core-collapse of a massive star at the end of its lifetime, its gravitational energy

$$U_{\text{grav}} \simeq \frac{3}{5} \frac{G_N M^2}{R_{NS}} \simeq 3 \times 10^{53} \text{ erg} \quad (111)$$

is released. Most of it is in the form of neutrinos of O(10) MeV, diffusing out of its core within O(10) s; about 1% of it (i.e. about the fraction of the neutrino energy deposited in the stellar layers on their way out) is enough to make the star explode and is eventually carried by the kinetic energy of the remnant ⁵. We can estimate thus

$$v_{SNR} = \sqrt{0.01 \frac{2U_{\text{grav}}}{M_{\text{SNR}}}} \simeq 10^{-2}. \quad (112)$$

This velocity, while non-relativistic, is clearly much larger than the sound speed in the ISM, and leads to a shockwave. The remnant follows different phases

- Ballistic expansion, during a few centuries, with $v_{SNR} \simeq \text{const.}$ and thus a radius of the SNR given by $R(t) \propto t$
- Sedov-Taylor phase ⁶, once the SNR has swept a quantity of mass comparable to the ejecta mass: A self similar solution relating the density, pressure, and temperature of the gas, and the distribution of the expansion velocity exists; it lasts for about 10^5 yrs, with $R(t) \propto t^{2/5}$.
- Snow-plow phase: eventually, cooling (radiative) processes cannot be neglected anymore. When the radiative cooling time of the gas becomes shorter than the expansion time, the SNR evolves conserving momentum at a more or less constant temperature and the radius of the shell expands as $R(t) \propto t^{1/4}$. This phase lasts some million years, typically. The name comes from the considerable mass accumulated behind the shock.
- ISM Merger: Eventually, the remnant dissipates into the ISM.

Most SNR we can “see” in radio, X, etc. are actually in the Sedov-Taylor phase. These observations show that they host energetic particles. Additionally, they present suitable conditions for acceleration (shocks) and also a sufficient power-budget to account for galactic CRs. They were recognised as a likely site for CR acceleration already in 1934, by Zwicky and Baade [38].

Exercise : Knowing that SN are estimated to happen 2-3 times per century in the Galaxy, each releasing a few times 10^{51} erg in kinetic energy, what is their “kinetic” luminosity? Compare that with the power needed to sustain a steady-state population of CRs, with integrated energy density of about $0.5\text{eV}/\text{cm}^3$ filling a confinement volume of the Milky Way assumed to be a cylinder with radius 15 kpc and height 4 kpc, and typical “lifetime” of $\tau_{CR} \simeq 10$ Myr. Is it enough for the SNRs to power CRs? What is the ratio of the two, or if you wish the efficiency of macroscopic kinetic energy conversion into CR acceleration?

Suggestion to go beyond: Study the Sedov-Taylor solution (can be found e.g. in [5]).

4. Confinement condition

One must require that the system must be able to contain the particle: its Larmor Radius r_L must be smaller than the size of the accelerator s . One can put different astrophysical objects in a log-log plot of magnetic field strength vs. size of the accelerator (this is known as *Hillas plot*, since [39]); if they fall to the left of a given diagonal downgoing line, they can at best contain and thus accelerate particles of the corresponding energy, since the product sB essentially determines the maximum rigidity. This suggests for instance that objects other than SNR must be involved in the acceleration of UHECRs, see fig. 13. One likely candidate are active galactic nuclei (at different possible sites, actually).

Part IV Collisions

Tackling E -loss limitation on E_{max} , mentioned in the previous section, opens up a big topic, namely collisional effects in CRs. These are crucial not only to set one limitation to the maximal energy of acceleration (in a finite time), but also yield a number of diagnostic channels, including acting as source term for high-energy neutrinos and photons.

⁵ A similar *kinetic* energy is also present in SNaE triggered by thermonuclear explosions following e.g. a binary white dwarf merger, or accretion onto a white dwarf. By the way, only about 1% of this kinetic energy is visible in optical photons. A SN event is much “brighter”, energetically speaking, than its light curve.

⁶ This is a classical, self-similar solution applying to a pointlike release of energy E , conserved in the expansion in a medium of constant density. It was found independently by the British Taylor and the Soviet Sedov around WWII time, in a completely different context than astrophysics, that I let you imagine; just be aware that the book in which Sedov presented his solution had a B-52 bomber on its cover!

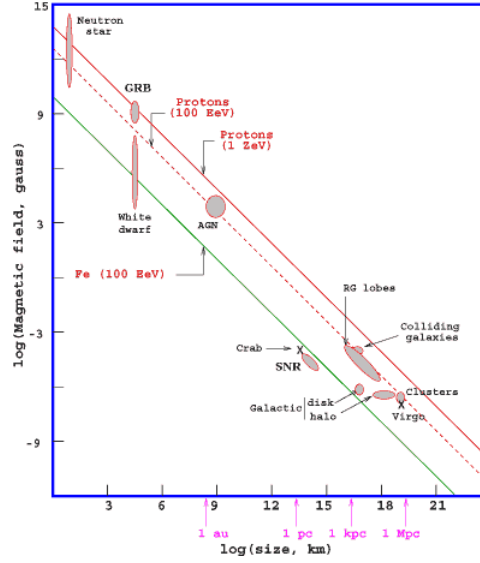


FIG. 13: Hillas diagram, modern version of the one first presented in [39]; see text for details.

Let us start by reminding that in a (relativistic) two-body collision $a + b \rightarrow \dots$, the following quantity is a relativistic invariant (square of the COM energy):

$$s = (p_a + p_b)^2 = m_a^2 + m_b^2 + 2(E_a E_b - \mathbf{p}_a \mathbf{p}_b) = m_a^2 + m_b^2 + 2E_a E_b (1 - \beta_a \beta_b \cos \vartheta). \quad (113)$$

If equated to the (square) of the sum of masses of the final state, this allows one to estimate threshold energies in the Lab frame.

Exercise Calculate the minimum energy in the lab for a CR proton, hitting another one at rest, to produce one antiproton. *Hint:* remembering that baryon number is conserved, what is the lightest final state containing an antiproton, i.e. what is the lightest X in $pp \rightarrow \bar{p} X$?

Another useful invariant in $a + b \rightarrow c + d$ is the (square) of the momentum transferred

$$t = (p_a - p_c)^2 = (p_b - p_d)^2. \quad (114)$$

For the case of an electron scattering with another charged particle (a proton, for instance) one has (prime is for outgoing quantities)

$$t = (p_e - p'_e)^2 = 2m_e^2 - 2E_e E'_e (1 - \beta_e \beta'_e \cos \vartheta) \rightarrow -4E_e E'_e \sin^2 \vartheta / 2, \quad (115)$$

where the last step is valid in the high-energy limit. Note that its value is negative, while the squared four-momentum of any real photon has $q^2 = 0$ (it's a virtual photon!). If you remember the strong angular dependence of Rutherford scattering, with $d\sigma/d\Omega \propto Z_1 Z_2 \alpha / \sin^4 \theta / 2$, this implies $d\sigma/d\Omega \propto 1/t^2$: the cross-section is dominated by small-angle scatterings! On the other hand, if one wants to produce a particle of mass M in a collision, a rough criterion must be $|t| > M^2$. So, the 'bulk' of the cross-section (what is mostly relevant for cosmic ray physics in the atmosphere, for instance) is dominated by small angle scatterings; machines like LHC focus instead on large-angle scatterings, which are associated to large exchanged momenta. Besides the relative rarity of very energetic CR, this is also the reason why CRs and high-energy collider physics have largely complementary targets. Nonetheless, there is a smaller community at LHC that is devoted to the so-called *forward* physics (the name comes from the fact that, loosely speaking, θ in formulae like the one above is very small). If curious, have a look e.g. at [40].

A collision can be associated to a *catastrophic* loss, when the primary particle disappears or has most of its energy transferred to other particles. In this case, the *mean-free-path* ℓ and its associated collision rate Γ are the key quantities to describe also the energy-loss spatial and time scales, respectively. ℓ is the average distance travelled in a medium of number density n before interacting. If σ is the cross-section of the interaction process, and β is the particle velocity, its mean-free-path and interaction rate are

$$\ell = \frac{1}{\sigma n}, \quad \Gamma = \sigma \beta n = \frac{\beta}{\ell} \quad (116)$$

One can also associate to a distance or size R , of background target density n , the dimensionless optical depth:

$$\tau = \frac{R}{\ell}. \quad (117)$$

Losses can also be *continuous*, if actually the primary particle retains its nature and most of its energy in each elementary process, so that a continuous description is more appropriate, characterised by the loss rate per unit time $-dE/dt$ (or analogously loss rate per unit space $-dE/dx$)

It is useful to define a characteristic loss timescale,

$$\tau_{\text{loss}} \equiv \frac{E}{-dE/dt}, \quad (118)$$

which is often a quick way to compare the relative importance of various processes, and can be compared with Γ^{-1} for catastrophic processes to gauge what is more important, energetically.

We will discuss collisional processes within the following scheme:

- Lepton interactions with fields/radiation (Synchrotron/Inverse Compton, basics of multimessenger approach).
- Lepton interactions with matter (Ionisation/Bremsstrahlung).
- Hadron interactions with photon fields (essentially for extragalactic CR propagation, as well as multimessenger astrophysics).
- Hadron interactions with matter (crucial for Galactic propagation, as well as for multimessenger astrophysics).
- Including interactions in the diffusion-loss equation (implications for CR spectra, secondary productions. . .)

For leptonic processes and applications, a much more complete reference (to which the treatment below is partially inspired to) is [41]. Before plunging into the list of processes, let us consolidate these concepts with the simple following application.

A. Pair production and the “gamma-ray horizon”

If we specialize Eq. (113) to the case $\gamma + \gamma \rightarrow e^+e^-$ for heads-on collision, we get

$$4E_\gamma\epsilon = (2m_e)^2 \implies E_\gamma > \frac{m_e^2}{\epsilon}. \quad (119)$$

The cross-sections behaves as

$$\sigma_{\gamma\gamma}(\beta) = \frac{3\pi\sigma_T}{16} (1 - \beta^2) \left[2\beta(\beta^2 - 2) + (3 - \beta^4) \ln\left(\frac{1 + \beta}{1 - \beta}\right) \right], \quad (120)$$

where β is either lepton velocity in the COM frame. Graphically, it peaks at about $\sigma_T/4$ at about twice the threshold energy, see Fig. 14.

Exercise Compute the energy of background photons at threshold for pair-production for incoming photons of 1 TeV or 1 PeV energy. What type of “light” are these bands corresponding to? In the case of CMB, described by a blackbody spectrum at 2.7 K, compute the mean-free path of a photon of typical PeV energies.

The exercise above is meant to illustrate the fact that the gamma-ray sky may not always be optically thin, with the e^\pm pair production mechanism constituting a serious limitation for the remote extragalactic sky already at hundred of GeV, for the near extragalactic sky at about 10 TeV, and even for Galactic objects in the PeV range (see the *photon horizon* in Fig. 15). Put otherwise, we expect that beyond the TeV range, we can only perform astronomy in the “local neighborhood”.

VII. SYNCHROTRON RADIATION

In the discussion of Sec. II, we have explicitly neglected any inelastic process. But, as we saw, in the presence of a magnetic field such as the one threading the ISM, a charged particle follows a helicoidal trajectory, with a typical gyroradius given by Eq. (22) and a typical gyrofrequency given by Eq. (23).

But a rotating charge is actually accelerated, and we know from basic electrodynamics that an accelerated charge radiates, see Fig. 16 for a cartoon. In the non-relativistic limit, the radiated power (or $-dE/dt$) is described by the Larmor formula

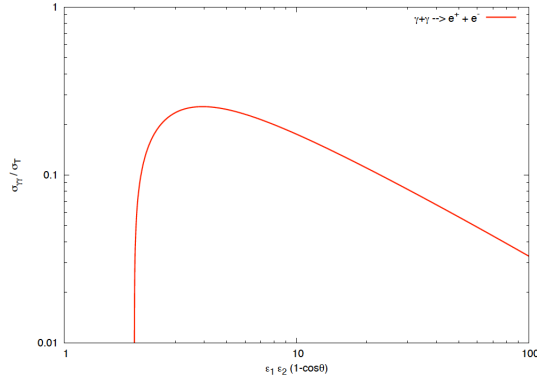


FIG. 14: Energy dependence of the pair-production cross-section.

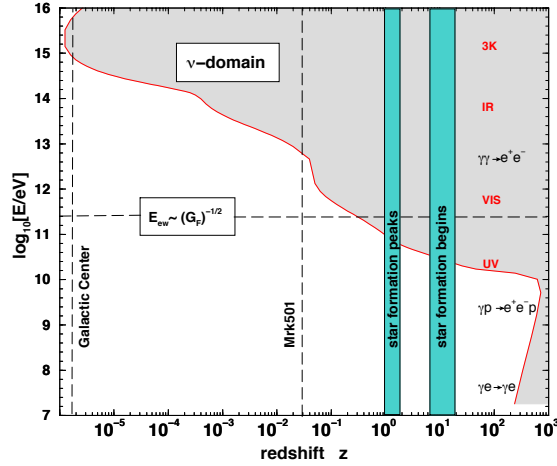


FIG. 15: Gamma-ray horizon (for a Hubble constant of $H_0=60 \text{ km s}^{-1} \text{ Mpc}^{-1}$ and a cold dark matter cosmology) due to various absorption processes (predominantly $\gamma - \gamma$ pair production in the extragalactic radiation field). The shaded area is invisible for gamma-ray astronomy [42].

$$\frac{dP}{d\Omega} = \frac{q^2 a^2 \sin^2 \phi}{4\pi} \Rightarrow P = \frac{2}{3} q^2 a^2, \quad (121)$$

ϕ being the angle with respect to the acceleration vector (dependence consistent with cartoon in Fig. 16)⁷. We shall assume familiarity with it, without re-deriving it (for more details on this and related topics in this and the following section, see also [41]). Note however how the dependence upon the square of the acceleration follows trivially from dimensional analysis (and the impossibility of dependence upon position or velocity because of Galilean or Poincaré invariance). The appearance of e^2 is also trivially following from the basic e.m. interaction vertex, squared when taking the amplitude square.

In fact, this formula is also valid in the relativistic limit, provided that a^2 is now replaced by the four-acceleration (or, four-force over mass) $a^2 \rightarrow a_\mu a^\mu$. This is because the radiated power is a Lorentz-invariant, as one can guess from the fact that dE and dt are both the 0-th components of four-vectors, transforming the same way.

A charge q moving with Lorentz factor γ with respect to the frame of the static magnetic field views an induced electric

⁷ This derives from

$$dP = \mathbf{S} \cdot d\vec{A} = \mathbf{S} \cdot \hat{\mathbf{n}} R^2 d\Omega, \quad (122)$$

R being the distance from the radiating source, $\hat{\mathbf{n}}$ the normal to the crossed surface, and the Poynting vector

$$\mathbf{S} = \frac{\mathbf{E} \times \mathbf{B}}{4\pi} = \frac{|\mathbf{E}|^2}{4\pi} \hat{\mathbf{S}}, \quad (123)$$

to be computed from the electrodynamics of a radiating charge moving non-relativistically, yielding $|\mathbf{E}|^2 \sim q^2 a^2 / R^2$.

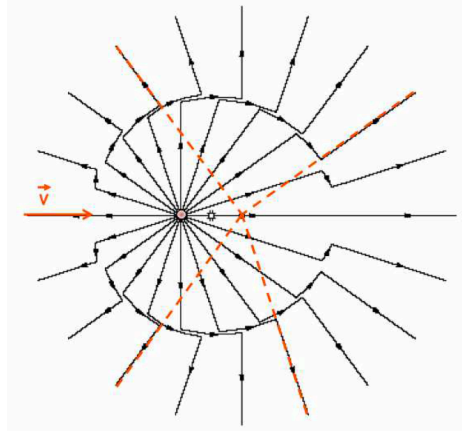


FIG. 16: Electric field due to a charge, initially in uniform motion, that is stopped within a short time δt . Nearby, the field had time to adjust and points to where the charge is (red dot). Far away, the field points to where the charge would be if it had not been stopped (orange point). There is then a region of space where the electric field has to change direction, corresponding to the propagating e.m. wave: its front propagates radially outwards, and the field of the wave (the $\Delta \mathbf{E}$ of the disturbance) is orthogonal to the propagating direction, null along the direction of the braking (which is the initial velocity one, where the two fields are already aligned), and the width of this region is $c\delta t$.

field equal to

$$\mathbf{E}' = -\gamma \mathbf{v} \times \mathbf{B}, \quad (124)$$

associated to the acceleration in the electron frame

$$\mathbf{a} = -\frac{q}{m} \gamma \mathbf{v} \times \mathbf{B}, \quad (125)$$

hence the synchrotron power (energy radiated away per unit time)

$$P_s = \frac{2q^4 \gamma^2}{3m^2} v^2 B^2 \sin^2 \theta. \quad (126)$$

i.e., proportional to γ^2 in the relativistic limit, as well as B^2 , itself proportional to the energy density stored in the B-field.

1. Beaming effect from relativistic motion

Remember the time dilation and space contraction by the same factor $\gamma(v)$ in a (primed) frame moving at velocity v with respect to the initial one, depending upon Lorentz transformation:

$$\boxed{t' = \gamma(t - \beta x) \quad x' = \gamma(x - \beta t)}. \quad (127)$$

From which one derives

$$\frac{dx}{dt} = \frac{\gamma(dx' + \beta dt')}{\gamma(dt' + \beta dx')} = \frac{u'_x + \beta}{1 + \beta u'_x}, \quad (128)$$

$$\frac{dy}{dt} = \frac{dy'}{\gamma(dt' + \beta dx')} = \frac{u'_y}{\gamma(1 + \beta u'_x)}. \quad (129)$$

This implies the aberration formula

$$\tan \theta \equiv \frac{u_y}{u_x} = \frac{u'_y}{\gamma(u'_x + \beta)} = \frac{u' \sin \theta'}{\gamma(\beta + u' \cos \theta')}. \quad (130)$$

This means that a photon ($u = c$) emitted at $\theta' = 0$ travels at $\theta = 0$, while a photon emitted at $\theta' = \pi/2$ travels at $\sin \theta \simeq \theta \simeq 1/\gamma$, as illustrated in Fig. 17.

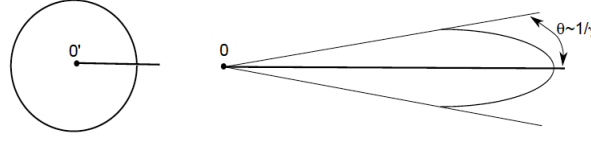


FIG. 17: Illustration of the beaming effect in the lab (unprimed frame) for an isotropic emission in the source (primed).

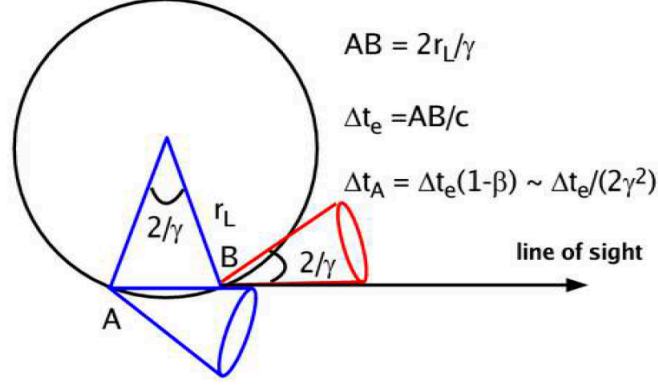


FIG. 18: Beaming effect.

2. Characteristic frequency of emission

To compute the spectrum of photons emitted in a time-varying emission process, one takes the Fourier transform of the signal. In the non-relativistic limit, one has simply a circular uniform motion, thus emission at the single frequency ν_g given (cyclotron line) given by Eq. (21). In the relativistic case, a major alteration is due to beaming (See sec. VII 1): The frequency spectrum is different because of sizable boost effects affecting the radiation timing: One must take into account that only during the fraction of the orbit within the beaming angle the emission is observed. The timescale of the observer is further different from the timescale of the emission. The time difference from the passage at point B and and point A is simply given by

$$\Delta t \equiv t_B - t_A = \frac{AB}{v} = r_L \frac{2}{\gamma} \frac{1}{v}. \quad (131)$$

For an observer at distance well beyond B along the direction AB, the duration of signal detected is

$$\Delta t_{\text{obs}} = t_B + \delta t_B^{\text{prop}} - (t_A + \delta t_A^{\text{prop}}) = \Delta t - AB/c = \frac{AB}{v} (1 - \beta) = \frac{AB}{v} \frac{(1 - \beta^2)}{1 + \beta} \simeq \frac{AB}{v} \frac{1}{2\gamma^2} \simeq \frac{r_L}{\gamma^3}. \quad (132)$$

As a poor man's proxy for a Fourier transform, we can estimate the typical frequency of the radiation (known as *synchrotron* radiation) as the inverse of the above, hence

$$\nu_s \simeq \frac{\gamma^3}{r_L} = \gamma^2 \frac{\omega_g}{2\pi} \Rightarrow E_s \simeq 500 \mu\text{eV} \frac{B}{\mu\text{G}} \left(\frac{E_e}{\text{GeV}} \right)^2. \quad (133)$$

The more complete calculation leads to a power emitted per unit frequency which is not monochromatic, rather with a behaviour $\sim \nu^{1/3} e^{-\nu/\nu_c}$, with the critical frequency ν_c of the same order as the ν_s above.

What about the spectrum from an ensemble of particles, say an electron population? For an electron spectrum of energy-differential number density $n(E) \propto E^{-\alpha}$, we have the following link

$$\nu_s = \left(\frac{E}{m_e} \right)^2 \nu_g \Rightarrow dE = \frac{m_e}{2\sqrt{\nu\nu_g}} d\nu. \quad (134)$$

The scaling of the synchrotron spectrum emitted with the B field and the index α can be estimated simply as follows (remember that $\nu_g \propto B$). In particular, the specific emissivity (power per unit solid angle per unit volume per unit

frequency) is

$$\epsilon(\nu)d\nu = \frac{1}{4\pi} P_s n(E) dE \propto E^2 B^2 E^{-\alpha} dE \propto \nu^{\frac{1-\alpha}{2}} B^{\frac{1+\alpha}{2}} d\nu. \quad (135)$$

So, from the slope typically in the radio-microwaves band $((1 - \alpha)/2)$ one can infer the slope of the parent electron distribution $(-\alpha)$.

To go beyond: The Green catalog of SNR is a continuously updated catalog of Galactic SNR observed at different wavelengths, available online at <https://www.mrao.cam.ac.uk/surveys/snrs/> Have a look to the quantities listed and find in particular the spectral index for the radio emission. What's the typical mean value for observed SNR? Compute this number, or take the value for some representative sources. Infer from this the slope of the parent electron distribution, and discuss how this compares to the observed slope for the observed electron spectrum. Reconsider it after studying the regime of energy loss dominated propagation (Sec.XI.C.1, notably eq. (172)).

VIII. INVERSE COMPTON

A. Thomson cross-section

Let's start from the classical problem of interaction of an electromagnetic wave with a charged particle, computing the power that this particle re-radiates. The acceleration is (Lorentz force over mass) $q(\mathbf{E} + \mathbf{v} \times \mathbf{B})$, which for $v \ll 1$ and considering that the electric and magnetic field of the wave have the same amplitude, gives an acceleration $q|\mathbf{E}|$ along the direction of the field. For a sinusoidal wave $E = E_0 \sin(\omega t + \phi)$ along some direction, the acceleration is along the same direction and of intensity $a = qE/m$, so that the Larmor formula gives for the (time-averaged) emitted power

$$\langle P \rangle = \frac{2}{3} q^2 \langle a^2 \rangle = \frac{2}{3} \frac{q^4}{m^2} \frac{E_0^2}{2}. \quad (136)$$

In scattering theory, the cross-section is the ratio of the radiated power to incident flux,

$$\sigma = \frac{\langle P \rangle}{|\langle \mathbf{S} \rangle|} = \frac{8\pi}{3} \frac{q^4}{m^2} \equiv \sigma_T \quad (\text{if } q = \pm e) \quad (137)$$

with σ_T is the well-known Thomson cross-section, and where the Poynting vector (incident energy per unit time and unit surface) is

$$|\langle \mathbf{S} \rangle| = \frac{|\langle \mathbf{E} \times \mathbf{B} \rangle|}{4\pi} = \frac{E_0^2}{8\pi}. \quad (138)$$

Note that in terms of u , the energy density in the e.m. field,

$$u = \left\langle \frac{|\mathbf{E}|^2}{8\pi} + \frac{|\mathbf{B}|^2}{8\pi} \right\rangle = \frac{E_0^2}{8\pi}, \quad (139)$$

one can also write

$$\langle P \rangle = \sigma_T u, \quad (140)$$

which clearly suggests a more microscopic interpretation (scattering rate—remember $c = 1!$ —onto the number of particles/photons in the field, times the average energy of the photons). Compare with Eq. (126): can you justify the interpretation of synchrotron power as up-scattering of 'virtual' photons associated to an external magnetic field?

1. Energy loss rate

The formula derived for the emission power in the non-relativistic case

$$\langle P \rangle = \sigma_T \tilde{u}, \quad (141)$$

is actually valid more in general since, loosely speaking, it's a dE/dt and energy and time transform the same way. The energy density \tilde{u} is the energy density in the frame comoving with the electron. In the lab frame where the electron is

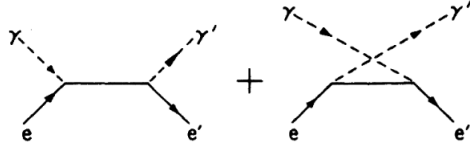


FIG. 19: Diagrams describing the Klein-Nishina process (tree-level electron photon scattering in QED).

moving at β , it can be expressed by remembering that $[u] = [\epsilon \times n]$, and that the number density n transforms as a time since both $dt d^3x$ (four-volume) and nd^3x (number of particles) are relativistic invariants. So, u transforms as the square of the energy,

$$\tilde{u} = u\gamma^2(1 - \beta \cos \alpha)^2, \quad (142)$$

which, for a isotropic radiation field, yields the angular average

$$\langle \tilde{u} \rangle = u\gamma^2 \left(1 + \frac{\beta^2}{3} \right) \quad (143)$$

since

$$\langle \cos^2 \alpha \rangle = \frac{1}{2} \int_{-1}^{+1} d(\cos \alpha) \cos^2 \alpha = \frac{1}{2} \frac{2}{3}. \quad (144)$$

The energy lost by the electrons per unit time being the difference of the scattered power minus incoming power $\sigma_T u$ (impinging photons had some energy, too!), we have

$$\boxed{-\frac{dE}{dt} = \sigma_T u \left[\gamma^2 \left(1 + \frac{\beta^2}{3} \right) - 1 \right] = \frac{4}{3} \gamma^2 \beta^2 u \sigma_T \simeq \frac{4}{3} \gamma^2 u \sigma_T.} \quad (145)$$

If u is interpreted as the energy density of both photon fields and magnetic field, this formula describes both synchrotron and IC losses (in the Thomson regime)!

Exercise Consider a (globally neutral) plasma of electrons and protons (remember: the two species are in tight e.m. coupling!), spherically symmetric of mass M and radius R , kept in equilibrium by the balance of gravity and radiation pressure. What is the luminosity (called *Eddington luminosity*) supporting such a “star” on the verge of disruption? Does our Sun satisfy that limit? If yes, it is close to it? If not, can you explain why?

B. The Klein-Nishina regime

Actually, one can look at the same process from a quantum point of view, as a two-body collision between a photon and an electron. The more general formula for differential cross-section derived by Klein & Nishina in 1929, based on QED (see the diagrams in Fig. 19):

$$\frac{d\sigma}{d\Omega} = \frac{3}{16\pi} \sigma_T \left(\frac{\epsilon_f}{\epsilon_i} \right)^2 \left(\frac{\epsilon_i}{\epsilon_f} + \frac{\epsilon_f}{\epsilon_i} - \sin^2 \theta \right), \quad (146)$$

$$\sigma = 2\pi \int_0^\pi \frac{d\sigma}{d\Omega} \sin \theta d\theta = \frac{3}{4} \sigma_T \left[\frac{1+x}{x^3} \left(\frac{2x(1+x)}{1+2x} - \ln(1+2x) \right) + \frac{1}{2x} \ln(1+2x) - \frac{1+3x}{(1+2x)^2} \right], \quad (147)$$

where $x \equiv \epsilon_i/m_e$, so that

$$\begin{aligned} \sigma(x) &\simeq \sigma_T(1 - 2x + \dots) & \text{for } x \ll 1 \text{ (Thomson)} \\ \sigma(x) &\simeq \frac{3}{8} \sigma_T \frac{1}{x} \left(\ln 2x + \frac{1}{2} \right) & \text{for } x \gg 1 \text{ (extreme KN)}. \end{aligned} \quad (148)$$

1. Compton kinematics

Let us focus on the kinematics of the quantum process. Impose energy momentum balance in a photon (momentum k)-electron (momentum p) scattering:

$$k_i^\mu + p_i^\mu = k_f^\mu + p_f^\mu, \quad (149)$$

and the on-shell condition for the electron mass, $m_e^2 = p_i^2 = p_f^2$, and that $k_{i,f}^2 = 0$:

$$m_e^2 = (p_i + k_i - k_f)_\mu (p_i + k_i - k_f)^\mu \implies m_e^2 = m_e^2 + 2(p_i k_i - p_i k_f - k_i k_f). \quad (150)$$

In the frame where the electron is at rest, $p_i = (m_e, 0, 0, 0)$. We choose the x-axis as the direction of the photon, and the outgoing direction generates with that the x-y plane. Then $k_i^\mu = \epsilon_i(1, 1, 0, 0)$, while $k_f^\mu = \epsilon_f(1, \cos \theta, \sin \theta, 0)$, so that

$$m_e(\epsilon_i - \epsilon_f) = \epsilon_i \epsilon_f (1 - \cos \theta) \implies \epsilon_f = \frac{\epsilon_i}{1 + \frac{\epsilon_i}{m_e}(1 - \cos \theta)}. \quad (151)$$

Note that unless the energy of the photons is of the order of the mass of the electron or larger in the electron rest-frame, the energy of the photons is only slightly altered (the ratio ϵ_i/m_e controls the energy change).

What happens if the electron is not at rest in the frame of interest ("lab"), rather has a velocity β ? Well, the above relation (151) is valid in a frame (let us denote it via a prime) boosted via $\gamma(\beta)$ with respect to the lab:

$$\epsilon'_f = \frac{\epsilon'_i}{1 + \frac{\epsilon'_i}{m_e}(1 - \cos \theta')}, \quad (152)$$

where $\epsilon'_i = \epsilon_i \gamma(1 - \beta \cos \alpha)$, where α is the angle between photon and electron in the Lab frame (θ' , as above, is the angle between outgoing and incoming photon directions). If we want to express ϵ'_f in the Lab frame, we need to perform the "reverse boost", now accounting for the emission angle α' in the comoving frame, such that

$$\epsilon_f = \gamma(1 + \beta \cos \alpha') \frac{\epsilon'_i}{1 + \frac{\epsilon'_i}{m_e}(1 - \cos \theta')} = \gamma^2 \epsilon_i \frac{(1 + \beta \cos \alpha')(1 - \beta \cos \alpha)}{1 + \frac{\epsilon_i}{m_e}(1 - \cos \theta')}. \quad (153)$$

In the limit where $\epsilon'_i/m_e \ll 1$ (which requires $\epsilon_i \gamma \ll m_e$, i.e. $\epsilon_i E_e \ll m_e^2$ in the Lab frame), one has

$$\epsilon_f \simeq \gamma^2 \epsilon_i (1 + \beta \cos \alpha')(1 - \beta \cos \alpha). \quad (154)$$

Also, for isotropically impinging radiation, the second (...) is averaging to 1 (and, as a consequence, also the first one, since the outgoing direction will be essentially isotropic in the electron comoving frame). Hence, a good estimate is

$$\epsilon_f \simeq \gamma^2 \epsilon_i = 30 \left(\frac{\epsilon_i}{\text{eV}} \right) \left(\frac{E_e}{\text{GeV}} \right)^2 \text{ MeV} \quad (155)$$

For this approximation to be correct, one requires $\epsilon_i E_e \ll m_e^2$ which implies $\epsilon_f < E_e$ as well. Note that while the scattering angle is arbitrary in the comoving frame, in the lab frame the outgoing radiation is beamed in the forward direction with an angle $1/\gamma$ (now you should be familiar with that!)

Exercise What is the maximum final energy of a photon in the Thomson regime ($\epsilon \ll m_e$), see Eq. (153)?

It is $4\gamma^2 \epsilon_i$

Exercise Have a look at Eq. (153): What is the typical energy in the KN regime?

C. Notions on SSC

Imagine that the synchrotron photons produced by an energetic electron populations also constitute the main target for further upscatter via inverse Compton. The resulting spectrum corresponds is dubbed Synchrotron-Self-Compton. We know the link between electron power-law index ($-\alpha$) and Syn. spectral index ($(1 - \alpha)/2$), which is also the same for the IC (check that you can repeat the same argument, at least in the Thomson regime!)

This means that, at least in the Thomson regime, SSC sources are expected to show a power law between $\gamma_{\min}^2 \nu_g$ and $\gamma_{\max}^2 \nu_g$, and another power-law parallel to the previous one from $\gamma_{\min}^4 \nu_g$ and $\gamma_{\max}^4 \nu_g$, where the γ_i 's refer to the parent

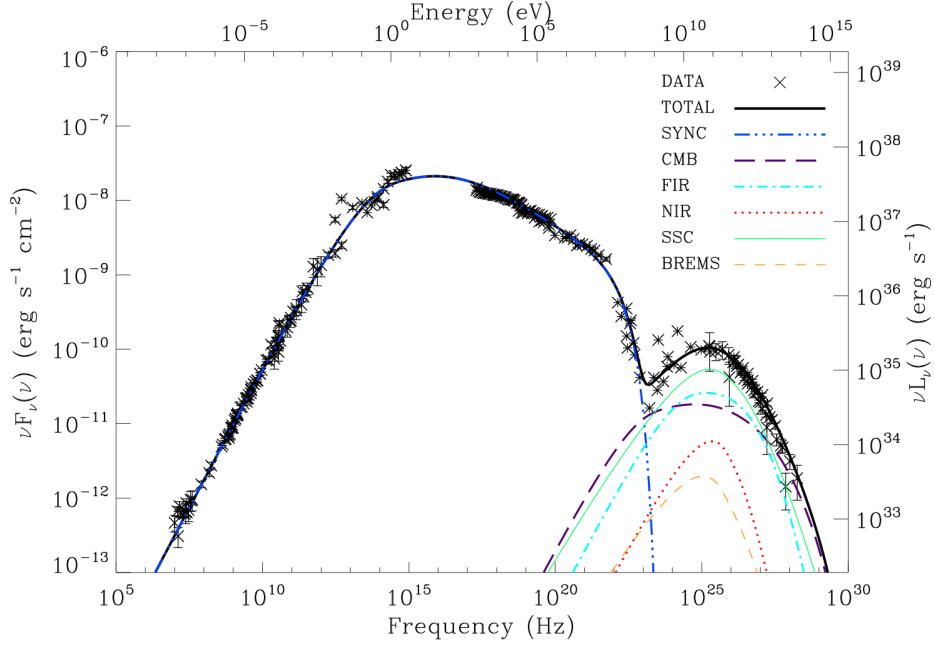


FIG. 20: The multiwavelength photon spectrum of the Crab nebula, also compared to models, taken from [43].

electron spectrum. Also note that the Syn. peak is proportional to the number of high-energy electrons, while the SSC peak, is quadratic in it (since also the target photon number is proportional to the high-energy electrons). I won't cover the physics of the sources, but if we are confident that SSC is realized, a lot of information can be gathered from the spectrum.

Exercise The Crab nebula, associated to the explosion of a SN in AD 1054, presents a roughly broken power-law spectrum, with a steepening around 5 eV, interpreted as synchrotron radiation, see Fig. 20. If we attribute this phenomenon to a “cooling break” (i.e. the electrons producing the photons below the break have a cooling lifetime longer than its age, and the ones producing photons above it have a shorter cooling timescale), determine the magnetic field in the source, and the energy of the electrons associated to this “break point”. What is the energy of IC photons produced when those electrons hit the very synchrotron photons at the break point?

IX. LEPTONIC INTERACTIONS WITH MATTER

A. Ionization and Coulomb interactions

When crossing a medium with density of electrons n_e , on dimensional grounds an electron undergoes an energy loss per unit length of the order of $\sigma_T n_e m_e f(E/m_e)$, with the dimensionless function $f(x)$ further depending on atomic or plasma properties of the medium (such as the electron binding energy or the plasma frequency). A simplified estimate comforting the above expression can be obtained as follows in a classical limit: Consider a non-relativistic electron crossing a medium containing electrons (“almost at rest”) with density n_e . If b is the impact parameter at which the energetic electron passes, and v its velocity, the target electron feels an impulsive force due to the CR electron electric field $F = e^2/b^2$ over a time $\delta t \sim b/v$ (factors of order unity are omitted), associated to a momentum gain $\Delta p = F \Delta t \sim e^2/(bv)$, or equivalently a gain of kinetic energy $\Delta E \sim (\Delta p)^2/m_e \sim e^4/(b^2 v^2 m_e)$. The energy-loss rate per unit length for the cosmic ray electron can be obtained by integrating over the individual losses,

$$-\frac{dE}{dx} = \int 2\pi b n_e \Delta E db \simeq 2\pi n_e \frac{e^4}{v^2 m_e} \ln \frac{b_{\max}}{b_{\min}} \simeq \frac{\sigma_T n_e m_e}{v^2} \ln \frac{b_{\max}}{b_{\min}} \quad (156)$$

where, apart from factors of order unity omitted above, the formula also depends on the so-called Coulomb logarithm: Qualitatively, b_{\min} is determined by the distance at which the collision leads to a deflection angle of order unity (a “hard” collision); b_{\max} is clearly dependent on the type of medium, related to bound electron orbital characteristics, or the effective

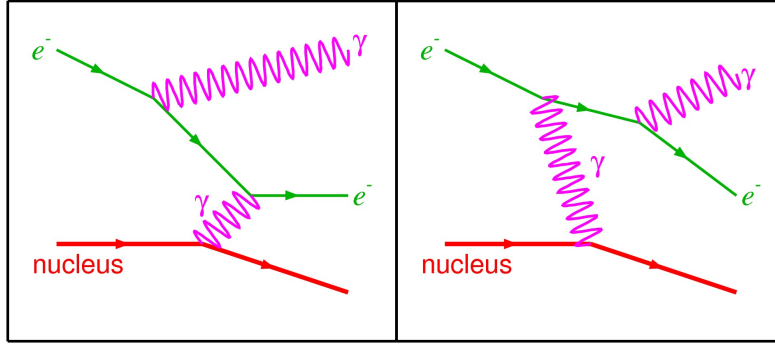


FIG. 21: Diagrams for Bremsstrahlung process.

plasma screening length. Typically, $\ln b_{\max}/b_{\min} \sim \mathcal{O}(10)$. Also note that the derivation requires the energy transfer to be non-relativistic, not the initial particle to be. In fact the result for a relativistic impinging particle is the same, since even if there is a time contraction $\Delta t \rightarrow \Delta t/\gamma$, the electric force increases by the same factor $F \rightarrow \gamma F$ (relativistic transformation of the electric field).

A more correct formula was computed by Bethe within quantum mechanics, and should be familiar from elementary physics courses,

$$-\frac{dE}{dx} = \frac{3}{2} \frac{\sigma_T m_e n_e}{v^2} \left[\log \left(\frac{E}{m_e} \right) + \kappa - \beta^2 \right] \quad (157)$$

where the dimensionless constant κ depends on the material crossed, but typically dominates the E -dependence. A number of corrections are needed at both low and high velocities, which however are not particularly relevant for us since at higher energy the electromagnetic energy transfer described here is hardly the dominant one, and at low-energy one exits the realm of interest for most cosmic ray phenomenology. It suffices to notice that in the non-relativistic regime the E-loss becomes less and less efficient with higher velocity, until it saturates (actually, grows logarithmically) at relativistic energies. But, by the time a particle is relativistic, other E-loss mechanisms dominate.

Exercise Remember Eq. (118). Estimate the range (and timescale) over which an electron with a kinetic energy of 60 keV stops in a ISM with density of 1 cm^{-3} .

The above considerations also apply to charged CRs, of course: We computed the energy transferred via interactions with the electrons in the medium via the impulsive electric field. So, the same considerations apply, but for the change in the force (now with factors e^2 replaced by $Z e^2$, so that the previous formulae acquire a factor Z^2 more. Also, since m_e sets the energy scale, these energy losses are *in percentage* way less efficient than for leptons *of the same velocity*.

Exercise Estimate the range (and timescale) over which a proton with a kinetic energy of 60 keV or 100 MeV stops in a ISM with density of 1 cm^{-3} .

B. Bremsstrahlung

The previously described process is a (quasi)elastic scattering between a charged energetic particle and electrons in the medium. But the energetic particle can also *radiate* a photon under the braking action of the nuclear electric fields. Its calculation requires a spectral decomposition of the Larmor formula, plus kinematical considerations similar to the ones previously developed, and will not be reported here. It suffices to know that this is the dominant X-ray emission process from clusters of galaxies.

A few heuristic considerations suffice: Since there is an extra photon leg attached (see Fig. 21) compared to the previous process, we can quickly estimate that it should be suppressed by a factor α , i.e. its cross section scales as

$$\sigma_{\text{Brems}} \sim \alpha Z^2 \sigma_T, \quad (158)$$

For relativistic electrons, it can also be shown that the energy loss rate scales linearly with energy, i.e.

$$-\frac{dE}{dt} \simeq \sigma_{\text{Brems}} n E. \quad (159)$$

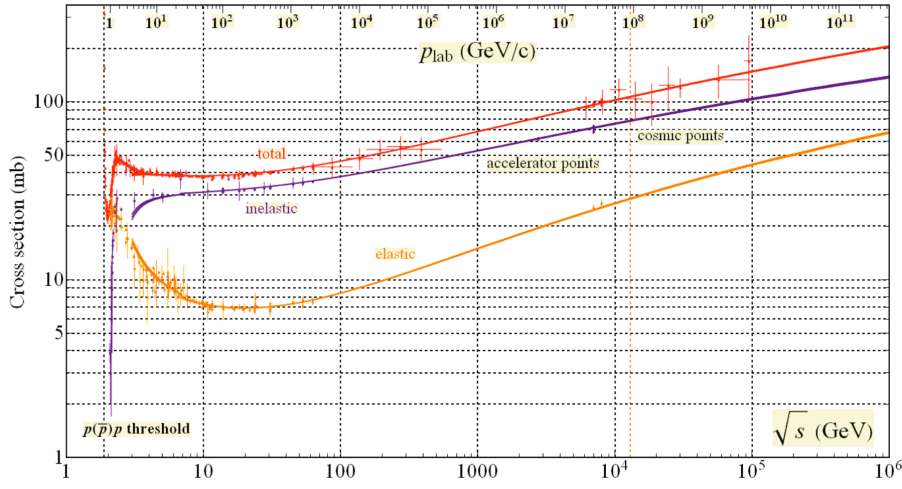


FIG. 22: Elastic and inelastic cross-section for pp scattering, from the PDG.

X. HADRONIC INTERACTIONS

For a particle of mass $m = Am_p$ and charge Ze , the Thomson cross-section σ_T scales as $\sigma_{\text{e.m.}}(m, Z) = Z^4 A^{-2} (m_e/m_p)^2 \sigma_T \simeq 3 \times 10^{-7} (Z^4/A^2) \sigma_T$, which immediately shows how much more inefficient the direct scattering photon-nucleus is compared to the photon-electron.

However, nucleons and nuclei are subject to the strong nuclear force, and the associated inelastic processes are much more important for energy losses, in collisions with matter but also with radiation (if above appropriate thresholds). One useful way to think intuitively about nuclear interactions is the good old Yukawa's idea, of an exchange of massive mediators (the pions), responsible for the relatively short-range of the interaction. Note that the numerous particle physics discoveries in the cosmic rays between the thirties and the fifties of the XX century (the muon, the pion, the strange hadrons...) are due to hadronic interactions of primary protons or nuclei in the atmosphere.

A. Generalities and spallation

The key property of reactions involving nucleon-nucleon, or more in general nucleus-nucleus, is that they are strong, but short range. Also, nucleons and nuclei, differently from leptons and photons, are not 'pointlike', but extended objects of radius approximately given by

$$R \simeq 1.2 A^{1/3} \text{ fm}. \quad (160)$$

Together, these properties suggest a total cross-section value of the order of

$$\sigma_{\text{tot}} \sim \pi R^2 \sim 45 A^{2/3} \text{ mb}, \quad (161)$$

which is a good rule of thumb (see Fig. 22). At a more microscopic level, this can be thought to arise from (possibly multiple) exchanges of pions with an interaction with "order 1" coupling, so that the nucleon nucleon cross-section is also of the order of $1/m_\pi^2$. At nucleon-nucleon level, inelastic processes are dominated by the emission of one or more pions (mostly in the forward direction). In a nuclear collision at GeV energies or above, however, the de Broglie wavelength $1/p \simeq 1/(\gamma m)$ is well below the nucleus size, so the nucleus is resolved in its constituents, and the nucleon typically strikes only one or a few nucleons⁸ (for multiple scatterings, more frequent for heavier nuclei). This "quasi-elastic" process if

⁸ Of course, what matters is the momentum exchanged in the process. Eventually, hard processes with the production of pions, for instance, become possible. Yet, remember that most interactions are relatively soft...

Product nucleus	Z	A	Parent nucleus								
			^{11}B	^{12}C	^{14}N	^{16}O	^{20}Ne	^{24}Mg	^{28}Si	^{56}Fe	
Lithium	3	6	12.9	12.6	12.6	12.6	12.6	12.6	12.6	12.6	17.4
		7	17.6	11.4	11.4	11.4	11.4	11.4	11.4	11.4	17.8
Beryllium	4	7	6.4	9.7	9.7	9.7	9.7	9.7	9.7	9.7	8.4
		9	7.1	4.3	4.3	4.3	4.3	4.3	4.3	4.3	5.8
Boron	5	10	15.8	2.9	1.9	1.9	1.9	1.9	1.9	1.9	4.1
		11	26.6	17.3	16.0	8.3	7.1	6.2	5.3	5.3	5.3
Carbon	6	10	—	3.9	3.3	2.9	2.1	1.6	1.2	0.5	—
		11	0.6	26.9	12.4	10.6	7.9	5.9	4.5	1.3	—
Nitrogen	7	12	—	—	38.1	32.7	13.5	10.1	7.6	4.7	—
		13	—	—	10.5	14.4	10.7	8.0	6.0	3.7	—
Oxygen	8	14	—	—	—	2.3	3.9	3.0	2.2	2.1	—
		15	—	—	—	10.7	3.6	2.7	2.0	1.5	0.5
Nitrogen	7	14	—	—	—	26.3	10.9	8.1	6.1	2.9	—
		15	—	—	—	31.5	10.0	7.5	5.7	4.3	—
Oxygen	8	16	—	—	—	—	3.4	2.6	1.9	1.6	—
		14	—	—	—	3.4	2.5	1.9	1.4	0.3	—
Oxygen	8	15	—	—	—	27.8	11.8	8.9	6.7	1.0	—
		16	—	—	—	—	27.0	13.5	10.2	3.9	—
Oxygen	8	17	—	—	—	—	15.5	11.6	8.7	4.1	—
		18	—	—	—	—	4.5	4.7	3.5	2.6	—

FIG. 23: Spallation cross-sections, in mb, From [1].

seen at the nucleon-level is however sufficient to give enough energy to the nucleon(s) to escape the bound state: The process where projectile or target nucleons are kicked out of the nucleus is known as *spallation*. Its cross-sections are only weakly dependent on energy, apart at low energies (typically below 100 MeV/nuc) where nuclear details are important. While more or less refined phenomenological models exist, these cross-sections are empirically measured and tabulated (see Fig. 23.) In this “superposition model”, most of the target nucleus remains essentially unaffected. This is confirmed by the fact that the *energy per nucleon* is approximately conserved, in such processes (this also explains the usefulness of plotting nuclear fluxes in terms of this variable E/A , notably at low-energies.) Note how partial cross-sections are a fraction of the estimate of Eq. (161), and typically the byproducts differing from the parent by a single nucleon or two are the preferred final states (e.g. ^{11}C and ^{11}B from ^{12}C , ^{14}N , ^{15}N from ^{16}O , ...) These are the most relevant catastrophic interactions for nuclei propagating in a “matter-rich” environment (as the Galactic disk, as opposed to the extragalactic space).

It is worth mentioning that quite often the projectile or target nucleus can end up in an unstable state and de-excite e.g. by gamma-ray emission, at typical energies of few MeV for nuclei at rest. Although this has long been recognized as a potential exquisite diagnostic tool for the study of energetic phenomena in the interstellar medium, the observational challenges in MeV gamma-ray astronomy make this field still in its infancy.

B. Adiabatic energy losses

An ultrarelativistic particle propagating over distances undergoing the “cosmological” stretching (Hubble expansion with rate $H(z)$) sees its wavelength stretched similarly. Hence

$$-\frac{1}{E} \frac{dE}{dt} = H(z) = H_0 \sqrt{\Omega_\Lambda + \Omega_M(1+z)^3}. \quad (162)$$

We expressed $H(z)$ in terms of the matter energy density (normalised to the critical one) $\Omega_M \simeq 0.3$, and the cosmological constant density parameter $\Omega_\Lambda \simeq 1 - \Omega_M \simeq 0.7$. H_0 is the current Hubble parameter, whose value is roughly of 70 km/s/Mpc.

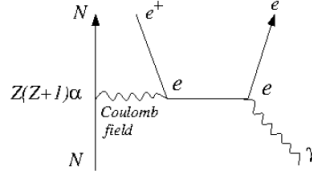
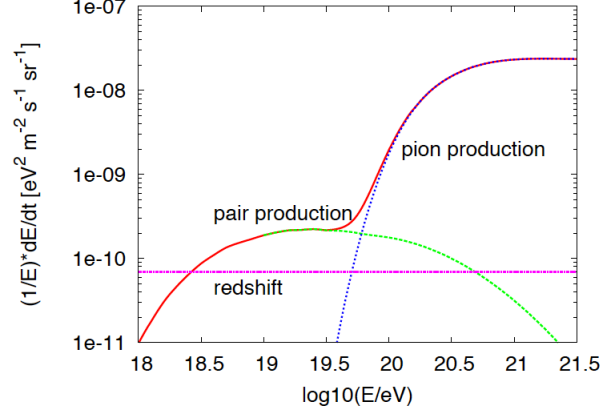


FIG. 24: Feynman diagram for the Bethe-Heitler process.

FIG. 25: Attenuation lengths at $z = 0$ for the main energy loss mechanisms for UHECR protons, from [45].

C. Bethe-Heitler process

It is the process $p + \gamma_{\text{CMB}} \rightarrow p + e^+ e^-$ (and, by extension, its analogous for nuclei). Its threshold is

$$m_p^2 + 2\epsilon_\gamma E_p (1 - \cos\theta) > (m_p + 2m_e)^2 \implies E_p \gtrsim \frac{m_e m_p}{\epsilon_\gamma} \simeq 2 \times 10^{18} \text{ eV}. \quad (163)$$

Its inelasticity is however rather low, of the order of $2m_e/m_p \simeq 10^{-3}$ at threshold (where the energy repartition basically follows the relative mass carried by the product, with the ensemble considered as a “decaying” particle). In its Feynman diagram, shown in Fig. 24, there are three interaction vertices, so not surprising its cross-section is of the order α^3 (or, if you wish, parametrically suppressed by a factor α compared to the Thomson cross-section). A rough estimate of the cross-section is

$$\sigma_{\text{BH}} \simeq \frac{\alpha^3}{m_e^2} Z^2 f(E, Z), \quad (164)$$

with $f(E, Z)$ of order one. Some more detailed parameterization can be found e.g. in [44]. For particles propagating over cosmological distances, if this channel is open onto the CMB photons it is important in limiting the range below the one due to Eq. (162). At low redshift, the associated energy-loss length is shown in green Fig. 25, which we see becomes more important than Eq. (162) above about $E \gtrsim 10^{18.5} \text{ eV}$. This mechanism also affects nuclei, for which it is comparatively more prominent since depending upon the nuclear charge as Z^2 .

D. Nuclear photodisintegration

For nuclei propagating over extragalactic distances, the photodisintegration process $A + \gamma \rightarrow (A - 1) + N + \gamma$ in the EBL (first) and CMB (at higher energies) is kinematically open. For typical nuclear binding energies of $\mathcal{O}(10) \text{ MeV}$, it is easy to check that the threshold lies at $E > 10^{19} \text{ eV}$ (just think that the threshold should be one order of magnitude higher than for the e^\pm pair production for the Bethe-Heitler.) with details depending on the nucleus: It typically damps the propagation of light nuclei before heavier one, with the Fe whose flux is only affected by this process closer to 10^{20} eV .

E. Inelastic pp collisions

This is the main energy-loss phenomenon affecting protons of Galactic Cosmic rays. If we specialize Eq. (113) to the case $p + p \rightarrow p + p(n) + \pi^0(\pi^+)$, neglecting the neutron-proton mass difference we get

$$2m_p^2 + 2E_p m_p > (2m_p + m_\pi)^2 \implies 2m_p E_p > 2m_p^2 + m_\pi^2 + 4m_p m_\pi \implies E_p > m_p + 2m_\pi + \frac{m_\pi^2}{2m_p} \simeq 1.2 \text{ GeV}. \quad (165)$$

Exercise: Without neglecting proton neutron mass difference, estimate the minimum energy needed to produce: i) at least one positive pion; ii) at least one negative pion in a pp reaction. *Hint:* impose baryon number, lepton number and electric charge conservation, and remember that free nucleons are not always the ground state of a multi-nucleon configuration!

F. $p\gamma$ collisions

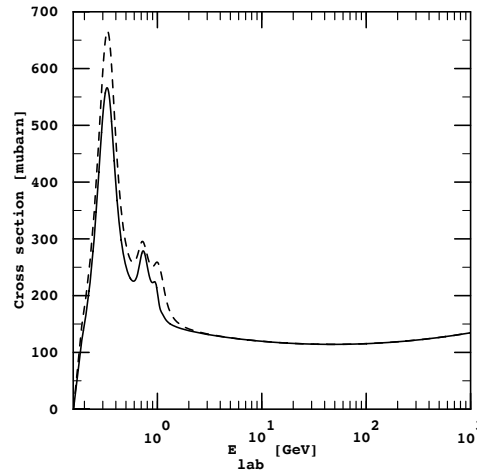


FIG. 26: The total photo-pion production cross section for protons (solid line) and neutrons (dashed line) as a function of the photon energy in the nucleon rest frame, E_{lab} .

If we specialize Eq. (113) to the case $p + \gamma \rightarrow p + \pi$, we get

$$m_p^2 + 2E_\gamma m_p > (m_p + m_\pi)^2 \implies E_\gamma > m_\pi + \frac{m_\pi^2}{2m_p} \simeq 145 \text{ MeV}, \quad (166)$$

where the numerical estimate is for π^0 . If the proton is instead relativistic, at threshold (heads-on)

$$m_p^2 + 4\epsilon_\gamma E_p > (m_p + m_\pi)^2 \implies E_p > \frac{2m_p m_\pi + m_\pi^2}{\epsilon_\gamma} \simeq 4 \times 10^{19} \text{ eV}, \quad (167)$$

for CMB photons. The inelasticity is of the order of $m_\pi/m_p \sim 15\%$ (actually a bit higher). The cross-section for this process, shown in Fig. 26, is dominated by the resonant production of a spin-3/2 and isospin 3/2 Δ^+ particle (of mass 1.232 MeV) just above threshold. Multi-particle processes dominate at much higher energy.

This process onto CMB photons is the most important process limiting the propagation of extragalactic protons, so dramatic to be known as *Greisen-Zatsepin-Kuzmin limit or cutoff* [46, 47].

Exercise: Based on the cross-section value of Fig. 26, compute the mean free path of a proton propagating in the CMB, and compare with Fig. 25. Differently from the BH process, here the inelasticity is quite high, hence losses are “catastrophic” and the concepts of mean free path and energy loss length blur. This is even more prominent given the steep CR spectrum, so that a proton losing a moderate fraction of its energy, even when surviving, contributes little to the flux at the lower energy.

XI. THE DIFFUSION-LOSS EQUATION: INCLUDING COLLISIONAL EFFECTS

In the light of what we have seen, the previously derived Eq. (85) requires some final generalizations concerning loss terms (besides a source term Q , to be provided by some theory of acceleration and injection). The two types of terms missing are “continuous energy losses” (such as Bremsstrahlung on the gas) and catastrophic ones, such as spallations and pp inelastic processes.

A. Catastrophic losses

These are treated as “source and sink terms” at the RHS of the propagation equation, since the species “changes nature” (disappears and/or evolves discontinuously in energy space). In particular, you are familiar with the fact that a radioactive species suffers of a term $-n/\tau$ (with n phase space density) at the RHS, where τ is its decay lifetime. Such a term is obviously present for unstable nuclei, apart for the generalization that in the lab frame, the decay time is boosted by the gamma factor of the nucleus: If τ_0 is the proper decay time of the species there is a $-\phi/(\gamma(p)\tau_0)$ at the RHS. For a species subject to collisional *interactions* that make it disappear, $1/(\gamma\tau_0) \rightarrow \Gamma$, with the interaction rate defined already in Eq. (A1), with n the gas target and the σ the cross-section for the specific process. Note how, differently from a decay, this term is in general space-dependent, and $\Gamma \rightarrow 0$ when the target density $n \rightarrow 0$. On the other hand, these interaction processes do produce secondary particles, so that they are also associated to *source* terms for other species. Sometimes, in fact, a specific channel may be negligible if considered a loss one for a species, but crucial as a source term for a secondary species (think of antiprotons produced in CR proton collisions). We can symbolically write this “secondary” source term for a species α as $\sum_{\beta} \Gamma_{\beta \rightarrow \alpha} \phi_{\beta}$. For nuclei sourced via spallation, if the transport equation is written in terms of Energy/nucleon, then this expression is almost exact, and not only symbolic. However, one should be aware that the true expression requires a convolution over energies (and the differential cross sections) since the secondaries have a degraded energy distribution with respect to the primaries.

B. Continuous energy losses

Under this category fall ionisation and Coulomb losses (however only important at energies below \sim GeV). In addition, electrons and positrons interact with the ISM emitting bremsstrahlung (again, only important at \sim few GeV energies), but also synchrotron radiation on the galactic magnetic fields and inverse Compton scattering on interstellar radiation fields, which are instead very important at tens of GeV or above. To deduce the form of such a term, let us consider the problem of the spectral intensity of particles only subject to injection and energy-losses. Since particles do not disappear once injected, a *continuity equation in E space holds*:

$$\frac{\partial F}{\partial t} + \frac{\partial}{\partial E}(\dot{E}F) = Q(E), \quad (168)$$

where $Q(E)$ is the injection term. If written in terms of phase space density or its angular average $\phi = F(E)/p^2$, the term corresponding to $\partial(\dot{E}F)/\partial E$ writes

$$-\frac{1}{p^2} \frac{\partial}{\partial p} \left[p^2 \left(\frac{dp}{dt} \right)_{\ell} \phi \right]. \quad (169)$$

C. The “complete” diffusion-loss equation and some benchmark solutions

For a coupled set of species α , we can thus write the master equations

$$\frac{\partial \phi_{\alpha}}{\partial t} - \frac{\partial}{\partial x_i} K_{ij} \frac{\partial \phi_{\alpha}}{\partial x_j} + u_i \frac{\partial \phi_{\alpha}}{\partial x_i} - \frac{1}{3} \frac{\partial u_i}{\partial x_i} \left(p \frac{\partial \phi_{\alpha}}{\partial p} \right) + \frac{1}{p^2} \frac{\partial}{\partial p} \left[p^2 \left(\frac{dp}{dt} \right)_{\ell} \phi_{\alpha} \right] - \frac{1}{p^2} \frac{\partial}{\partial p} \left(p^2 K_{pp} \frac{\partial \phi_{\alpha}}{\partial p} \right) = q - \Gamma \phi_{\alpha} + \sum_{\beta} \phi_{\beta} \Gamma_{\beta \rightarrow \alpha}, \quad (170)$$

where we have identified in color the terms introduced previously in this section. Note that each term in the above equation has the dimension of ϕ /time. One can thus define “characteristic timescales” (analogous to Eq. (118)) which allow for a quick parametric assessment of the importance of each term. Public available codes exist that allow for a numerical (such as GALPROP, DRAGON) or semi-analytical (USINE) solution of the problem. It is important however to grasp the key features of these terms via some analytical, limiting solution, notably of the steady state problem.

1. E-loss dominated propagation

If continuous energy loss timescales are the shortest ones (or the only one of relevance, in “quasi-homogeneous” problems), the steady state equation approximates to

$$-\frac{1}{p^2} \frac{\partial}{\partial p} \left[p^2 \left(\frac{dp}{dt} \right)_\ell \phi_\alpha \right] = q \implies \phi(p) \propto -\frac{1}{p^2 (dp/dt)_\ell} \int^p dp' q(p') p'^2, \quad (171)$$

which, for $q \propto p^{-s}$ and $(dp/dt)_\ell \propto -p^\ell$, leads to

$$\phi(p) \propto p^{-s-\ell+1}. \quad (172)$$

Namely, *the resulting spectrum is $\ell - 1$ softer than the injected one*. It turns out that for CR leptons, the above situation is close to truth, with ionization and Coulomb Energy losses ($\ell \simeq 0$) dominating at low-energies (spectrum is harder than the source), eventually overcome by bremsstrahlung energy losses ($\ell \simeq 1$, spectrum matching the source one) and Compton-Synchrotron energy losses ($\ell \simeq 2$ steeper spectrum). Note also that the diffusion-continuous loss problem (at least for space-independent loss term) is reduced to the diffusion problem (and thus to Eq. (63)) via a variable transformation into a “pseudo-time”, see for instance Sec. II in [48], where the adaptation of the Green’s function method to a geometry with boundaries is also shown.

2. Catastrophic loss for diagnostics: Secondaries over primaries

Let us apply the previous equation to the case of secondaries, i.e. nuclei only produced by spallation during propagation, such as the above-mentioned Boron, Lithium, and Beryllium. The distribution of secondaries in the plane, $\phi_S(p)$ is sourced by the injected nuclides per unit time, i.e. $q_0(p) \rightarrow \phi_P \Gamma_{P \rightarrow S}$, ϕ_P being the primary population. Hence we obtain the solution for the ratio of primary to secondary distribution; prove that

$$\frac{\phi_S(p)}{\phi_P(p)} \simeq \Gamma_{P \rightarrow S} \tau_{\text{eff}, P} \simeq \Gamma_{P \rightarrow S} \frac{H h}{K(p)}. \quad (173)$$

where the second relation holds if collisions are subdominant with respect to diffusion (which is not true at low energies!). Since, at least in principle, $\Gamma_{P \rightarrow S} h$ can be inferred by independent means, from this ratio (for instance, Boron-to-Carbon ratio in CRs) one can gauge the value of the “diffusive” ratio H/K , including its energy dependence.

Exercise: Modify eq. (67) to account for a catastrophic loss term, of the type $-2h \Gamma_\sigma \phi_P \delta(z)$. Consider the same equation written for secondaries, i.e. without primary source term q , but sourced by primary spallation, i.e. $2h \Gamma_{P \rightarrow S} \phi_P \delta(z)$. Prove eq. (173).

3. Principles underlying dark matter searches via CRs

The previous exercise suggests that, by measuring some secondary to primary ratios (such as the “classical” Boron over Carbon), one can infer the universal function $\tau_d(p)$ through which one should be able to predict *all* other secondary to primary ratios, provided that the relevant nuclear data are known. This is essentially the case, so that within uncertainties one finds that the $\tau_d(p)$ function inferred from analysing different S/P are consistent.

Now, imagine that there is some species that is purely secondary in conventional physics, but that admits some exotic *primary* source: Observing the flux of this species in excess of the secondary prediction may offer a discovery tool. Alternatively, if the species is observed in accordance with the expectations, bounds on such an exotic primary term can be set.

The most widely considered exotic primary source of CRs is from dark matter annihilations⁹, notably if DM is in the form of WIMPs. In particular, these processes should produce equal yields of SM particles and antiparticles, so that the search for DM in antiparticles (and antinuclei, in principle) is greatly enhanced by the lack of primary antiparticles in the conventional scenario.

⁹ Other exotic mechanism sometimes considered are dark matter decays, or the evaporation via the Hawking process of rather light black holes produced in the early universe.

Positrons were once believed to be essentially secondary particles, but now it is universally acknowledged that there is a primary component, probably due to PWN, becoming dominant in at $E \gtrsim 10$ GeV, so that their usefulness as a DM discovery tool has been somewhat undermined (albeit they can be still used to set bounds).

Antiprotons are currently studied as a promising discovery channel. In principle, they are sources by mostly CR protons (and to some extent He nuclei) impinging onto the ISM gas. Knowing the steady state fluxes of protons and He, and knowing the propagation properties from studies such as S/P ones, should make us capable of predicting power on the secondary contribution to antiprotons. However, you should be aware of the fact that this approach is not without difficulties. One of these difficulties consists in the fact that *primary* fluxes turn out to depend upon astrophysical parameters in a different way than secondary fluxes. Hence, further (astrophysical) constraints are typically needed for tight searches. To illustrate this point, let us consider the following toy model

$$-\frac{\partial}{\partial z} \left(K \frac{\partial \phi_X}{\partial z} \right) = q_X(p) - 2h \Gamma_\sigma \phi_X \delta(z). \quad (174)$$

where the production of antiprotons q_X is considered uniform over the vertical (diffusive) extent $\pm H$. Although not geometrically correct, since the whole, extended DM halo hosts the antiproton sources, this tries to capture the fact that, for a DM origin the source is much more vertically extended than the thin disk for the conventional astrophysical model where they arise as secondaries.

I invite you to show as a simple **Exercise** that eq. (174) implies

$$\frac{1}{\tau_{\text{eff}}(p)} \phi_X^0 = \frac{H}{h} q_X(p), \quad (175)$$

where $\tau_{\text{eff}}(p)$ is the same defined in Eq. (??). Note that now the expected antiproton signal from DM depends on one extra parameter, the ratio H/h as opposed to the product Hh entering τ_d . This extra dependence makes physical sense, because it is linear in the size of the volume from which one collects injected particles.

Imagine now that the actual flux at the Earth is made of two contributions: An astrophysical one plus a DM one. Even if the respective source terms were exactly known (which is not true, think for instance of cross-section uncertainties), one has to account for propagation effects. And even if the “astrophysical” ones were under control (e.g. B/C ratio, etc.), so that secondary to primary ratio allows one to determine τ_d from observations (but there are errors associated to that!), the DM contribution is subject to further *astrophysical/propagation* uncertainties, which are more difficult to reduce, since they depend *differently* from the astrophysical parameters. Although some handles exist (such as radioactive CRs for the above example of H determination), this “propagation problem” is one of the main difficulties to keep in mind associated to these types of searches. Put otherwise: Astrophysical uncertainties in new physics searches do not factor out, even when “normalising” to other channels. These “systematic” uncertainties are the main limitations in pushing the sensitivity of these probes.

D. On some limitations of the theory presented

Eq. (170) above is used in almost all phenomenological treatments of Galactic CR propagation. Needless to say, this is still an approximation. The two major limitations of this treatment are:

- The requirement that the scattering centers are moving non-relativistically. This is crucial in obtaining a hierarchy between the isotropic and anisotropic part of the CR distribution, the latter in turn being dominated by the dipole term. This is certainly inadequate in relativistic environments (such as gamma-ray bursts, or most candidate sources for ultra-high energy cosmic rays), where a technical difficulty is that the distribution function retains a non-trivial angular dependence.
- At a more conceptual level, we have performed some further approximations. First, we assumed that a kinetic description in terms of the single-particle distribution function is suitable, i.e. we neglected particle-particle correlations terms (entering higher-order equations of the BBGKY (Bogoliubov-Born-Green-Kirkwood-Yvon) hierarchy), implicitly adopting the so-called *plasma approximation*. More importantly, even the single particle distribution functions f_a (for

the species a) are ruled by Maxwell-Vlasov equations

$$\frac{\partial f_a}{\partial t} + \mathbf{v} \cdot \frac{\partial f_a}{\partial \mathbf{x}} + \frac{q_a}{m_a} (\mathbf{E} + \mathbf{v} \times \mathbf{B}) \cdot \frac{\partial f_a}{\partial \mathbf{v}} = 0. \quad (176)$$

$$\nabla \times \mathbf{B} = \frac{\partial \mathbf{E}}{\partial t} + 4\pi \left(\mathbf{j}_{\text{ext}} + \sum_b q_b \int d\mathbf{p} \mathbf{v}_b f_b \right) \quad (177)$$

$$\nabla \times \mathbf{E} = -\frac{\partial \mathbf{B}}{\partial t} \quad (178)$$

$$\nabla \cdot \mathbf{B} = 0 \quad (179)$$

$$\nabla \cdot \mathbf{E} = 4\pi \left(\rho_{\text{ext}} + \sum_b q_b \int d\mathbf{p} f_b \right) \quad (180)$$

$$(181)$$

where ρ_{ext} and \mathbf{j}_{ext} represent external charge densities and currents due to non-dynamical components of the medium, such as the background thermal plasma. In general, we see that *the CR themselves contribute to generate the fields in which they propagate*. This coupling has been ignored. A simple way to convince oneself that some coupling must be accounted for, in order to guarantee the consistency of the previous description, is to think about the isotropisation process. If CR tend to be isotropized in the frame of the plasma, where does the initial CRs momentum go? In fact, it constitute a current, acting as one of the sources of the e.m. waves of similar type to the ones onto which CRs scatter. Put otherwise, we have taken the magnetic perturbations as given externally, but truly they are dynamically coupled to the CRs. This *non-linear approach* to CR acceleration and propagation is at the forefront of current research.

Part V

Multimessenger astrophysics

The examples previously discussed combine different probes (e.g. B, C, proton ... spectra) to make predictions on yet another observable (antiproton flux) and make us acquire diagnostic power for a different phenomenon (indirect searches of DM). This philosophy is extremely common in high-energy astrophysics. Often it also involves neutral particles, photons and neutrinos, since they are produced by charged CRs. We saw examples of these channels when dealing with leptonic energy losses. Here we focus on hadronic production channels, which are behind a key expectation in high-energy astrophysics: The link of neutrino fluxes with (hadronically produced) high-energy photons, the link holding *at the source*. This has been crucial to build expectations for both diffuse neutrino fluxes and point-like ones, and in the end to set the experimental size of neutrino detectors, recently seeing the first detections.

XII. SPECTRA OF PION DECAY BYPRODUCTS

A. Gamma spectra emitted in neutral pion decays

Let us consider the neutral pion decay process, $\pi^0 \rightarrow \gamma\gamma$: The photons are back-to-back in the π^0 frame (momentum conservation), each carrying $E_\gamma = m_\pi/2 \simeq 67.5$ MeV (energy conservation). If the pion moves at β , in the Lab frame the energy of the photon emitted is $m_\pi\gamma(1 + \beta \cos\theta)/2$, θ being the angle of the emitted photons with respect to the the direction of flight of the pion. Hence, the maximal and minimal energy of the photons is

$$E_{\text{min}}^{\text{max}} = \frac{m_\pi}{2} \gamma (1 \pm \beta), \quad (182)$$

i.e. from 0 to E_π in the ultra-relativistic limit. Also note that there is a one-to-one correspondence between photon energy and emission angle, whose law is

$$dE = \frac{m_\pi}{2} \gamma \beta d \cos \theta. \quad (183)$$

Since the pion is a scalar particle, its decay products are emitted isotropically, i.e. (just normalizing to one)

$$\frac{dN}{d\Omega} = \frac{1}{4\pi} \implies dN = \frac{1}{2} d \cos \theta, \quad (184)$$

hence the energy distribution of the photons is

$$\frac{dN}{dE} = \frac{1}{m_\pi \gamma \beta} = \frac{1}{E_\pi \beta} = \frac{1}{\sqrt{E_\pi^2 - m_\pi^2}}, \quad (185)$$

i.e. flat in energy space, between $E_{\min} \simeq 0$ and $E_{\max} \simeq E_\pi$ in the relativistic limit. Basically, one expects a box spectrum, symmetric around $m_\pi/2$. In log-Energy space,

$$\frac{1}{2}(\log E^{\min} + \log E^{\max}) = \log \sqrt{E^{\min} E^{\max}} = \log \left(\frac{m_\pi}{2} \sqrt{\gamma^2 (1 - \beta^2)} \right) = \log \left(\frac{m_\pi}{2} \right), \quad (186)$$

i.e. *the center of the interval is half the pion mass, independently of the pion energy distribution, hence of the parent nucleon distribution.* This is dubbed “pion bump” and considered in principle the cleanest signature of hadronic origin of a gamma-ray spectrum. (In practice, very often one has only access to the high-energy tail of the spectrum!)

A useful approximation for the spectrum of pions from hadronic interaction is the delta approximation, where a fixed inelasticity is considered,

$$E_\pi \simeq \kappa_\pi E_p. \quad (187)$$

Then (assuming for simplicity a pure hydrogen target and relativistic projectiles)

$$q_\pi(E_\pi) = n_H \int dE_p \delta(E_\pi - \kappa_\pi E_p) \sigma_{pp \rightarrow \pi}(E_p) \Phi(E_p) = \frac{n_H}{\kappa_\pi} \sigma_{pp \rightarrow \pi} \left(\frac{E_\pi}{\kappa_\pi} \right) \Phi \left(\frac{E_\pi}{\kappa_\pi} \right), \quad (188)$$

where $\sigma_{pp \rightarrow \pi}(E_p)$ is the pion-production cross section, rising quickly above threshold to $\mathcal{O}(100)$ mb and then growing only slowly with energy (logarithmically), not unlikely the overall inelastic cross-section ($\delta(\dots)\sigma_{pp \rightarrow \pi}$ is a “simple” way to write the differential cross section that a proton of energy E_p produces a pion of energy E_π . For more advanced formulae, see e.g. [49] or [50])

To a leading order, the pion source spectrum at E_π is thus proportional to the proton flux at an energy $E_p = E_\pi/\kappa_\pi$ (with sizable corrections due to the cross-section energy dependence relevant close to threshold). The photon spectrum is then trivially obtained as

$$q_\gamma(E_\gamma) = 2 \int_{E_\pi^{\min}(E_\gamma)}^\infty dE_\pi \frac{dN}{dE} q(E_\pi) = 2 \int_{E_\gamma + \frac{m_\pi^2}{4E_\gamma}}^\infty dE_\pi \frac{q(E_\pi)}{\sqrt{E_\pi^2 - m_\pi^2}}, \quad (189)$$

where the minimum energy of the pion to produce a photon of energy E_γ , $E_\pi^{\min}(E_\gamma)$, is given by the relation linking the maximal energy of a photon produced by a pion of E_π . Note that the last step follows from the properties

$$E_\gamma^{\max} E_\gamma^{\min} = \frac{m_\pi^2}{4}, \quad E_\gamma^{\max} + E_\gamma^{\min} = E_\pi. \quad (190)$$

For a given energy E_π , the maximum energy of the photons is

$$E_\gamma^{\max} = E_\pi - E_\gamma^{\min} = E_\pi - \frac{m_\pi^2}{4E_\gamma^{\max}}, \quad (191)$$

hence solving for E_π by inversion it follows

$$E_\pi^{\min}(E_\gamma) = E_\gamma + \frac{m_\pi^2}{4E_\gamma}. \quad (192)$$

To go beyond, optional exercise: Compute the *shape* of $q_\gamma(E_\gamma)$ for some test pion source term, such as a power-law, a gaussian, etc. For a more advanced/realistic application, you can also use the fitting formula of Eq. (1) in [51] and the approximation $q_\pi(E_\pi) \propto \Phi_p \left(\frac{E_\pi}{\kappa_\pi} \right)$. Plot $q_\gamma(E_\gamma)$ in linear scale and $E_\gamma^2 q_\gamma(E_\gamma)$ in log-log one. Compare with [51].

B. Neutrino spectra emitted in charged pion decays

For the process $\pi \rightarrow \mu + \nu$, the spectrum is monochromatic in the pion rest frame, at an energy satisfying (neutrino assumed massless)

$$(p_\pi - p_\nu)^2 = p_\mu^2 \implies E_\nu^* = \frac{m_\pi^2 - m_\mu^2}{2m_\pi} \simeq 29.8 \text{ MeV}. \quad (193)$$

If the pion moves at β , in the Lab frame the energy of the neutrino emitted is $E_\nu = E_\pi^* \gamma (1 + \beta \cos \theta)$, θ being the angle of the emitted neutrino with respect to the the direction of flight of the pion. Hence, the maximal energy of the neutrinos is

$$E_\nu^{\max} = \frac{m_\pi^2 - m_\mu^2}{2m_\pi} \gamma (1 + \beta) \simeq \frac{m_\pi^2 - m_\mu^2}{2m_\pi} 2\gamma = \left(1 - \frac{m_\mu^2}{m_\pi^2}\right) E_\pi \equiv \lambda E_\pi \simeq 0.427 E_\pi, \quad (194)$$

where the last equalities hold for very relativistic pions, $\beta \simeq 1$. Similarly to what seen for photons, inverting the latter given the minimum pion energy yielding a given neutrino energy, hence

$$q_\nu(E_\nu) = \int_{E_\pi^{\min}(E_\nu)}^\infty dE_\pi \frac{dN}{dE} q(E_\pi) = \int_{E_\nu/\lambda}^\infty dE_\pi \frac{q(E_\pi)}{\lambda E_\pi}. \quad (195)$$

Note that Eq. (185) holds unchanged for neutrinos and, given that $dE_\nu = E_\nu^* \gamma \beta d \cos \theta$, the energy distribution of the neutrinos is

$$\frac{dN}{dE} = \frac{1}{2E_\nu^* \gamma \beta} \simeq \frac{1}{\lambda E_\pi}. \quad (196)$$

For a power-law form of $q_\pi(E_\pi)$, the above expression indicates that the neutrino from pion decay has the same power-law.

Similar considerations (but a bit more involved) can be applied to the muon spectrum from the pion decay and, in turn, to its three body decay $\mu \rightarrow e + \nu \bar{\nu}$ to yield the complete neutrino spectrum. Note that the muons from charged pion decays are also the main parents of the so-called *secondary* electrons and positrons in CRs. In particular, until a few years ago, it was believed that most CR positrons in the GeV-TeV range should originate via this mechanism (ultimately coming from $pp \rightarrow \pi^+$ reactions and analogous nuclear processes), while now a sizable contribution of primary sources seems favoured.

It is worth noting that each process producing a π^0 is associated to a process producing a π^+ (that is the case of $p\gamma \rightarrow p\pi^0$, associated to $p\gamma \rightarrow n\pi^+$) or to both π^+ and π^- : For the pp process one is practically always well above threshold, multipion production is frequent, and isospin symmetry yields equal numbers of π^0 , π^+ , and π^- . For the $p\gamma$ process, one is often close to threshold and the number of π^- is much lower than the one of π^0 and π^+ , which are instead comparable. Similarly, the energies of the two types of particles are similar, within a factor of 2: neutrinos carry a fraction between 1/4 and 1/2 of the parent pion, while photons exactly a fraction 1/2 of it. We will discuss below some implications of this link.

XIII. DIFFUSE EXTRAGALACTIC FLUXES

Since there is virtually no neutrino horizon (the optical depth = 1 is attained for cosmological epochs), any population of neutrino sources will lead to a diffuse neutrino flux whose spectrum depends on the source spectrum and the cosmic evolution of the population.

Let us consider a typical source with the (all flavor, but can be generalised to flavour-dependent) neutrino yield $\frac{dN_\nu}{d\varepsilon_\nu}(\varepsilon_\nu, z)$ in $[\text{GeV}^{-1} \text{s}^{-1}]$, where ε_ν is the energy of neutrinos at production. Its integral over energy gives the number of neutrinos per second emitted at the source. In principle, the spectrum can have an intrinsic dependence on z , as indicated, but in the following we assume that this is not the case (so that neutrino sources are “standard candles”). This means that the luminosity, given by

$$L_\nu = \int_{\varepsilon_{\min}}^{\varepsilon_{\max}} d\varepsilon_\nu \varepsilon_\nu \frac{dN_\nu}{d\varepsilon_\nu} = \text{const.} \quad (197)$$

The differential diffuse neutrino flux at the Earth, $\frac{d\phi_\nu}{dE_\nu}(E_\nu)$ in $[\text{GeV}^{-1} \text{cm}^{-2} \text{s}^{-1} \text{sr}^{-1}]$, from a population of these sources with cosmic evolution $\mathcal{F}(z)$ (density in comoving volume) in $[\text{Mpc}^{-3}]$ or $[\text{cm}^{-3}]$ is given by

$$\frac{d\phi_\nu}{dE_\nu}(E_\nu) = \frac{1}{4\pi} \int dz \frac{d\mathcal{V}_c}{dz} \mathcal{F}(z) \frac{1}{4\pi d_c^2} \frac{dN_\nu}{d\varepsilon_\nu} [(1+z)E_\nu] = \frac{1}{4\pi} \int dz \frac{\mathcal{F}(z)}{H(z)} \frac{dN_\nu}{d\varepsilon_\nu} [(1+z)E_\nu], \quad (198)$$

where E_ν is the neutrino energy at Earth, $\mathcal{V}_c = 4\pi d_c^3/3$ is the comoving volume and d_c is the comoving distance, related to the *luminosity distance* d_L via $d_c(z) = d_L(z)/(1+z)$. $d\mathcal{V}_c/dz = 4\pi d_c^2(z)/H(z)$, and $H(z) = H_0 \sqrt{\Omega_\Lambda + \Omega_M(1+z)^3}$ is the Hubble rate. The total number of sources contributing is

$$\int dz \frac{d\mathcal{V}_c}{dz} \mathcal{F}(z) = N_{\text{tot}}. \quad (199)$$

Note also that the total power received per unit surface and solid angle writes (in the second step, I set $y \equiv (1+z)E_\nu$):

$$\mathcal{P}_\nu \equiv \int dE_\nu E_\nu \frac{d\phi_\nu}{dE_\nu}(E_\nu) = \int dy \frac{y}{4\pi} \frac{dN_\nu(y)}{d\varepsilon_\nu} \int dz \frac{\mathcal{F}(z)}{(1+z)^2 H(z)} = \frac{L_\nu \mathcal{F}(0)}{4\pi H_0} \int \frac{dz}{(1+z)^2} \frac{\mathcal{F}(z)}{\mathcal{F}(0)} \frac{H_0}{H(z)} \equiv \frac{L_\nu \mathcal{F}(0) \xi_z}{4\pi H_0} \quad (200)$$

where the cosmological effect is encoded uniquely in the dimensionless coefficient ξ_z , usually an order 1 factor. Note the degeneracy L_ν vs. $\mathcal{F}(0)$: With the sole observable \mathcal{P}_ν we cannot disentangle fewer sources with higher luminosity from numerous sources with lower luminosities (for that, other observables like the number of multiplets/clusters of events can be used). \mathcal{P}_ν is fixed by the diffuse flux observations of IceCube.

Neutrino production through charged pion and kaon decay is associated to a γ -ray yield

$$\varepsilon_\gamma \frac{dN_\gamma}{d\varepsilon_\gamma} = \frac{4}{3\kappa} \left[\varepsilon_\nu \frac{dN_\nu}{d\varepsilon_\nu} \right]_{\varepsilon_\nu = \varepsilon_\gamma/2}, \quad (201)$$

where the neutral to charged pion ratio $\kappa \approx 1$ for the $p\gamma$ scenario, since one has 1 neutral pion each π^+ pion (negligible production of π^-) and neutrinos carry 3/4 of the energy of the (charged) pion, while photons carry the totality of the (neutral) pion energy. For the pp channel, multi-pion production (in the isospin symmetric limit) dominates, so that $\kappa = 2$, since there are twice as many charged pions per neutral one.

Note that Eq. (201) is a *minimal* Ansatz on the γ -ray flux, since it ignores any further leptonic contribution which would have no neutrino counterpart. While propagating from the sources (assumed transparent) to the Earth, γ -rays initiate electromagnetic cascades by pair-production on and inverse-Compton scattering off the CMB and EBL, resulting in a diffuse γ -ray flux at the Earth with energies $\lesssim 1$ TeV. The exact spectral shape of the diffuse γ -ray flux depends on the cosmic evolution $\mathcal{F}(z)$ and the distance to the sources. In the limit of fully developed cascades, with some approximations one can derive analytically a universal spectral shape for the diffuse γ -ray flux [2, 52]. This is given by:

$$n_\gamma(E_\gamma) = \begin{cases} (K/\mathcal{E}_X)(E_\gamma/\mathcal{E}_X)^{-3/2} & \text{at } E_\gamma \leq \mathcal{E}_X \equiv \frac{1}{3}\mathcal{E}_\gamma \frac{\varepsilon_{\text{CMB}}}{\varepsilon_{\text{EBL}}} \simeq 1.2 \times 10^8 \text{ eV} \\ (K/\mathcal{E}_X)(E_\gamma/\mathcal{E}_X)^{-2} & \text{at } \mathcal{E}_X \leq E_\gamma \leq \mathcal{E}_\gamma \\ 0 & \text{at } E_\gamma > \mathcal{E}_\gamma \equiv \frac{m_e^2}{\varepsilon_{\text{EBL}}} \simeq 3.9 \times 10^{11} \text{ eV} \end{cases} \quad (202)$$

where the normalisation is given in terms of the total injection energy E_s as

$$K = \frac{E_s}{\mathcal{E}_X (2 + \ln \mathcal{E}_\gamma/\mathcal{E}_X)}. \quad (203)$$

In comparing different choices of $\mathcal{F}(z)$ it may be appropriate to compute the spectrum numerically, in order to account for the spectra of the background photons and the fact that for the closest sources the cascade development may not be complete. Barring these complications, the main message to retain is that even if photons are subject to energy reprocessing, as long as there is no “leakage” from the gamma-ray band, we should expect that $\mathcal{P}_\gamma^{\text{had}} = 4\mathcal{P}_\nu/(3\kappa)$.

Fermi-LAT has measured the isotropic energy density above ~ 1 GeV as being

$$\frac{4\pi}{c} \mathcal{P}_\gamma^{>1 \text{ GeV}} = 5.7 \times 10^{-7} \text{ eV/cm}^3 \quad (204)$$

which is basically fully accounted for (within errors) by the unresolved part of known populations of gamma-ray emitters which *do not show significant correlations* with the arrival directions of IceCube neutrinos. Unless our understanding of the gamma-ray sky is deeply flawed, we are currently in the situation where $\mathcal{P}_\gamma^{\text{obs}} - \mathcal{P}_\gamma^{\text{known}} \lesssim \mathcal{P}_\nu$. This has been used in the literature to raise the possibility that most of the sources contributing to the IceCube flux are actually *opaque* (i.e. the associated gamma-rays are degraded to MeV or even thermal energies before escaping the sources). See for instance [53] and refs. therein.

A similar but slightly looser argument [54] was used at the end of past century to argue that, attributing UHE-CRs above 10^{19} eV to extragalactic sources, one should expect a neutrino flux above ~ 10 PeV of $\mathcal{P}_\nu^{>10 \text{ PeV}} \lesssim 2 \times 10^{-8} \text{ GeV cm}^{-2} \text{ s}^{-1} \text{ sr}^{-1}$. Assuming a relevant cross-section of about $2 \times 10^{-33} \text{ cm}^2$, a medium of density $n \simeq 1 \text{ g/cm}^3$ (water, ice), the rate of events in a volume of $V \text{ cm}^3$ writes (assuming half-sky acceptance)

$$\Gamma = 2\pi\sigma N_A \frac{\mathcal{P}_\nu^{>10 \text{ PeV}}}{10 \text{ PeV}} V_{\text{cm}^3} \simeq 1 \times 10^{-32} 6 \times 10^{23} \frac{2 \times 10^{-8}}{10^7} \text{ events/s} \simeq 10^{-15} V_{\text{cm}^3} \text{ events/yr}. \quad (205)$$

This implies that we need a detector of linear size $V_{\text{cm}^3}^{1/3} \simeq (10^{15})^{1/3} \simeq 10^5 \text{ cm} = \text{km}$ in order to detect a few events per year! This was one of the arguments used to set the goal of a km^3 telescope in order to start neutrino astronomy. Perhaps coincidentally, perhaps not, it turned out to be correct!

To go beyond (optional more advanced exercise): Study e.g. [52] to gain a deeper understanding of the origin of the universal spectrum of Eq. (202).

To go beyond (optional more advanced exercise): Use Eq. (204), and the fact that the energy density that IceCube has detected in PeV neutrinos is of $2.7 \times 10^{-9} \text{ eV/cm}^3$, to infer a bound on the possible violation of Lorentz-invariance in the neutrino sector, according to the argument developed in [55].

Appendix A: Recap: Collisional random motions

The mean-free-path ℓ is the average distance travelled by a particle moving at velocity β in a medium of number density n before interacting. It is associated to the collision rate Γ , which has the dimensions of an inverse timescale. If σ is the cross-section of the interaction process, its mean-free-path and interaction rate are

$$\ell = \frac{1}{\sigma n}, \quad \Gamma = \sigma \beta n = \frac{\beta}{\ell} \quad (\text{A1})$$

For an opaque source of radius R , the optical depth is

$$\tau = \frac{R}{\ell}. \quad (\text{A2})$$

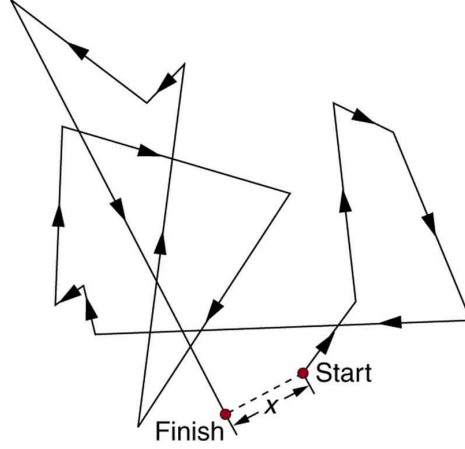


FIG. 27: Typical displacement vectors in a random motion.

For a “random motion” with vectors of average length ℓ and random direction after each bounce, see Fig. 27, the average distance X a particle moves away from its initial position vanishes, i.e.

$$\langle X \rangle_N = \left\langle \sum \vec{r}_i \right\rangle = 0. \quad (\text{A3})$$

However, its variance is (vectors randomly directed and of comparable lengths ℓ):

$$\langle X^2 \rangle_N = \left\langle \left(\sum_i \vec{r}_i \right) \cdot \left(\sum_j \vec{r}_j \right) \right\rangle = \sum_i \langle r_i^2 \rangle + \ell^2 \sum_{i \neq j} \langle \cos \theta_{ij} \rangle = \ell^2 N \quad (\text{A4})$$

How many scatterings are typically experienced by a particle before escaping a source with optical depth τ ? One has to require

$$\langle X^2 \rangle_N = R^2 \Rightarrow N = \tau^2 \quad (\text{A5})$$

How long does it take to escape? Obviously

$$t_{\text{esc}} = \Gamma^{-1} N = \frac{\tau^2}{\Gamma} = \frac{\tau R}{\beta}. \quad (\text{A6})$$

The law of Eq. (A4) is the discrete version of a diffusive propagation, with N proportional to the time elapsed via the constant Γ . We can thus guess the continuum limit

$$\langle X^2 \rangle(t) = \ell^2 \Gamma t = \ell \beta t, \quad (\text{A7})$$

or $X^2 \propto K t$ with the diffusion coefficient K roughly given by $K \propto \ell \beta$ (We have been omitting numerical constants depending on the space dimensions, see after Eq. (63) for a more rigorous calculation).

Appendix B: From Liouville equation to BBGKY hierarchy

a. Liouville Equation

Consider a classical¹⁰ system of N point-like particles, whose evolution is dictated by the hamiltonian H . If we denote by \vec{q}_k the canonical coordinate and by \vec{p}_k the conjugate momentum for the k -th particle, its motion is described by

$$\dot{\vec{q}}_k = \frac{\partial H}{\partial \vec{p}_k}, \quad (\text{B1})$$

$$\dot{\vec{p}}_k = -\frac{\partial H}{\partial \vec{q}_k}. \quad (\text{B2})$$

For simplicity of notation, let us define collectively the coordinates $\{\vec{q}_k, \vec{p}_k\}$ as τ_k . The most general information on the system is contained in its N -particle distribution function $\mathcal{F}(\tau_1, \dots, \tau_k, \dots, \tau_N)$, normalized to 1 over all the phase-space, which describes the probability to find particle 1 around $\vec{\tau}_1$, particle k around $\vec{\tau}_k$, etc. Of course, for identical particles the function is invariant under name re-labelling, which we shall assume henceforth. The volume element in phase space is preserved by the Hamiltonian evolution, which is equivalent to the following *Liouville theorem*

$$\frac{d}{dt} \mathcal{F} = 0, \quad (\text{B3})$$

which can also be rewritten in terms of *Poisson brackets* $\{\cdot, \cdot\}$ or the equations of motion,

$$\frac{\partial}{\partial t} \mathcal{F} - \{H, \mathcal{F}\} = 0, \iff \frac{\partial}{\partial t} \mathcal{F} - \sum_{k=1}^N \left[\frac{\partial H}{\partial \vec{q}_k} \cdot \frac{\partial \mathcal{F}}{\partial \vec{p}_k} - \frac{\partial H}{\partial \vec{p}_k} \cdot \frac{\partial \mathcal{F}}{\partial \vec{q}_k} \right] = 0. \quad (\text{B4})$$

In the simple case where H can be written as sum of kinetic energy $T_k(\vec{p}_k)$ plus (external) potential energy $U_k(\vec{q}_k)$, i.e.

$$H = \sum_k (T_k + U_k), \quad (\text{B5})$$

the Liouville theorem writes

$$\left[\frac{\partial}{\partial t} + h_N \right] \mathcal{F} = 0, \quad (\text{B6})$$

where

$$h_N(\vec{\tau}_1, \dots, \vec{\tau}_k, \dots, \vec{\tau}_N) = \sum_{k=1}^N \left[\frac{\partial T_k}{\partial \vec{p}_k} \cdot \frac{\partial}{\partial \vec{q}_k} - \frac{\partial U_k}{\partial \vec{q}_k} \cdot \frac{\partial}{\partial \vec{p}_k} \right]. \quad (\text{B7})$$

Note how this is the sum of N identical pieces, but for relabelling. If we integrate over all particle coordinate but the nr. 1, switch derivative and integral (and multiply times a factor N to ensure symmetrization over all particles, see below) we get

$$\left[\frac{\partial}{\partial t} + \dot{\vec{q}}_1 \cdot \frac{\partial}{\partial \vec{q}_1} - \frac{\partial U_1}{\partial \vec{q}_1} \cdot \frac{\partial}{\partial \vec{p}_1} \right] f^{(1)} = 0, \quad (\text{B8})$$

¹⁰ Classical kinetic theory can be argued to provide a good approximation if particle densities n are low enough that inter-particle distances are very large compared with the De Broglie wavelength, i.e. one is well above Heisenberg uncertainty limit: $n^{-1/3} p \gg 1$.

where we defined

$$f^{(1)}(\vec{\tau}_1) = N \int \mathcal{F} d\vec{\tau}_2, \dots d\vec{\tau}_N. \quad (\text{B9})$$

This $f^{(1)}(\vec{\tau}_1)$ is the particle density distribution function that we introduced in Eq. (34). It obeys an eq. formally identical to the Liouville eq. (B6) (with eq. (B7)), but this is valid only for this “separable” single particle hamiltonian.

In most cases, however, H can be written as sum of kinetic energy $T_k(\vec{p}_k)$, (external) potential energy $U_k(\vec{q}_k)$ and 2-body interaction energy $V_{kl}(|\vec{q}_k - \vec{q}_l|)$ between particle k and l , namely

$$H = \sum_k (T_k + U_k) + \sum_{k < l} V_{kl}. \quad (\text{B10})$$

In this sufficiently general case the Liouville theorem writes

$$\left[\frac{\partial}{\partial t} + h_N \right] \mathcal{F} = 0, \quad (\text{B11})$$

where

$$h_N(\vec{\tau}_1, \dots, \vec{\tau}_k, \dots, \vec{\tau}_N) = \sum_{k=1}^N \left[\frac{\partial T_k}{\partial \vec{p}_k} \cdot \frac{\partial}{\partial \vec{q}_k} - \frac{\partial U_k}{\partial \vec{q}_k} \cdot \frac{\partial}{\partial \vec{p}_k} \right] + \frac{1}{2} \sum_{k,l=1}^N \vec{W}_{kl} \cdot \left(\frac{\partial}{\partial \vec{p}_k} - \frac{\partial}{\partial \vec{p}_l} \right) \quad (\text{B12})$$

and we defined the 2-body “force” $\vec{W}_{kl} \equiv -\frac{\partial V_{kl}}{\partial \vec{q}_k}$. To deal with that, let us sketch the more general treatment.

b. BBGKY hierarchy

Virtually in no case of physical interest (i.e. with interactions!) one has access to the complete information on the system encoded in \mathcal{F} . In order to describe a partial (incomplete) information of the system, it turns useful to define “reduced” distribution functions by integrating over all but a few variables. In particular, we define $f^{(1)}(\vec{\tau}_1) \equiv \langle \sum_{k=1}^N \delta(\tau'_1 - \tau_k) \rangle$, so that

$$f^{(1)}(\vec{\tau}_1) = N \int \mathcal{F} \delta(\tau'_1 - \tau_k) d\vec{\tau}_1 d\vec{\tau}_2, \dots d\vec{\tau}_N = N \int \mathcal{F} d\vec{\tau}_2, \dots d\vec{\tau}_N, \quad (\text{B13})$$

note the pre-factor N coming out in association to the labelling-invariance. More in general, one defines

$$\begin{aligned} f^{(\ell)}(\tau'_1, \tau'_2, \dots, \tau'_\ell) &\equiv \left\langle \sum_{k=1}^N \sum_{l=1, l \neq k}^N \sum_{m=1, m \neq k, l, \dots}^N \delta(\tau'_1 - \tau_k) \delta(\tau'_2 - \tau_l) \dots \delta(\tau'_\ell - \tau_m) \right\rangle \\ &= \frac{N!}{(N-\ell)!} \int f^{(N)}(\tau'_1, \dots, \tau'_\ell, \tau_{\ell+1}, \dots, \tau_N) d\vec{\tau}_{\ell+1}, \dots d\vec{\tau}_N, \end{aligned} \quad (\text{B14})$$

so that the pre-factor gives the number of ordered ℓ -plets ($f^{(1)}$ gives a particle density, $f^{(2)}$ the density of ordered pairs, etc.) It is also useful to rewrite the operator in Eq. (B12) as follows

$$h_N(\vec{\tau}_1, \dots, \vec{\tau}_k, \dots, \vec{\tau}_N) = h_\ell(\vec{\tau}_1, \dots, \vec{\tau}_\ell) + h_{N-\ell}(\vec{\tau}_{\ell+1}, \dots, \vec{\tau}_N) + \sum_{k=1}^{\ell} \sum_{l=\ell+1}^N \vec{W}_{kl} \cdot \left(\frac{\partial}{\partial \vec{p}_k} - \frac{\partial}{\partial \vec{p}_l} \right). \quad (\text{B15})$$

The previous form of Liouville's equation can be transformed into a chain of coupled equations, each one connecting the ℓ -th reduced distribution function to the $(\ell + 1)$ - density probability function as follows

$$\left(\frac{\partial}{\partial t} + h_\ell \right) f^{(\ell)} = - \sum_{k=1}^{\ell} \int d\vec{\tau}_{\ell+1} \vec{W}_{k, \ell+1} \cdot \frac{\partial}{\partial \vec{p}_k} f^{(\ell+1)}(\vec{\tau}_1, \dots, \vec{\tau}_{\ell+1}). \quad (\text{B16})$$

This set of coupled equations is known as the *BBGKY (Bogoliubov–Born–Green–Kirkwood–Yvon) hierarchy* and, without further approximations, it contains in principle the same information as the Liouville equation from which it was derived.

The set of Eqs. (B16) are equally challenging to solve as the Liouville Equation they were derived from. On the other hand, in most practical cases only a few distribution functions are of interest. By a suitable truncation to some order ℓ (with an approximation for $f^{(\ell+1)}$ in terms of $f^{(1)}, \dots, f^{(\ell)}$), the BBGKY hierarchy turns into a *closed* system made of only a few equations. Which approximation is most suitable to a given problem is of course subject to physical or heuristic arguments. In particular, the first equation writes

$$\left[\frac{\partial}{\partial t} + \dot{\vec{q}}_1 \cdot \frac{\partial}{\partial \vec{q}_1} - \frac{\partial U_1}{\partial \vec{q}_1} \cdot \frac{\partial}{\partial \vec{p}_1} \right] f^{(1)} = - \int d\tau_2 \vec{W}_{12} \frac{\partial f^{(2)}}{\partial \vec{p}_1}. \quad (\text{B17})$$

which can be proven to reduce to the Boltzmann equation under the hypothesis that our system is only subject to binary interactions from a potential V_{12} of range $\lambda \ll d$, with d being the typical distance between particles, and Boltzmann's "molecular chaos" hypothesis, or "Stosszahl Ansatz"

$$f^{(2)}(t, \tau_1, \tau_2) \rightarrow f^{(1)}(t, \tau_1) f^{(1)}(t, \tau_2). \quad (\text{B18})$$

-
- [1] M. Longair, "high energy astrophysics", Cambridge Univ. Press.
- [2] V. S Berezinskii et al. "Astrophysics of cosmic rays" (edited by V.L Ginzburg) Amsterdam: North-Holland, 1990.
- [3] R. Schlickeiser, "Cosmic ray astrophysics," Berlin, Germany: Springer (2002) 519 p
- [4] G. Sigl, "Astroparticle Physics: Theory and Phenomenology", Atlantis Studies in Astroparticle Physics and Cosmology (2017).
- [5] M. Vietri, "Foundations of High-Energy Astrophysics", The Univ. of Chicago press (2008).
- [6] R. Blandford & D. Eichler, Phys. Rep. 154, 1 (1987).
- [7] John Kirk, notes on Particle Acceleration www.mpi-hd.mpg.de/personalhomes/kirk/publications/saasfee.ps.gz
- [8] Kip S. Thorne and Roger D. Blandford, *Modern Classical Physics (Optics, Fluids, Plasmas, Elasticity, Relativity, and Statistical Physics)* Princeton University Press, 2017
- [9] M. Kachelriess, P. D. Serpico and M. Teshima, "The Galactic magnetic field as spectrograph for ultrahigh energy cosmic rays," *Astropart. Phys.* **26**, 378-386 (2006) [arXiv:astro-ph/0510444 [astro-ph]].
- [10] J. D. Finke, L. C. Reyes, M. Georganopoulos, K. Reynolds, M. Ajello, S. J. Fegan and K. McCann, "Constraints on the Intergalactic Magnetic Field with Gamma-Ray Observations of Blazars," *Astrophys. J.* **814**, no. 1, 20 (2015) [arXiv:1510.02485 [astro-ph.HE]].
- [11] M. S. Pshirkov, P. G. Tinyakov and F. R. Urban, "New limits on extragalactic magnetic fields from rotation measures," *Phys. Rev. Lett.* **116**, no. 19, 191302 (2016) [arXiv:1504.06546 [astro-ph.CO]].
- [12] T. Akahori *et al.*, "Cosmic Magnetism in Centimeter and Meter Wavelength Radio Astronomy," *Publ. Astron. Soc. Jap.* **70**, no. 1, R2 (2018) [arXiv:1709.02072 [astro-ph.HE]].
- [13] T. R. Jaffe, "Practical Modeling of Large-Scale Galactic Magnetic Fields: Status and Prospects," *Galaxies* **7**, no.2, 52 (2019) [arXiv:1904.12689 [astro-ph.GA]].
- [14] A. Esmaili and P. D. Serpico, "Gamma-ray bounds from EAS detectors and heavy decaying dark matter constraints," *JCAP* **1510**, no. 10, 014 (2015) [arXiv:1505.06486 [hep-ph]].
- [15] S. Abdollahi *et al.* [Fermi-LAT Collaboration], "A gamma-ray determination of the Universe's star formation history," *Science* **362**, no. 6418, 1031 (2018) [arXiv:1812.01031 [astro-ph.HE]].
- [16] Arthur H. Compton "A Geographic Study of Cosmic Rays" *Phys. Rev.* **43**, 387 (1933)
- [17] Bruno Rossi, "Interpretation of Cosmic-Ray Phenomena" *Rev. Mod. Phys.* **20**, 537 (1948)
- [18] J. W. Cronin, "The 1953 cosmic ray conference at Bagnères de Bigorre: The Birth of sub atomic physics," *Eur. Phys. J. H* **36** (2011), 183-201 [arXiv:1111.5338 [physics.hist-ph]].
- [19] C. Sørmer' s First Communication, 1934, available at <https://articles.adsabs.harvard.edu/pdf/1933POsIO...1J...1S>.
- [20] <https://arxiv.org/pdf/0704.3250v1.pdf>
- [21] Rossi & Greisen, *Rev. Mod. Phys.* **13**, 240 (1940)
- [22] J. Matthews, *Astroparticle Physics* **22** (2005) 387397.
- [23] V. Tatischeff and S. Gabici, "Particle acceleration by supernova shocks and spallogenic nucleosynthesis of light elements," *Ann. Rev. Nucl. Part. Sci.* **68**, 377 (2018) [arXiv:1803.01794 [astro-ph.HE]].
- [24] R. A. Treumann, R. Nakamura and W. Baumjohann, "Relativistic transformation of phase-space distributions," *Ann. Geophys.* **29**, 1259-1265 (2011) [arXiv:1105.2120 [physics.space-ph]].
- [25] Earl, J.A., Jokipii, J.R., Morfill, G.: *Astrophys. J. Lett.* **331**, 91 (1988)
- [26] Webb, G.M.: *Astrophys. J.* **340**, 1112 (1989)
- [27] P.L. Bhatnagar, E.P. Gross, M. Krook, "A Model for Collision Processes in Gases. I. Small Amplitude Processes in Charged and Neutral One-Component Systems" *Phys. Rev. D* **94** (1954) 511.
- [28] P. Mertsch and M. Ahlers, "Cosmic ray small-scale anisotropies in quasi-linear theory," *JCAP* **11**, 048 (2019) [arXiv:1909.09052 [astro-ph.HE]].

- [29] P. Mertsch, “Cosmic ray electrons and positrons from discrete stochastic sources,” *JCAP* **02**, 031 (2011) [arXiv:1012.0805 [astro-ph.HE]].
- [30] Y. Genolini, P. Salati, P. Serpico and R. Taillet, “Stable laws and cosmic ray physics,” *Astron. Astrophys.* **600**, A68 (2017) [arXiv:1610.02010 [astro-ph.HE]].
- [31] V. H. M. Phan, F. Schulze, P. Mertsch, S. Recchia and S. Gabici, “Stochastic Fluctuations of Low-Energy Cosmic Rays and the Interpretation of Voyager Data,” *Phys. Rev. Lett.* **127**, no.14, 141101 (2021) [arXiv:2105.00311 [astro-ph.HE]].
- [32] Y. Gholini *et al.*, “Cosmic-ray transport from AMS-02 B/C data: benchmark models and interpretation,” *Phys. Rev. D* **99**, no. 12, 123028 (2019) [arXiv:1904.08917].
- [33] T. I. Gombosi *et al.*, “The Telegraph Equation in Charged Particle Transport”, *Astrophys. J.* **403**, 377 (1993)
- [34] Y. E. Litvinenko, F. Effenberger and R. Schlickeiser, “The telegraph approximation for focused cosmic-ray transport in the presence of boundaries,” *Astrophys. J.* **806**, no.2, 217 (2015) [arXiv:1505.05134 [physics.space-ph]].
- [35] L. J. Gleeson and W. I. Axford, “Solar Modulation of Galactic Cosmic Rays,” *Astrophys. J.* **154**, 1011 (1968).
- [36] P. Mertsch, “A new analytic solution for 2nd-order Fermi acceleration,” *JCAP* **12**, 010 (2011) [arXiv:1110.6644 [astro-ph.HE]].
- [37] E. Fermi, “On the Origin of the Cosmic Radiation,” *Phys. Rev.* **75**, 1169-1174 (1949)
- [38] W. Baade and F. Zwicky, “On Super-Novae,” *Proc. Nat. Acad. Sci.* **20**, no.5, 254-259 (1934)
- [39] A. M. Hillas, “The Origin of Ultrahigh-Energy Cosmic Rays,” *Ann. Rev. Astron. Astrophys.* **22**, 425-444 (1984)
- [40] K. Akiba *et al.* “LHC Forward Physics,” *J. Phys. G* **43**, 110201 (2016) [arXiv:1611.05079 [hep-ph]].
- [41] G. Ghisellini, “Radiative Processes in High Energy Astrophysics,” *Lect. Notes Phys.* **873**, 1 (2013) [arXiv:1202.5949 [astro-ph.HE]].
- [42] J. G. Learned and K. Mannheim, “High-energy neutrino astrophysics,” *Ann. Rev. Nucl. Part. Sci.* **50**, 679 (2000).
- [43] J. Martin, D. F. Torres and N. Rea, “Time-dependent modeling of pulsar wind nebulae: Study on the impact of the diffusion-loss approximations,” *Mon. Not. Roy. Astron. Soc.* **427**, 415 (2012) [arXiv:1209.0300 [astro-ph.HE]].
- [44] M. J. Chodorowski, A. Zdziarski and M. Sikora, *Astrophys. J.* **400**, 181 (1992).
- [45] M. Kachelriess, “Lecture notes on high energy cosmic rays,” arXiv:0801.4376 [astro-ph].
- [46] K. Greisen, “End to the cosmic ray spectrum?,” *Phys. Rev. Lett.* **16**, 748 (1966).
- [47] G. T. Zatsepin and V. A. Kuzmin, “Upper limit of the spectrum of cosmic rays,” *JETP Lett.* **4**, 78 (1966)
- [48] T. Delahaye, R. Lineros, F. Donato, N. Fornengo and P. Salati, “Positrons from dark matter annihilation in the galactic halo: Theoretical uncertainties,” *Phys. Rev. D* **77**, 063527 (2008) [arXiv:0712.2312 [astro-ph]].
- [49] S. R. Kelner, F. A. Aharonian and V. V. Bugayov, “Energy spectra of gamma-rays, electrons and neutrinos produced at proton-proton interactions in the very high energy regime,” *Phys. Rev. D* **74**, 034018 (2006) Erratum: [*Phys. Rev. D* **79**, 039901 (2009)] [astro-ph/0606058].
- [50] E. Kafexhiu, F. Aharonian, A. M. Taylor and G. S. Vila, “Parametrization of gamma-ray production cross-sections for pp interactions in a broad proton energy range from the kinematic threshold to PeV energies,” *Phys. Rev. D* **90**, no. 12, 123014 (2014) [arXiv:1406.7369 [astro-ph.HE]].
- [51] M. Ackermann *et al.* [Fermi-LAT Collaboration], “Detection of the Characteristic Pion-Decay Signature in Supernova Remnants,” *Science* **339**, 807 (2013) [arXiv:1302.3307 [astro-ph.HE]].
- [52] V. Berezhinsky and O. Kalashev, “High energy electromagnetic cascades in extragalactic space: physics and features,” *Phys. Rev. D* **94**, no.2, 023007 (2016) doi:10.1103/PhysRevD.94.023007 [arXiv:1603.03989 [astro-ph.HE]].
- [53] A. Capanema, A. Esmaili and P. D. Serpico, “Where do IceCube neutrinos come from? Hints from the diffuse gamma-ray flux,” *JCAP* **02**, 037 (2021) [arXiv:2007.07911 [hep-ph]].
- [54] E. Waxman and J. N. Bahcall, “High-energy neutrinos from astrophysical sources: An Upper bound,” *Phys. Rev. D* **59**, 023002 (1999) [arXiv:hep-ph/9807282 [hep-ph]].
- [55] E. Borriello, S. Chakraborty, A. Mirizzi and P. D. Serpico, “Stringent constraint on neutrino Lorentz-invariance violation from the two IceCube PeV neutrinos,” *Phys. Rev. D* **87**, no.11, 116009 (2013) [arXiv:1303.5843 [astro-ph.HE]].